Spring 2015

Nonlinear Waves on a String with Inhomogeneous Properties

Robert Arredondo
University of New Hampshire, Durham

NONLINEAR WAVES ON A STRING WITH INHOMOGENEOUS PROPERTIES

BY

ROBERT ARREDONDO

BSMET, University of Lowell, Lowell MA, 1989

MSME, University of Massachusetts, Lowell MA, 1993

DISSERTATION

Submitted to the University of New Hampshire

in Partial Fulfillment of

the Requirements for the Degree of

Doctor of Philosophy

in

Mechanical Engineering

May, 2015

This dissertation has been examined and approved in partial fulfillment of the requirements for the degree of Doctor of Philosophy in Mechanical Engineering by:

Thesis/Dissertation Director, John P. McHugh,
Associate Professor of Mechanical Engineering

Gregory P. Chini,
Associate Professor of Mechanical Engineering

Yannis P. Korkolis,
Assistant Professor of Mechanical Engineering

Mark Lyon, Associate Professor of Mathematics

John F. Gibson, Assistant Professor of Mathematics

On December 15, 2014

Original approval signatures are on file with the University of New Hampshire Graduate School.

ACKNOWLEDGMENTS

I would like to thank Associate Professor of Mechanical Engineering John P. McHugh for acting as my advisor for this thesis project. His help was instrumental in guiding and helping me to complete this project. His courses in Computational Fluid Dynamics and Viscous Flow with an introduction to asymptotic methods was most helpful for this work. Also I would like to thank Associate Professor of Mechanical Engineering Gregory P. Chini for his knowledge in teaching a course in Asymptotic Methods. I would like to thank the other members of my thesis committee Associate Professor of Mechanical Engineering Yannis P. Korkolis, Associate Professor of Mathematics Mark Lyon, and Assistant Professor of Mathematics John F. Gibson for participating on the committee and offering valuable assistance on this project.

I would like to thank the University of New Hampshire for providing graduate student office space for me to work on this project while on campus.

I would also like to express my thanks to my wife Cathy Arredondo who has given me endless support and encouragement throughout the entire project.

Contents

List of Tables

List of Figures

ABSTRACT

NONLINEAR WAVES ON A STRING

WITH INHOMOGENEOUS PROPERTIES

by

Robert Arredondo

University of New Hampshire, May, 2015

Nonlinear waves on an infinite string with a rapid change in properties at one location are treated. The string is an idealized version of more complex configurations in both fluids and solids. This idealized version treats the property change as an interface with a discontinuity in properties. Packets of waves are then considered with a reduced model, here a set of nonlinear Schrödinger (NLS) equations. The stress and the displacement must both be matched at the interface, resulting in dynamic and kinematic interfacial conditions. The dynamic condition produces an inhomogeneous effect that cannot be treated successfully with separation-of-variables. This inhomogeneity is treated here with a time-evolution approach using Laplace transforms. The results show that this inhomogeneity creates a mean longitudinal displacement on both sides of the interface and a shift in the position of the interface as the waves transit the interface. This mean longitudinal displacement corresponds to a sustained strain in the string. The mean longitudinal displacement develops three distinct features. One feature has a length scale that is half the wave-length of the incident waves, while the lengths of the other two features have the same order as the length of the wave packet. The position of maximum strain as a result of this mean is often at the interface, depending on parameter values. These results apply to a variety of applications, such as waves in ocean ice, Rayleigh waves caused by earthquakes, internal waves in the oceans and atmosphere, as well as waves in stretched cables.

Chapter 1

INTRODUCTION

Waves are ubiquitous in natural and man-made systems, and they often have a dramatic effect on the observable features of these systems. Waves are most easily classified by their restoring force, such as gravity, rotation, and elasticity. The behavior of the waves may depend quite strongly on the character of these different restoring forces. However, there are often features of wave behavior that are shared by different types of waves. One such feature is the wave behavior near a region where properties change rapidly.

Waves of all types are routinely treated with the slowly-varying assumption. Slowly-varying generally means that the length for a change in any feature that affects the waves is much longer than the length of an individual wave. Such features include the material properties, a wave packet shape, and the strength of nonlinear effects. The results with this slowly-varying approximation reliably predict many aspects of wave propagation.

However, the background state may not be slowly varying, and in fact may contain very sudden changes in properties. One example of this fact appears in the character of the ice field in arctic regions. The ocean in arctic regions is covered with a relatively thin ice layer. Waves have been observed to form on this ice layer, see Campbell [1], analogous to ocean waves. These ice waves have both gravity and the elasticity of the ice as restoring forces. The waves are likely to result in fracture of the ice and may accelerate the disintegration of the polar ice caps, generating much recent interest in the problem. For example, Wang [2] considered solitary waves with an elastic model of ice, while Korobkin [3] investigates linear waves in a channel with an elastic

ice sheet. Measurements of ice thickness show wildly varying values over very short distances, apparently mostly due to the shape of the ice bottom. Thus long waves, as in Wang [2], when encountering these thickness variations would respond in a manner similar to that predicted here.

Another application of the present results is the propagation of waves created by earthquakes. An earthquake creates a wave field in the Earth that is often modeled as wave propagation in an elastic media. However real earthquake waves travel through many different regions with different material properties, e.g. loosely packed sand, hard packed gravel, solid bedrock, etc. These different materials have different elastic properties and the interface between these regions is often quite distinct. Again, the waves would respond to these interfaces in a manner similar to that analyzed here.

Cables and wires are common in many man-made structures. Many types of excitation will cause packets of waves to propagate along the cables. Different size cables that are rigidly connected are accurately modeled with the results given here.

In general, a rapid or sudden change in the properties of the media will likely cause a similar rapid change in the behavior of the waves, and this is a violation of the common assumption of slowly-varying material conditions. Nonlinear waves that are rapidly varying are very difficult to treat, yet can be extremely important. The one configuration with rapidly varying properties that may still be treated within the slowly-varying assumption is the case where the properties change abruptly, such that they may be modeled with a discontinuity in properties. This discontinuity is an interface, with corresponding interfacial conditions. The main subject of this thesis is the weakly nonlinear theory of waves that are evolving slowly but impinge on an interface of material properties for the important case of waves on an elastic string.

The linear model of waves propagating on a string results in the second-order

wave equation,

$$u_{tt} = c^2 u_{xx},$$

where u is the string displacement, t is time, x is position, and c is the phase speed. The subscripts used here indicate differentiation. The general wave solution to this equation is

$$u = F(x \pm ct),$$

where F is any function with sufficient differentiability. These waves do not disperse and are generally called 'hyperbolic' waves. A general discussion of the second-order wave equation appears in many texts, see for example Whitham [4] and Bland [5].

Nonlinear effects with larger amplitude motions may be important for several reasons. The material may have a constitutive behavior that is strongly nonlinear or even non-elastic. For many common engineering materials these effects are small and thus these material nonlinearities are ignored here. Other nonlinear effects may appear as a result of purely geometric deformation, and these effects are included. Nonlinear elasticity is reviewed in the book by Antman [6].

The physical model treated here is an infinite string consisting of two semi-infinite segments, each with different material properties, joined together at the interface. The interfacial conditions are that the displacement and tension must be continuous at the interface point. Bland [5] and Fetter and Walecka [7] discuss the linear solution for transverse waves with this same configuration. Morse and Ingard [8] and Beyer [9] give the nonlinear equations for constant property strings, but do not provide a general solution.

Nonlinear waves in discontinuous or inhomogeneous media have been treated recently in a variety of physical problems. Ellermeier [10] considers weakly nonlinear acoustic waves in non-uniform infinite and finite layered media; the medium in this case is an ideal gas and the non-uniformities are variable cross-section and density

stratification. Chakraborty and Gopalakrishnan [11, 12] consider numerical solutions to nonlinear wave propagation in Functionally Graded Materials (FGM). FGM are engineered materials which exhibit the desired variation of material properties along spatial directions. The FGM properties in Chakraborty and Gopalakrishnan vary over a finite spatial distance, unlike the sudden change in properties for the string treated here. Mortell and Seymour [13] also consider nonlinear waves in FGM, but seek a solution where the inhomogeneity interaction between strong stratification and nonlinear material properties can be chosen to yield combinations of linear exact solutions as in Whitham [4]. Iizuka and Wadati [14] study nonlinear waves in one-dimensional inhomogeneous lattice structures using the Korteweg-de Vries (KdV) wave equation. Yajima [15] and Iizuka and Wadati [16] treat the reflection and transmission of soliton waves through a one-dimensional lattice structure, again using the KdV equation.

The present work considers slowly evolving nonlinear monochromatic waves traveling in a packet, similar to the many studies of dispersive waves. The wave packet impinges on an interface, creating a reflected wave packet and a transmitted wave packet, see Figure 1.1. The incident, reflected, and transmitted wave packets must respect the nonlinear interfacial conditions, as well as the nonlinearities in the governing equations. Furthermore, the incident and reflected wave packets exist together on one side of the string, creating a nonlinear wave interaction. The nonlinear evolution during this stage is determined in this thesis. Of particular importance is a mean longitudinal displacement that occurs. One of the goals of the present work is to precisely determine this mean longitudinal displacement.

The governing equations are derived in Chapter 2 for a nonlinear one-dimensional wave equation for transverse and longitudinal displacements for a constant or smooth property string. In Chapter 3, the string is allowed to experience a sudden change

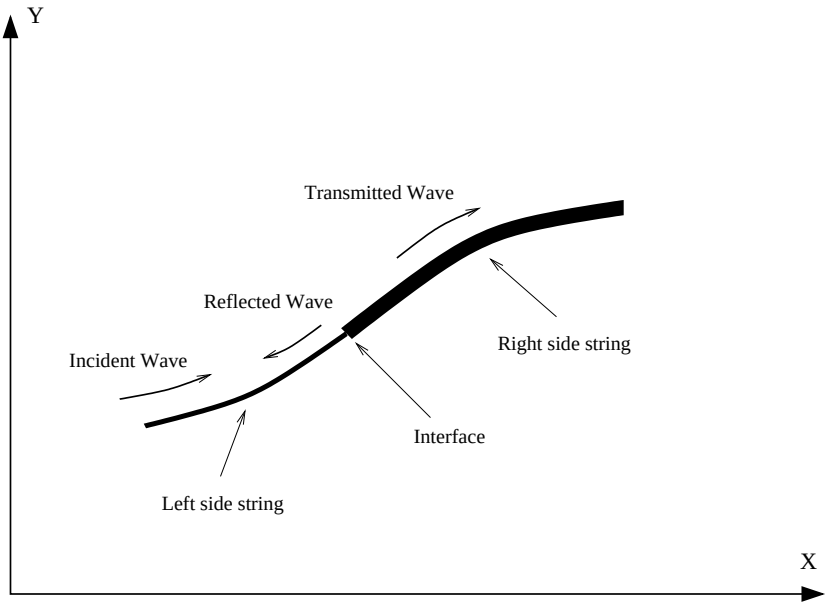

Figure 1.1: Wave Packet Direction

in properties and the interface conditions are developed. Chapter 4 addresses the neglect of quadratic and higher level terms in the governing equations and the interface conditions and the linear solution is presented. Chapter 5 develops the weakly nonlinear wave equations from the governing equations and the interface conditions. In Chapter 6, the weakly nonlinear solution is determined for each side of the string. The dynamic interface condition could not be satisfied due to an inhomogeneous term which requires special treatment. An initial value approach using Laplace transforms is used. In Chapter 7, the third-order equations produce secular terms which must be suppressed. This results in three NLS equations in terms of the incident, reflected, and transmitted wave packet amplitudes. Chapter 8 presents the solution to the NLS equations using numerical integration to solve for the wave packet amplitudes and to show the resultant behavior of the mean longitudinal displacement equations.

Chapter 9 gives the results from the numerical simulations for various cases of three dimensionless parameter ratios which emerge. These parameter ratios are var-

ied systematically to show their effects. It was found that a purely transverse incident wave produces longitudinal waves and a mean longitudinal displacement when interacting with an interface where properties change suddenly. This mean longitudinal displacement can be either positive or negative depending upon the parameters and can have an effect that spans outward from the interface along each side of the string with decreasing values away from the interface point. The shape of the mean longitudinal displacement curve has unique features attributable to various terms in the mean longitudinal displacement equations. The mean longitudinal displacement also induces a strain in the string near the interface. Chapter 10 presents a conclusion of the results.

Chapter 2

GOVERNING EQUATIONS

Consider an infinite string with smoothly varying properties along its length. Initially the string is parallel to the abscissa. The properties of the string are dictated by the mass density per unit length ρ, the elastic modulus E, and the cross-sectional area A. Figures 2.1 and 2.2 are schematics of an infinitesimal element of the string in the reference and deformed positions. The displacements u, v are defined by

$$u = x - X, \tag{2.1}$$

$$v = y - Y, \tag{2.2}$$

where X, Y are the initial or reference positions, and x, y are the deformed positions.

The angle ψ between the element at time $t + \delta t$ and the abscissa is given by

$$\tan\psi = \lim_{\delta X \to 0} \left(\frac{\delta Y + \delta v}{\delta X + \delta u} \right) = \left[\frac{\left(\frac{\partial Y}{\partial X} + \frac{\partial v}{\partial X} \right)}{\left(1 + \frac{\partial u}{\partial X} \right)} \right]. \tag{2.3}$$

Using subscript notation to denote derivatives, (2.3) becomes

$$\tan\psi = \left(\frac{Y_X + v_X}{1 + u_X} \right). \tag{2.4}$$

The elongational strain ϵ is defined as

$$\epsilon = \lim_{\delta X \to 0} \frac{\left\{ [(\delta X + \delta u)^2 + (\delta Y + \delta v)^2]^{1/2} - [\delta X^2 + \delta Y^2]^{1/2} \right\}}{\delta X}, \tag{2.5}$$

which reduces to

$$\epsilon = [(1 + u_X)^2 + (Y_X + v_X)^2]^{1/2} - [1 + Y_X^2]^{1/2}. \tag{2.6}$$

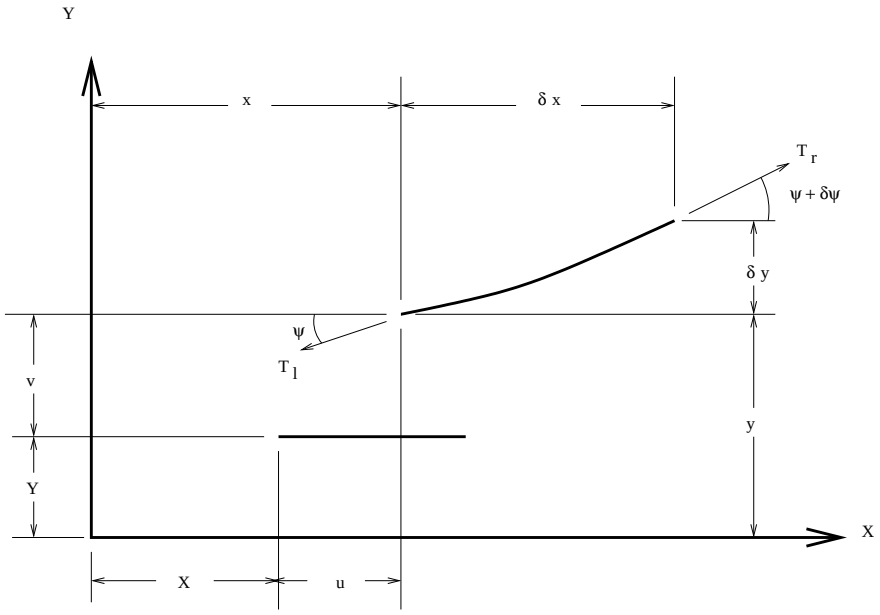

Figure 2.1: String Element - Reference and Deformed Positions

Since the string in the initial or reference position is parallel to the abscissa,

$$Y_X = 0. \tag{2.7}$$

Equations (2.4) and (2.6) become, respectively,

$$\tan\psi = \left(\frac{v_X}{1+u_X}\right), \tag{2.8}$$

$$\epsilon = \left[(1+u_X)^2 + v_X^2\right]^{1/2} - 1. \tag{2.9}$$

The equations of motion along the horizontal and vertical directions are derived using Newton's Second Law of motion,

$$\vec{F} = m\vec{a}, \tag{2.10}$$

where $\vec{F}$ represents the sum of the forces acting on the string, m is the mass of the string, and $\vec{a}$ is the acceleration. Applied to the string element, the horizontal force component gives

$$T\cos\psi\Big|_{x+\delta x, y+\delta y} - T\cos\psi\Big|_{x,y} = \rho u_{tt}\,\delta X.$$

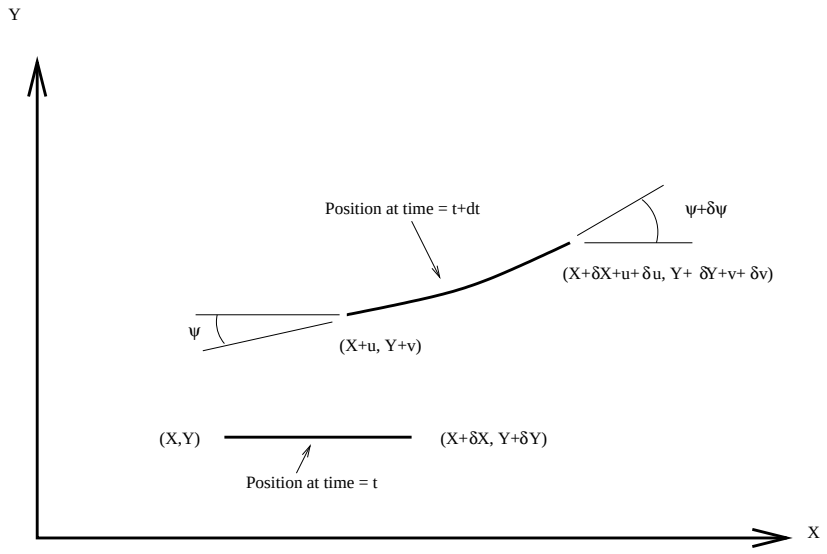

Figure 2.2: String Element Coordinate Endpoints

Add and subtract

$$T\cos\psi\Big|_{x,y+\delta y}$$

and rearrange to get

$$\left[T\cos\psi\Big|_{x+\delta x,y+\delta y} - T\cos\psi\Big|_{x,y+\delta y}\right] + \left[T\cos\psi\Big|_{x,y+\delta y} - T\cos\psi\Big|_{x,y}\right] = \rho u_{tt}\,\delta X. \quad (2.11)$$

Divide both sides by δX and add δx and δy as appropriate to get

$$\left[\frac{T\cos\psi\Big|_{x+\delta x,y+\delta y} - T\cos\psi\Big|_{x,y+\delta y}}{\delta x}\right]\frac{\delta x}{\delta X} + \left[\frac{T\cos\psi\Big|_{x,y+\delta y} - T\cos\psi\Big|_{x,y}}{\delta y}\right]\frac{\delta y}{\delta X} = \rho u_{tt}. \quad (2.12)$$

Take the limit as δX goes to zero, to obtain

$$\frac{\partial(T\cos\psi)}{\partial x}\frac{\partial x}{\partial X} + \frac{\partial(T\cos\psi)}{\partial y}\frac{\partial y}{\partial X} = \rho u_{tt}. \quad (2.13)$$

However, direct reference to the current state is unnecessary, as the quantity on the left is merely $\partial/\partial X$,

$$\frac{\partial(T\cos\psi)}{\partial X} = \rho u_{tt}. \tag{2.14}$$

The vertical force component can also be treated in a similar matter resulting in

$$\frac{\partial(T\sin\psi)}{\partial X} = \rho v_{tt}. \tag{2.15}$$

In linear theory, (see Chapter 4), the tension in the string is considered constant and the angle of the string element is assumed very small. Here the tension is assumed non-constant and the angle of the string segment is not restrained to be infinitesimal, resulting in the important nonlinear effects.

The tension in the string is defined using Hooke's Law as

$$T = T_0 + E\,A\,\epsilon, \tag{2.16}$$

where T_0 is the initial tension and ϵ is the elongational strain. Combining (2.16) and (2.9) gives

$$T = T_0 + E\,A\left[\left[(1+u_X)^2 + v_X^2\right]^{1/2} - 1\right]. \tag{2.17}$$

After expanding, using trigonometric identities, and rearranging, (2.14) and (2.15) become

$$\begin{aligned} -\left(\frac{T_0 - EA}{\rho}\right)\left[(1+u_X)v_X v_{XX} - v_X^2 u_{XX}\right] \\ + \frac{EA}{\rho}u_{XX}\left[(1+u_X)^2 + v_X^2\right]^{3/2} \\ = \left[(1+u_X)^2 + v_X^2\right]^{3/2} u_{tt}, \end{aligned} \tag{2.18}$$

$$\begin{aligned} \left(\frac{T_0 - EA}{\rho}\right)\left[(1+u_X)^2 v_{XX} - (1+u_X)v_X u_{XX}\right] \\ + \frac{EA}{\rho}v_{XX}\left[(1+u_X)^2 + v_X^2\right]^{3/2} \\ = \left[(1+u_X)^2 + v_X^2\right]^{3/2} v_{tt}. \end{aligned} \tag{2.19}$$

Define

$$c_\lambda^2 = \frac{EA}{\rho}, \tag{2.20}$$

$$c_\tau^2 = \frac{T_0}{\rho}, \tag{2.21}$$

where c_λ and c_τ will be shown to be the longitudinal and transverse wave speeds, respectively. Use these definitions in (2.20) and (2.21) to obtain

$$\begin{aligned} -(c_\tau^2 - c_\lambda^2)\big[(1+u_X)v_X v_{XX} - v_X^2 u_{XX}\big] & \\ +c_\lambda^2 u_{XX}\big[(1+u_X)^2 + v_X^2\big]^{3/2} & \\ = \big[(1+u_X)^2 + v_X^2\big]^{3/2} u_{tt}, & \end{aligned} \tag{2.22}$$

$$\begin{aligned} (c_\tau^2 - c_\lambda^2)\big[(1+u_X)^2 v_{XX} - (1+u_X)v_X u_{XX}\big] & \\ +c_\lambda^2 v_{XX}\big[(1+u_X)^2 + v_X^2\big]^{3/2} & \\ = \big[(1+u_X)^2 + v_X^2\big]^{3/2} v_{tt}. & \end{aligned} \tag{2.23}$$

The nonlinear equations (2.22) and (2.23) cannot be solved in general, and a weakly nonlinear approach is pursued here. The binomial series is used to simplify the terms in (2.22) and (2.23) with fractional exponent. The binomial series is

$$(1+\beta)^n = 1 + n\beta + \frac{n(n-1)}{2!}\beta^2 + \frac{n(n-1)(n-2)}{3!}\beta^3 + \cdots, \tag{2.24}$$

where $|\beta| < 1$. For small amplitude displacements where $\left|(u_X^2 + 2u_X + v_X^2)\right| < 1$, this leads to

$$\big[(1+u_X)^2 + v_X^2\big]^{3/2} = 1 + 3u_X + 3u_X^2 + \frac{3}{2}v_X^2 + u_X^3 + \frac{3}{2}u_X v_X^2 + \cdots. \tag{2.25}$$

Use (2.25) in (2.22) and (2.23) and keep only cubic terms to obtain the final form of the nonlinear governing equations as

$$u_{tt} - c_\lambda^2 u_{XX} = (c_\lambda^2 - c_\tau^2)\big[(1-2u_X)v_X v_{XX} - v_X^2 u_{XX}\big] + \cdots, \tag{2.26}$$

$$v_{tt} - c_\tau^2 v_{XX} = (c_\lambda^2 - c_\tau^2)\left[(1 - 2u_X)v_X u_{XX} + \left(u_X - u_X^2 + \frac{3}{2}v_X^2\right)v_{XX}\right] + \cdots. \quad (2.27)$$

Close examination of (2.26) and (2.27) show that all nonlinear terms have a common coefficient of

$$(c_\lambda^2 - c_\tau^2). \quad (2.28)$$

If the wave speeds are equal, the nonlinear terms vanish from the governing equations. The severity of nonlinear behavior of the nonlinear terms is dictated by the difference between the squares of the two wave speeds.

Chapter 3

THE INTERFACE

Now the string is allowed to have a sudden change in properties at one location, conveniently chosen to be $X = 0$. Each segment of the string has constant or smooth properties: E, A, and ρ. An incident wave packet is created at the left end of the string and travels to the right toward the interface. When the incident wave packet reaches the interface both a reflected wave packet and a transmitted wave packet are created. The reflected waves travel to the left toward $X = -\infty$ and the transmitted waves travel to the right toward $X = +\infty$.

At the interface the solution must obey both kinematic and dynamic conditions. The kinematic condition requires the displacement to be continuous at $X = 0$:

$$\big[u\big]_l = \big[u\big]_r, \tag{3.1}$$

$$\big[v\big]_l = \big[v\big]_r, \tag{3.2}$$

on $X = 0$ where the subscript l and r represent left and right sides of the string respectively.

The dynamic condition requires the tension T to be continuous, see Figure 3.1. The Cartesian components of the tension give

$$\big[T\cos\psi\big]_l = \big[T\cos\psi\big]_r, \tag{3.3}$$

$$\big[T\sin\psi\big]_l = \big[T\sin\psi\big]_r, \tag{3.4}$$

on $X = 0$.

Use (2.8) and (2.17) along with trigonometric identities to get

$$T\cos\psi = \frac{(T_0 - EA)(1+u_X)}{\Big[(1+u_X)^2 + v_X^2\Big]^{1/2}} \;+\; EA\,(1+u_X), \tag{3.5}$$

$$T\sin\psi = \frac{(T_0 - EA)v_X}{\Big[(1+u_X)^2 + v_X^2\Big]^{1/2}} \;+\; EA\,v_X. \tag{3.6}$$

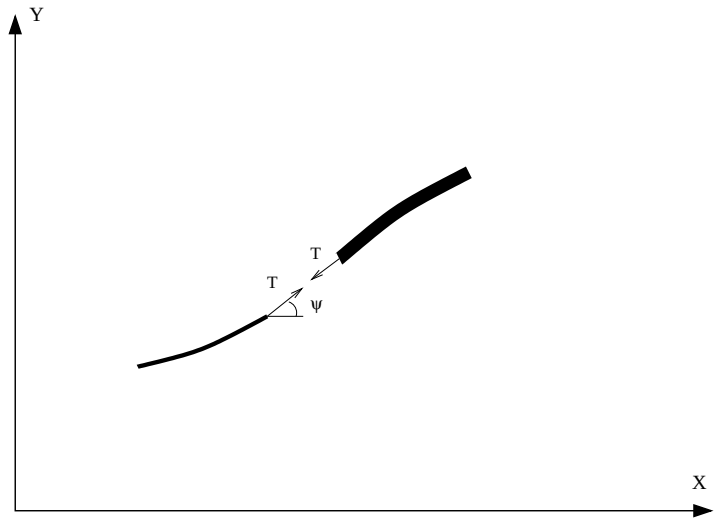

Figure 3.1: Interface Forces

Expand the denominator in a binomial series (2.24), to eliminate the fractional exponent,

$$T\cos\psi = T_0\left(1 - \frac{1}{2}v_X^2 + u_X v_X^2\right) \;+\; EA\left(u_X + \frac{1}{2}v_X^2 - u_X v_X^2\right), \tag{3.7}$$

$$T\sin\psi = T_0\left(v_X - u_X v_X + u_X^2 v_X - \frac{1}{2}v_X^3\right) \;+\; EA\left(u_X v_X - u_X^2 v_X + \frac{1}{2}v_X^3\right), \tag{3.8}$$

where quartic and higher terms have been neglected.

Finally the dynamic conditions at the interface are

$$\left[T_0\left(u_X v_X^2 - \frac{1}{2}v_X^2\right) \;+\; EA\left(u_X + \frac{1}{2}v_X^2 - u_X v_X^2\right)\right]_l = \left[T_0\left(u_X v_X^2 - \frac{1}{2}v_X^2\right) \;+\; EA\left(u_X + \frac{1}{2}v_X^2 - u_X v_X^2\right)\right]_r, \tag{3.9}$$

$$\left[T_0\left(v_X - u_X v_X + u_X^2 v_X - \frac{1}{2}v_X^3\right) + EA\left(u_X v_X - u_X^2 v_X + \frac{1}{2}v_X^3\right)\right]_l$$
$$= \left[T_0\left(v_X - u_X v_X + u_X^2 v_X - \frac{1}{2}v_X^3\right) + EA\left(u_X v_X - u_X^2 v_X + \frac{1}{2}v_X^3\right)\right]_r, \quad (3.10)$$

on $X = 0$.

Chapter 4

LINEAR SOLUTION

Neglecting all quadratic and higher level terms in (2.26), (2.27), (3.1), (3.2), (3.9), and (3.10) results in

$$u_{tt} - c_\lambda^2 u_{XX} = 0, \tag{4.1}$$

$$v_{tt} - c_\tau^2 v_{XX} = 0, \tag{4.2}$$

and

$$\big[u\big]_l = \big[u\big]_r, \tag{4.3}$$

$$\big[v\big]_l = \big[v\big]_r, \tag{4.4}$$

$$\Big[(EA)u_X\Big]_l = \Big[(EA)u_X\Big]_r, \tag{4.5}$$

$$\big[v_X\big]_l = \big[v_X\big]_r, \tag{4.6}$$

at $X = 0$. The linear governing equations (4.1) and (4.2) allow two well-known basic wave types, transverse waves, where $u = 0$, $v \neq 0$, and longitudinal waves, where $u \neq 0$, $v = 0$. A transverse wave traveling to the right has the solution

$$v = Ae^{i(kX - \sigma t)} + A^* e^{-i(kX - \sigma t)}, \tag{4.7}$$

$$u = 0. \tag{4.8}$$

where

$$\sigma = kc_\tau, \tag{4.9}$$

where k is the wave number and σ is the wave frequency. The coefficient A is the amplitude of the wave and the circumflex (*) indicates complex conjugate. Hence c_τ (defined earlier) is clearly the wave speed of a linear transverse wave.

A longitudinal traveling wave moving to the right has the solution

$$u = Ae^{i(kX-\sigma t)} + A^* e^{-i(kX-\sigma t)}, \tag{4.10}$$

$$v = 0. \tag{4.11}$$

where

$$\sigma = kc_\lambda. \tag{4.12}$$

and here c_λ is the wave speed of the longitudinal wave.

The nonlinear theory that follows will treat primarily transverse waves. Nonlinear transverse waves will create a longitudinal structure, as will be seen. In contrast, pure longitudinal waves do not create a transverse wave component, and hence transverse waves are more complex.

Now focus on transverse waves, (4.7) and (4.8). When the interface is included, the incident waves alone are not sufficient to satisfy the interfacial conditions, e.g. for transverse waves, (4.7) does not satisfy (4.4) and (4.6). Reflected and transmitted waves must be included. On the left side of the string both the incident and reflected waves are present,

$$v_l = Ae^{i(k_l X-\sigma t)} + A^* e^{-i(k_l X-\sigma t)} + Be^{i(k_l X+\sigma t)} + B^* e^{-i(k_l X+\sigma t)}, \tag{4.13}$$

where A and B are the magnitudes of the incident and reflected wave respectively, and k_l is the wave number on the left. On the right side of the string are transmitted waves, given by

$$v_r = Ce^{i(k_r X-\sigma t)} + C^* e^{-i(k_r X-\sigma t)}, \tag{4.14}$$

where C is the magnitude and k_r is the wave number of the transmitted waves. The interfacial conditions (4.4) and (4.6) give

$$A + B^* = C, \tag{4.15}$$

$$k_l(A - B^*) = k_r C. \tag{4.16}$$

After rearranging,

$$B^* = \mathcal{R}A, \tag{4.17}$$

$$C = \mathcal{T}A. \tag{4.18}$$

where $\mathcal{R}$ and $\mathcal{T}$ are the reflection and transmission coefficients, respectively,

$$\mathcal{R} = \left[\frac{k_l - k_r}{k_l + k_r}\right], \tag{4.19}$$

$$\mathcal{T} = \left[\frac{2k_l}{k_l + k_r}\right]. \tag{4.20}$$

Furthermore, the incident, reflected, and transmitted waves must have the same frequency σ.

Chapter 5

WEAKLY NONLINEAR WAVES

The transverse waves are assumed to exist in a packet with a length that is much larger than the length of an individual wave. The small parameter ε is a measure of the ratio of the individual wavelength to the packet length. Introduce slow scales for both time and position,

$$X_m = \varepsilon^m X, \tag{5.1}$$

$$t_m = \varepsilon^m t, \tag{5.2}$$

where

$$m = 0, 1, 2. \tag{5.3}$$

The amplitude of the wave is also assumed to be small, as measured by the small parameter α. The displacement (u, v) is expanded in a power series in α,

$$u = \alpha u_1 + \alpha^2 u_2 + \alpha^3 u_3 + \cdots, \tag{5.4}$$

$$v = \alpha v_1 + \alpha^2 v_2 + \alpha^3 v_3 + \cdots. \tag{5.5}$$

In order to achieve the final results, the two small parameters α and ε must be of the same order. The following choice achieves this requirement and simplifies the analysis:

$$\varepsilon = \alpha. \tag{5.6}$$

The governing equations (2.26) and (2.27) (repeated here for convenience) are

$$u_{tt} - c_\lambda^2 u_{XX} = (c_\lambda^2 - c_\tau^2)\big[(1 - 2u_X)v_X v_{XX} - v_X^2 u_{XX}\big],$$

$$v_{tt} - c_\tau^2 v_{XX} = (c_\lambda^2 - c_\tau^2)\left[(1 - 2u_X)v_X u_{XX} + \left(u_X - u_X^2 + \frac{3}{2}v_X^2\right)v_{XX}\right].$$

Use (5.1), (5.2), (5.4), (5.5), and (5.6) in (2.26) and (2.27), rearrange, and collect powers of ε to obtain

$$u_{1,t_0t_0} - c_\lambda^2 u_{1,X_0X_0} = 0, \tag{5.7}$$

$$v_{1,t_0t_0} - c_\tau^2 v_{1,X_0X_0} = 0, \tag{5.8}$$

$$u_{2,t_0t_0} - c_\lambda^2 u_{2,X_0X_0} = 2c_\lambda^2 u_{1,X_0X_1} - 2u_{1,t_0t_1} - c_0^2 v_{1,X_0} u_{1,X_0,X_0} + c_0^2 v_{1,X_0} v_{1,X_0,X_0}, \tag{5.9}$$

$$v_{2,t_0t_0} - c_\tau^2 v_{2,X_0X_0} = 2c_\tau^2 v_{1,X_0X_1} - 2v_{1,t_0t_1} + c_0^2 v_{1,X_0} u_{1,X_0,X_0} + c_0^2 u_{1,X_0} v_{1,X_0,X_0}, \tag{5.10}$$

$$\begin{aligned} u_{3,t_0t_0} - c_\lambda^2 u_{3,X_0X_0} = {} & c_\lambda^2 u_{1,X_1X_1} - u_{1,t_1t_1} + 2c_\lambda^2 u_{1,X_0X_2} - 2u_{1,t_0t_2} \\ & + 2c_\lambda^2 u_{2,X_0X_1} - 2u_{2,t_0t_1} - c_0^2 v_{1,X_0} u_{2,X_0X_0} + c_0^2 v_{1,X_0} v_{2,X_0X_0} \\ & - c_0^2 v_{2,X_0} u_{1,X_0X_0} + c_0^2 v_{2,X_0} v_{1,X_0X_0} - c_0^2 v_{1,X_1} u_{1,X_0X_0} + c_0^2 v_{1,X_1} v_{1,X_0X_0} \\ & - 2c_0^2 v_{1,X_0} u_{1,X_0X_1} + 2c_0^2 v_{1,X_0} v_{1,X_0X_1} - 2c_0^2 u_{1,X_0} v_{1,X_0} v_{1,X_0X_0}, \end{aligned} \tag{5.11}$$

$$\begin{aligned} v_{3,t_0t_0} - c_\tau^2 v_{3,X_0X_0} = {} & c_\tau^2 v_{1,X_1X_1} - v_{1,t_1t_1} + 2c_\tau^2 v_{1,X_0X_2} - 2v_{1,t_0t_2} \\ & + 2c_\tau^2 v_{2,X_0X_1} - 2v_{2,t_0t_1} + c_0^2 v_{1,X_1} u_{1,X_0X_0} + c_0^2 v_{1,X_0} u_{2,X_0X_0} \\ & + c_0^2 v_{2,X_0} u_{1,X_0X_0} + c_0^2 u_{1,X_1} v_{1,X_0X_0} + c_0^2 u_{1,X_0} v_{2,X_0X_0} + c_0^2 u_{2,X_0} v_{1,X_0X_0} \\ & - c_0^2 (u_{1,X_0})^2 v_{1,X_0X_0} + 2c_0^2 v_{1,X_0} u_{1,X_0X_1} + 2c_0^2 u_{1,X_0} v_{1,X_0X_1} \\ & + \frac{3}{2} c_0^2 (v_{1,X_0})^2 v_{1,X_0X_0} - 2c_0^2 u_{1,X_0} v_{1,X_0} u_{1,X_0X_0}. \end{aligned} \tag{5.12}$$

where

$$c_0^2 = (c_\lambda^2 - c_\tau^2). \tag{5.13}$$

Recall the kinematic interfacial conditions (3.1) and (3.2) (repeated here),

$$\big[u\big]_l = \big[u\big]_r,$$

$$\big[v\big]_l = \big[v\big]_r,$$

on $X = 0$.

Treat these conditions in the same manner as the above governing equations to obtain

$$\big[u_1\big]_l = \big[u_1\big]_r, \tag{5.14}$$

$$\big[v_1\big]_l = \big[v_1\big]_r, \tag{5.15}$$

$$\big[u_2\big]_l = \big[u_2\big]_r, \tag{5.16}$$

$$\big[v_2\big]_l = \big[v_2\big]_r, \tag{5.17}$$

on $X = 0$. Note that the third order interfacial conditions are unnecessary.

The dynamic interfacial conditions (3.3) and (3.4) (repeated here) are

$$\big[T\cos\psi\big]_l = \big[T\cos\psi\big]_r,$$

$$\big[T\sin\psi\big]_l = \big[T\sin\psi\big]_r,$$

on $X = 0$, where

$$T\cos\psi = T_0\bigg(1 - \frac{1}{2}v_X^2 + u_X v_X^2\bigg) \;+\; EA\bigg(u_X + \frac{1}{2}v_X^2 - u_X v_X^2\bigg),$$

$$T\sin\psi = T_0\bigg(v_X - u_X v_X + u_X^2 v_X - \frac{1}{2}v_X^3\bigg) \;+\; EA\bigg(u_X v_X - u_X^2 v_X + \frac{1}{2}v_X^3\bigg).$$

Again, treat as before:

$$\big[EA\,u_{1,X_0}\big]_l = \big[EA\,u_{1,X_0}\big]_r, \tag{5.18}$$

$$\big[T_0\,v_{1,X_0}\big]_l = \big[T_0\,v_{1,X_0}\big]_r, \tag{5.19}$$

$$\bigg[\frac{1}{2}(EA - T_0)(v_{1,X_0})^2 + EA(u_{2,X_0} + u_{1,X1})\bigg]_l = \bigg[\frac{1}{2}(EA - T_0)(v_{1,X_0})^2 + EA(u_{2,X_0} + u_{1,X1})\bigg]_r, \tag{5.20}$$

$$\Big[(EA - T_0)u_{1,X_0}v_{1,X_0} + T_0(v_{2,X_0} + v_{1,X_1})\Big]_l = \Big[(EA - T_0)u_{1,X_0}v_{1,X_0} + T_0(v_{2,X_0} + v_{1,X_1})\Big]_r, \tag{5.21}$$

on $X = 0$.

Chapter 6

WEAKLY NONLINEAR SOLUTION

As stated previously, the incident wave packet travels toward the interface from the left. Interaction with the interface creates reflected and transmitted wave packets. During this interaction, incident, reflected, and transmitted waves exist simultaneously, while a short time later only the reflected and transmitted waves remain, traveling in opposite directions. During this entire period, the right-side of the string only has transmitted waves. There are no changes in string properties encountered as the transmitted wave moves away from the interface, making it equivalent to an incident wave problem with smooth or constant string properties. It is therefore simpler and will be discussed first.

6.1 Right Side of String

If the incident wave is chosen to be a transverse wave, then the transmitted wave will also be primarily a transverse wave of the form

$$u_1 = 0, \tag{6.1}$$

$$v_1 = C_{11}e^{i(k_r X_0 - \sigma t_0)} + C_{11}^* e^{-i(k_r X_0 - \sigma t_0)}, \tag{6.2}$$

where k_r is the wave number on the right side of the string and σ is the wave frequency ($\sigma = c_\tau k_r$). The coefficient C_{11} may be a function of all the slow variables. The first subscript on C_{ij} denotes the order while the second subscript will be explained later. Use (6.1) to simplify (5.7) through (5.12) to obtain

$$u_{1,t_0t_0} - c_\lambda^2 u_{1,X_0X_0} = 0, \tag{6.3}$$

$$v_{1,t_0t_0} - c_\tau^2 v_{1,X_0X_0} = 0, \tag{6.4}$$

$$u_{2,t_0t_0} - c_\lambda^2 u_{2,X_0X_0} = c_0^2 v_{1,X_0} v_{1,X_0,X_0}, \tag{6.5}$$

$$v_{2,t_0t_0} - c_\tau^2 v_{2,X_0X_0} = 2c_\tau^2 v_{1,X_0X_1} - 2v_{1,t_0t_1}, \tag{6.6}$$

$$\begin{aligned} u_{3,t_0t_0} - c_\lambda^2 u_{3,X_0X_0} &= 2c_\lambda^2 u_{2,X_0X_1} - 2u_{2,t_0t_1} - c_0^2 v_{1,X_0} u_{2,X_0X_0} \\ &+c_0^2 v_{1,X_0} v_{2,X_0X_0} + c_0^2 v_{2,X_0} v_{1,X_0X_0} + c_0^2 v_{1,X_1} v_{1,X_0X_0} + 2c_0^2 v_{1,X_0} v_{1,X_0X_1}, \end{aligned} \tag{6.7}$$

$$\begin{aligned} v_{3,t_0t_0} - c_\tau^2 v_{3,X_0X_0} &= c_\tau^2 v_{1,X_1X_1} - v_{1,t_1t_1} + 2c_\tau^2 v_{1,X_0X_2} - 2v_{1,t_0t_2} + 2c_\tau^2 v_{2,X_0X_1} \\ &-2v_{2,t_0t_1} + c_0^2 v_{1,X_0} u_{2,X_0X_0} + c_0^2 u_{2,X_0} v_{1,X_0X_0} + \frac{3}{2} c_0^2 (v_{1,X_0})^2 v_{1,X_0X_0}. \end{aligned} \tag{6.8}$$

Note that (6.1) and (6.2) satisfy the first-order equations (6.3) and (6.4).

Substitute (6.2) into (6.6). The inhomogeneous terms of (6.6) produce the secular terms

$$2ik_r c_\tau \left[c_\tau \frac{\partial C_{11}}{\partial X_1} + \frac{\partial C_{11}}{\partial t_1} \right] e^{i(k_r x_0 - \sigma t_0)}, \tag{6.9}$$

$$-2ik_r c_\tau \left[c_\tau \frac{\partial C_{11}^*}{\partial X_1} + \frac{\partial C_{11}^*}{\partial t_1} \right] e^{-i(k_r x_0 - \sigma t_0)}. \tag{6.10}$$

To suppress these terms,

$$\left[c_\tau \frac{\partial C_{11}}{\partial X_1} + \frac{\partial C_{11}}{\partial t_1} \right] = \left[c_\tau \frac{\partial C_{11}^*}{\partial X_1} + \frac{\partial C_{11}^*}{\partial t_1} \right] = 0. \tag{6.11}$$

The solution here is

$$C_{11} = C_{12} e^{i(k_r X_1 - \sigma t_1)}, \tag{6.12}$$

$$C_{11}^* = C_{12}^* e^{-i(k_r X_1 - \sigma t_1)}, \tag{6.13}$$

where C_{12} may be a function of (X_2, t_2). The second subscript is a reassignment of the coefficient which may be functions of the next order slow scales and not the current slow scales.

When the first-order solution is combined with the linear solution, the combination is merely a linear wave with slightly different wave number and frequency. These two orders are now merged by redefining the variables k_r and σ as

$$k_r \to (\varepsilon + 1)k_r, \tag{6.14}$$

$$\sigma \to (\varepsilon + 1)\sigma. \tag{6.15}$$

The linear solution is now

$$v_1 = C_{12}e^{i(k_r X_0 - \sigma t_0)} + C_{12}^* e^{-i(k_r X_0 - \sigma t_0)}. \tag{6.16}$$

All of the inhomogeneous terms in (6.6) are secular and have been suppressed. Therefore the solution for v_2 consists of the homogeneous solution alone,

$$v_2 = C_{21}e^{i(k_r X_0 - \sigma t_0)} + C_{21}^* e^{-i(k_r X_0 - \sigma t_0)}. \tag{6.17}$$

where C_{21} and C_{21}^* are arbitrary. Set $C_{21} = C_{21}^* = 0$ to get

$$v_2 = 0. \tag{6.18}$$

Solve (6.5) using (6.16) to obtain homogeneous and particular parts for longitudinal displacement to get

$$u_{2H} = C_{22}e^{i(k_r X_0 - \sigma t_0)} + C_{22}^* e^{-i(k_r X_0 - \sigma t_0)}, \tag{6.19}$$

$$u_{2P} = -\frac{ik_r}{4}\left[C_{12}^2 e^{i2(k_r X_0 - \sigma t_0)} - C_{12}^{*\,2} e^{-i2(k_r X_0 - \sigma t_0)}\right], \tag{6.20}$$

where subscripts H and P denote homogeneous and particular. Again choose $C_{22} = C_{22}^* = 0$ to get

$$u_2 = -\frac{ik_r}{4}\left[C_{12}^2 e^{i2(k_r X_0 - \sigma t_0)} - C_{12}^{*\,2} e^{-i2(k_r X_0 - \sigma t_0)}\right]. \tag{6.21}$$

6.2 Left Side of String

On the left side of the string there are two waves, incident and reflected. Both the incident and reflected waves are transverse waves with displacements of the form

$$u_1 = 0, \tag{6.22}$$

$$v_1 = A_{11}e^{i(k_l X_0 - \sigma t_0)} + A_{11}^* e^{-i(k_l X_0 - \sigma t_0)} + B_{11}e^{i(k_l X_0 + \sigma t_0)} + B_{11}^* e^{-i(k_l X_0 + \sigma t_0)}, \tag{6.23}$$

where k_l is the wave number on the left side of the string and σ is the wave frequency ($\sigma = c_\tau k_l$). The amplitudes A_{11} and B_{11} may be functions of all the slow variables. Since $u_1 = 0$ for the left side, then equations (6.3) through (6.8) are equally valid for the left side. Note that (6.22) and (6.23) satisfy the first-order equations (6.3) and (6.4).

The second-order solution must satisfy the inhomogeneous equations (6.5) and (6.6). Substitute (6.23) into (6.6). The inhomogeneous terms in (6.6) produce secular terms that result in

$$2ik_l c_\tau \left[c_\tau \frac{\partial A_{11}}{\partial X_1} + \frac{\partial A_{11}}{\partial t_1} \right] e^{i(k_r x_0 - \sigma t_0)}, \tag{6.24}$$

$$-2ik_l c_\tau \left[c_\tau \frac{\partial A_{11}^*}{\partial X_1} + \frac{\partial A_{11}^*}{\partial t_1} \right] e^{-i(k_r x_0 - \sigma t_0)}, \tag{6.25}$$

$$2ik_l c_\tau \left[c_\tau \frac{\partial B_{11}}{\partial X_1} + \frac{\partial B_{11}}{\partial t_1} \right] e^{i(k_r x_0 + \sigma t_0)}, \tag{6.26}$$

$$-2ik_l c_\tau \left[c_\tau \frac{\partial B_{11}^*}{\partial X_1} + \frac{\partial B_{11}^*}{\partial t_1} \right] e^{-i(k_r x_0 + \sigma t_0)}. \tag{6.27}$$

To suppress these terms,

$$\left[c_\tau \frac{\partial A_{11}}{\partial X_1} + \frac{\partial A_{11}}{\partial t_1} \right] = \left[c_\tau \frac{\partial A_{11}^*}{\partial X_1} + \frac{\partial A_{11}^*}{\partial t_1} \right] = 0, \tag{6.28}$$

$$\left[c_\tau \frac{\partial B_{11}}{\partial X_1} + \frac{\partial B_{11}}{\partial t_1} \right] = \left[c_\tau \frac{\partial B_{11}^*}{\partial X_1} + \frac{\partial B_{11}^*}{\partial t_1} \right] = 0. \tag{6.29}$$

The solution is

$$A_{11} = A_{12}e^{i(k_l X_1 - \sigma t_1)}, \tag{6.30}$$

$$A_{11}^* = A_{12}^* e^{-i(k_l X_1 - \sigma t_1)}, \tag{6.31}$$

$$B_{11} = B_{12}e^{i(k_l X_1 - \sigma t_1)}, \tag{6.32}$$

$$B_{11}^* = B_{12}^* e^{-i(k_l X_1 - \sigma t_1)}, \tag{6.33}$$

where A_{12} and B_{12} may be functions of (X_2, t_2).

As in the previous section, this contribution from the second-order may be merged with the new linear solution. Use (6.15) and

$$k_l \to (\varepsilon + 1)k_l, \tag{6.34}$$

to write the linear solution as

$$v_1 = A_{12}e^{i(k_l X_0 - \sigma t_0)} + A_{12}^* e^{-i(k_l X_0 - \sigma t_0)} + B_{12}e^{i(k_l X_0 - \sigma t_0)} + B_{12}^* e^{-i(k_l X_0 - \sigma t_0)}. \tag{6.35}$$

Since all inhomogeneous terms in (6.6) have now been suppressed, the final solution for v_2 consists of only a homogeneous part,

$$v_2 = A_{22}e^{i(k_l X_0 - \sigma t_0)} + A_{22}^* e^{-i(k_l X_0 - \sigma t_0)} + B_{22}e^{i(k_l X_0 + \sigma t_0)} + B_{22}^* e^{-i(k_l X_0 + \sigma t_0)}. \tag{6.36}$$

Setting $A_{22} = A_{22}^* = B_{22} = B_{22}^* = 0$ gives

$$v_2 = 0. \tag{6.37}$$

Solve (6.5) using (6.35) to obtain homogeneous and particular parts for longitudinal displacement,

$$u_{2H} = A_{21}e^{i(k_l X_0 - \sigma t_0)} + A_{21}^* e^{-i(k_l X_0 - \sigma t_0)} + B_{21}e^{i(k_l X_0 + \sigma t_0)} + B_{21}^* e^{-i(k_l X_0 + \sigma t_0)}, \tag{6.38}$$

$$\begin{aligned} u_{2P} = -\frac{ik_l}{4}\Big[&(A_{11})^2 e^{i2(k_l X_0 - \sigma t_0)} - (A_{11}^*)^2 e^{-i2(k_l X_0 - \sigma t_0)} \\ &+ (B_{11})^2 e^{i2(k_l X_0 + \sigma t_0)} - (B_{11}^*)^2 e^{-i2(k_l X_0 + \sigma t_0)}\Big] \\ &- \frac{ik_l}{2c_\lambda^2}\left(c_\lambda^2 - c_\tau^2\right)\Big[A_{11}B_{11}e^{i2k_l X_0} - A_{11}^* B_{11}^* e^{-i2k_l X_0}\Big]. \end{aligned} \tag{6.39}$$

Set $A_{21} = A_{21}^* = B_{21} = B_{21}^* = 0$ to get

$$u_2 = -\frac{ik_l}{4}\Big[(A_{11})^2 e^{i2(k_l X_0 - \sigma t_0)} - (A_{11}^*)^2 e^{-i2(k_l X_0 - \sigma t_0)} + (B_{11})^2 e^{i2(k_l X_0 + \sigma t_0)} - (B_{11}^*)^2 e^{-i2(k_l X_0 + \sigma t_0)}\Big] - \frac{ik_l}{2c_\lambda^2}\big(c_\lambda^2 - c_\tau^2\big)\Big[A_{11}B_{11}e^{i2k_l X_0} - A_{11}^* B_{11}^* e^{-i2k_l X_0}\Big]. \quad (6.40)$$

6.3 Interface Conditions

The solution thus far is (6.1), (6.16), (6.18), (6.21), (6.22), (6.35), (6.37), and (6.40) repeated here using appropriate subscripts l and r for the left and right sides:

$$[u_1]_l = [u_1]_r = 0, \quad (6.41)$$

$$[v_1]_l = A_{12}e^{i(k_l X_0 - \sigma t_0)} + A_{12}^* e^{-i(k_l X_0 - \sigma t_0)} + B_{12}e^{i(k_l X_0 + \sigma t_0)} + B_{12}^* e^{-i(k_l X_0 + \sigma t_0)}, \quad (6.42)$$

$$[v_1]_r = C_{12}e^{i(k_r X_0 - \sigma t_0)} + C_{12}^* e^{-i(k_r X_0 - \sigma t_0)}, \quad (6.43)$$

$$[u_2]_l = -\frac{ik_l}{4}\Big[(A_{12})^2 e^{i2(k_l X_0 - \sigma t_0)} - (A_{12}^*)^2 e^{-i2(k_l X_0 - \sigma t_0)} + (B_{12})^2 e^{i2(k_l X_0 + \sigma t_0)} - (B_{12}^*)^2 e^{-i2(k_l X_0 + \sigma t_0)}\Big] - \frac{ik_l}{2c_\lambda^2}\big(c_\lambda^2 - c_\tau^2\big)\Big[A_{12}B_{12}e^{i2k_l X_0} - A_{12}^* B_{12}^* e^{-i2k_l X_0}\Big], \quad (6.44)$$

$$[u_2]_r = \frac{ik_r}{4}\Big[{C_{12}^*}^2 e^{-2i(k_r X_0 - \sigma t_0)} - C_{12}^2 e^{2i(k_r X_0 - \sigma t_0)}\Big], \quad (6.45)$$

$$[v_2]_l = [v_2]_r = 0. \quad (6.46)$$

The kinematic and dynamic interface conditions, (5.14) through (5.21), must be satisfied at the interface where $X = 0$. Since the initial tension T_0 equal on both

sides of the string and v_1 is independent of X_1, (6.41) and (6.46) may be used to reduce the eight interfacial conditions (5.14) to (5.21) to four:

$$\big[v_1\big]_l = \big[v_1\big]_r, \tag{6.47}$$

$$\big[u_2\big]_l = \big[u_2\big]_r, \tag{6.48}$$

$$\big[v_{1,X_0}\big]_l = \big[v_{1,X_0}\big]_r, \tag{6.49}$$

$$\left[\frac{1}{2}(EA - T_0)(v_{1,X_0})^2 + EA(u_{2,X_0})\right]_l = \left[\frac{1}{2}(EA - T_0)(v_{1,X_0})^2 + EA(u_{2,X_0})\right]_r, \tag{6.50}$$

on $X = 0$. Use (6.42) and (6.43) in (6.47) and note that the three waves have the same frequency σ, resulting in

$$C_{12} = A_{12} + B_{12}^*, \tag{6.51}$$

$$C_{12}^* = A_{12}^* + B_{12}, \tag{6.52}$$

on $X = 0$. This is the same relationship found in the linear solution (4.15). Differentiate (6.42) and (6.43) and substitute into (6.49) to get the following additional relationships:

$$C_{12} = \frac{k_l}{k_r}\big(A_{12} - B_{12}^*\big), \tag{6.53}$$

$$C_{12}^* = \frac{k_l}{k_r}\big(A_{12}^* - B_{12}\big), \tag{6.54}$$

on $X = 0$. Combine (6.51), (6.52), (6.53), and (6.54) to get

$$B_0 = \mathcal{R}A_0^*, \tag{6.55}$$

$$B_0^* = \mathcal{R}A_0, \tag{6.56}$$

where $A_0 = A_{12}(X = 0)$ and $B_0 = B_{12}(X = 0)$. Combine (6.51), (6.52), (6.55), and (6.56) to get

$$C_0 = \mathcal{T}A_0, \tag{6.57}$$

$$C_0^* = \mathcal{T} A_0^*, \tag{6.58}$$

where $C_0 = C_{12}(X = 0)$ and $\mathcal{R}$ and $\mathcal{T}$ were defined previously as the reflection and the transmission coefficients, respectively, (4.19) and (4.20).

6.4 Initial Condition Problem

There is an inhomogeneous term in the dynamic interfacial condition (6.50) that the solution up to this point has not included. This term requires special treatment. The solutions given in (6.41) through (6.46) are based on the separation-of-variables method, where space and time are treated separately. A separation-of-variables approach to the extra inhomogeneous term fails to satisfy the boundary condition at $X \to \pm\infty$. Instead, an initial value approach using Laplace transforms is pursued here.

This additional part of the solution that balances the inhomogeneous term in the dynamic interfacial condition must satisfy the homogeneous equation for the string,

$$u_{2,t_0t_0} - c_\lambda^2 u_{2,X_0X_0} = 0. \tag{6.59}$$

The kinematic and dynamic boundary conditions at the interface may be written as

$$\big[u_2(0,t_0)\big]_l - \big[u_2(0,t_0)\big]_r = 0, \tag{6.60}$$

$$\Big[EA(u_{2,X_0}(0,t_0))\Big]_l - \Big[EA(u_{2,X_0}(0,t_0))\Big]_r = f(0,t_0), \tag{6.61}$$

where

$$f(0,t_0) = \left[\frac{1}{2}\big(EA - T_0\big)\Big[v_{1,X_0}(0,t_0)\Big]^2\right]_r - \left[\frac{1}{2}\big(EA - T_0\big)\Big[v_{1,X_0}(0,t_0)\Big]^2\right]_l. \tag{6.62}$$

Initial Conditions at $t_0 = 0$ are

$$u_2(X_0,0) = 0, \tag{6.63}$$

$$u_{2,t_0}(X_0, 0) = 0. \tag{6.64}$$

The Laplace transform is defined as

$$\mathcal{L}\Big[g(X_0, t_0)\Big] = \int_0^\infty g(X_0, t_0)\, e^{-st_0} dt_0 = G(X_0, s), \tag{6.65}$$

where g is any function and G is it's Laplace transform.

Use (6.65) to transform (6.59), (6.60), (6.61), (6.63), and (6.64) to get

$$s^2\, U(X_0, s) - c_\lambda^2 U(X_0, s)_{X_0 X_0} = 0, \tag{6.66}$$

$$\Big[U(0, s)\Big]_l - \Big[U(0, s)\Big]_r = 0, \tag{6.67}$$

$$\Big[EA(U_{X_0}(0, s))\Big]_l - \Big[EA(U_{X_0}(0, s))\Big]_r = F(0, s), \tag{6.68}$$

where

$$F(0,s) = \frac{2k_l^2 k_r^2}{(k_l + k_r)^2}\Big[\big(EA\big)_l - \big(EA\big)_r\Big]\Bigg\{ \int_0^\infty (A_0)^2\, e^{-i2\sigma t_0} e^{-st_0} dt_0 + \int_0^\infty (A_0^*)^2\, e^{i2\sigma t_0} e^{-st_0} dt_0 - 2\int_0^\infty A_0 A_0^*\, e^{-st_0} dt_0 \Bigg\}, \tag{6.69}$$

and $U(X_0, s)$ represents the Laplace transform of $u_2(X_0, t_0)$.

The general solution to (6.66) is

$$U(X_0, s) = \tilde{A}(s)\, e^{-s(X_0/c_\lambda)} + \tilde{B}(s)\, e^{s(X_0/c_\lambda)}. \tag{6.70}$$

For the left side of the string choose $\tilde{A}(s) = 0$ to achieve acceptable behavior as $X_0 \to -\infty$ and likewise for the right side of the string choose $\tilde{B}(s) = 0$ for $X_0 \to +\infty$. This gives

$$U_l(X_0, s) = \tilde{B}_l(s)\, e^{s(X_0/c_\lambda)_l}, \tag{6.71}$$

$$U_r(X_0, s) = \tilde{A}_r(s)\, e^{-s(X_0/c_\lambda)_r}, \tag{6.72}$$

where subscripts have been added to indicate sides of the domain. Apply the kinematic boundary condition (6.67) to get

$$\tilde{A}_r(s) = \tilde{B}_l(s) = \tilde{D}(s), \tag{6.73}$$

on $X = 0$. This gives the following solutions for (6.66):

$$U_l(X_0, s) = \tilde{D}(s)\, e^{s(X_0/c_\lambda)_l}, \tag{6.74}$$

$$U_r(X_0, s) = \tilde{D}(s)\, e^{-s(X_0/c_\lambda)_r}. \tag{6.75}$$

Use (6.74) and (6.75) in (6.68) to get

$$\left\{ \left[\frac{EA}{c_\lambda}\right]_l + \left[\frac{EA}{c_\lambda}\right]_r \right\} s\ \tilde{D}(s) = F(0, s) \tag{6.76}$$

Use (6.69) in (6.76), solve for $\tilde{D}(s)$, then use (6.74) and (6.75), rearrange and simplify to get

$$U_l(X_0, s) = \left[\frac{(EA)_l - (EA)_r}{(EA/c_\lambda)_l + (EA/c_\lambda)_r}\right] \frac{2k_l^2 k_r^2}{(k_l + k_r)^2} * \left\{ \int_0^\infty \left[(A_0)^2\, e^{-i2\sigma t_0} + (A_0^*)^2\, e^{i2\sigma t_0} - 2A_0A_0^*\right] e^{-st_0} dt_0 \right\} \frac{e^{s(X_0/c_\lambda)_l}}{s}, \tag{6.77}$$

$$U_r(X_0, s) = \left[\frac{(EA)_l - (EA)_r}{(EA/c_\lambda)_l + (EA/c_\lambda)_r}\right] \frac{2k_l^2 k_r^2}{(k_l + k_r)^2} * \left\{ \int_0^\infty \left[(A_0)^2\, e^{-i2\sigma t_0} + (A_0^*)^2\, e^{i2\sigma t_0} - 2A_0A_0^*\right] e^{-st_0} dt_0 \right\} \frac{e^{-s(X_0/c_\lambda)_r}}{s}. \tag{6.78}$$

Multiply (6.77) and (6.78) by e^{st} and integrate from 0 to ∞ to inverse Laplace transform the equations to get

$$u(X_0, t_0)_l = \left[\frac{(EA)_l - (EA)_r}{(EA/c_\lambda)_l + (EA/c_\lambda)_r}\right] \frac{2k_1^2 k_2^2}{(k_1 + k_2)^2} * \int_0^\infty \left\{ \int_0^\infty \left[(A_0)^2\, e^{-i2\sigma t_0} + (A_0^*)^2\, e^{i2\sigma t_0} - 2A_0A_0^*\right] e^{-st_0} dt_0 \right\} \frac{e^{s(X_0/c_\lambda)_l} e^{st_0}}{s}\, ds, \tag{6.79}$$

$$u(X_0, t_0)_r = \left[\frac{(EA)_l - (EA)_r}{(EA/c_\lambda)_l + (EA/c_\lambda)_r}\right] \frac{2k_1^2 k_2^2}{(k_1 + k_2)^2} * \int_0^\infty \left\{ \int_0^\infty \left[(A_0)^2\, e^{-i2\sigma t_0} + (A_0^*)^2\, e^{i2\sigma t_0} - 2A_0A_0^*\right] e^{-st_0} dt_0 \right\} \frac{e^{-s(X_0/c_\lambda)_r} e^{st_0}}{s}\, ds, \tag{6.80}$$

where the RHS has been left in integral form.

6.5 Evaluation of the Integrals

The inner integral in (6.79) and (6.80) can be sub-divided into three sub-integrals. The coefficient A_0 only depends weakly on t_2, hence an asymptotic approximation can be found for each sub-integral with repeated application of integration by parts. The three integral solutions are, e.g.

$$\int_0^\infty A_0^2 e^{-(s+i2\sigma)} dt_0 = A_0^2 \int_0^\infty e^{-(s+i2\sigma)} dt_0 + O(\varepsilon^2). \tag{6.81}$$

Essentially A_0^2 may be removed from the integral here (and below),

$$\int_0^\infty e^{-(s+i2\sigma)t_0} dt_0 = \frac{1}{(s+i2\sigma)} + O(\varepsilon^2), \tag{6.82}$$

$$\int_0^{\infty,} e^{-(s-i2\sigma)t_0} dt_0 = \frac{1}{(s-i2\sigma)} + O(\varepsilon^2), \tag{6.83}$$

$$\int_0^\infty e^{-st_0} dt_0 = \frac{1}{s} + O(\varepsilon^2). \tag{6.84}$$

Neglect terms of ε^2 and higher and use (6.82), (6.83), and (6.84) in (6.79) and (6.80) to obtain

$$u_l(X_0, t_0) = \left[\frac{(EA)_l - (EA)_r}{(EA/c_\lambda)_l + (EA/c_\lambda)_r}\right] \frac{2k_l^2 k_r^2}{(k_l + k_r)^2} * \int_0^\infty \left\{ (A_0)^2 \frac{1}{(s+i2\sigma)} + (A_0^*)^2 \frac{1}{(s-i2\sigma)} - 2A_0 A_0^* \frac{1}{s} \right\} \frac{e^{s(t_0 + X_0/c_\lambda)_l}}{s}\, ds, \tag{6.85}$$

$$u_r(X_0, t_0) = \left[\frac{(EA)_l - (EA)_r}{(EA/c_\lambda)_l + (EA/c_\lambda)_r}\right] \frac{2k_l^2 k_r^2}{(k_l + k_r)^2} * \int_0^\infty \left\{ (A_0)^2 \frac{1}{(s+i2\sigma)} + (A_0^*)^2 \frac{1}{(s-i2\sigma)} - 2A_0 A_0^* \frac{1}{s} \right\} \frac{e^{s(t_0 - X_0/c_\lambda)_r}}{s}\, ds. \tag{6.86}$$

After rearrangement, the remaining integrals can each be segmented into three sub-integrals with the coefficients removed from within the sub-integral (as treated earlier) to give

$$u_l(X_0,t_0) = \left[\frac{(EA)_l-(EA)_r}{(EA/c_\lambda)_l+(EA/c_\lambda)_r}\right]\frac{2k_l^2k_r^2}{(k_l+k_r)^2}\left\{(A_0)^2\int_0^\infty \frac{e^{s(t_0+X_0/c_\lambda)}}{s(s+i2\sigma)}\,ds \right.$$
$$\left. +(A_0^*)^2\int_0^\infty \frac{e^{s(t_0+X_0/c_\lambda)}}{s(s-i2\sigma)}\,ds - 2A_0A_0^*\int_0^\infty \frac{e^{s(t_0+X_0/c_\lambda)}}{s^2}\,ds\right\}, \quad (6.87)$$

$$u_r(X_0,t_0) = \left[\frac{(EA)_l-(EA)_r}{(EA/c_\lambda)_l+(EA/c_\lambda)_r}\right]\frac{2k_l^2k_r^2}{(k_l+k_r)^2}\left\{(A_0)^2\int_0^\infty \frac{e^{s(t_0-X_0/c_\lambda)}}{s(s+i2\sigma)}\,ds \right.$$
$$\left. +(A_0^*)^2\int_0^\infty \frac{e^{s(t_0-X_0/c_\lambda)}}{s(s-i2\sigma)}\,ds - 2A_0A_0^*\int_0^\infty \frac{e^{s(t_0-X_0/c_\lambda)}}{s^2}\,ds\right\}. \quad (6.88)$$

The remaining six sub-integrals can each be treated with contour integration using Cauchy's residue theorem:

$$\int_C G(X,s)\,e^{st}ds = 2\pi i\sum_{i=0}^{n} res\big[G(X,s)e^{st}\big], \quad (6.89)$$

The contour used consists of a line at $s=\gamma$ which is to the right of all singularities and an semi-circular arc of radius R centered at $s=\gamma$. The two parts of the contour can be represented by a line integral and an integral over the semi-circular arc as

$$\int_{C_R} G(X,s)\,e^{st}ds + \int_{L_R} G(X,s)\,e^{st}ds = 2\pi i\sum_{i=0}^{n} res\big[G(X,s)\,e^{st}\big]. \quad (6.90)$$

Taking the limit as $R\to\infty$, the integral over the semi-circular arc is zero and the remaining integral becomes

$$\frac{1}{2\pi i}\int_{\gamma-i\infty}^{\gamma+i\infty} G(X,s)\,e^{st}ds = \sum_{i=0}^{n} res\big[G(X,s)\,e^{st}\big]. \quad (6.91)$$

Define

$$Q_l = \left(t_0 + \frac{X_0}{c_\lambda} \right)_l , \tag{6.92}$$

$$Q_r = \left(t_0 - \frac{X_0}{c_\lambda} \right)_r . \tag{6.93}$$

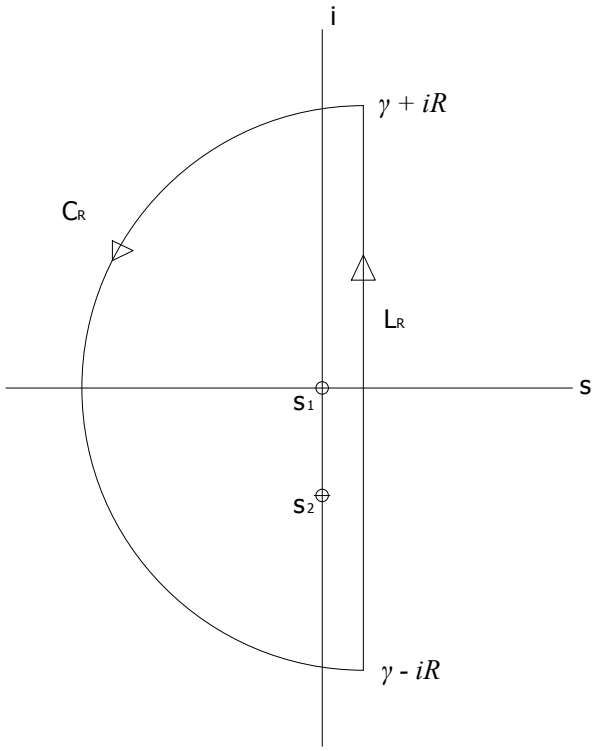

Figure 6.1: Contour Integration Including Poles

For $Q_l, Q_r > 0$, the semi-circle is chosen to the left of the $s = \gamma$ line with all singularities inside the closed contour, see Figure 6.1. Note: Only one contour integral figure is shown here. For $Q_l, Q_r < 0$, the semi-circle is chosen to the right with no singularities inside.

For $Q_l, Q_r > 0$, the integrals have simple poles and are not multi-valued, thus the

residue at each singularity is given by

$$res(s_n) = \frac{1}{(m-1)!} \lim_{s \to a} \frac{\partial^{(m-1)}}{\partial s^{(m-1)}} \big[(s-a)^m f(s)\big], \tag{6.94}$$

where m is the order of the pole, and $s = a$ is the pole location. For $Q_l, Q_r > 0$ the integral solutions are

$$\frac{1}{2\pi i} \int_{\gamma - i\infty}^{\gamma + i\infty} \frac{e^{sQ_l}}{s(s + i2\sigma)}\, ds = \frac{1}{i2\sigma} \Big[1 - e^{-i2\sigma Q_l}\Big], \tag{6.95}$$

$$\frac{1}{2\pi i} \int_{\gamma - i\infty}^{\gamma + i\infty} \frac{e^{sQ_l}}{s(s - i2\sigma)}\, ds = -\frac{1}{i2\sigma} \Big[1 - e^{i2\sigma Q_l}\Big], \tag{6.96}$$

$$\frac{1}{2\pi i} \int_{\gamma - i\infty}^{\gamma + i\infty} \frac{e^{sQ_l}}{s^2}\, ds = Q_l, \tag{6.97}$$

$$\frac{1}{2\pi i} \int_{\gamma - i\infty}^{\gamma + i\infty} \frac{e^{sQ_r}}{s(s + i2\sigma)}\, ds = \frac{1}{i2\sigma} \Big[1 - e^{-i2\sigma Q_r}\Big], \tag{6.98}$$

$$\frac{1}{2\pi i} \int_{\gamma - i\infty}^{\gamma + i\infty} \frac{e^{sQ_r}}{s(s - i2\sigma)}\, ds = -\frac{1}{i2\sigma} \Big[1 - e^{i2\sigma Q_r}\Big], \tag{6.99}$$

$$\frac{1}{2\pi i} \int_{\gamma - i\infty}^{\gamma + i\infty} \frac{e^{sQ_r}}{s^2}\, ds = Q_r. \tag{6.100}$$

For $Q_l, Q_r < 0$, the integrals do not contain singularities and are zero.

Substitute (6.95), (6.96), (6.97), (6.98), (6.99), and (6.100) into (6.87) and (6.88) and recall the particular solutions (6.40) and (6.21). The final longitudinal displacement may be written as

$$\begin{aligned} u_2(X_0, t_0)_l = -\frac{ik_l}{4} \Big[& (A_{12})^2 e^{i2(k_l X_0 - \sigma t_0)} - (A_{12}^*)^2 e^{-i2(k_l X_0 - \sigma t_0)} \\ & + (B_{12})^2 e^{i2(k_l X_0 + \sigma t_0)} - (B_{12}^*)^2 e^{-i2(k_l X_0 + \sigma t_0)} \Big] \\ & - \frac{ik_l}{2c_\lambda^2} \big(c_\lambda^2 - c_\tau^2\big) \Big[A_{12} B_{12} e^{i2k_l X_0} - A_{12}^* B_{12}^* e^{-i2k_l X_0} \Big] + \bar{W}_l, \end{aligned} \tag{6.101}$$

$$u_2(X_0,t_0)_r = -\frac{ik_r}{4}\left[(C_{12})^2 e^{i2(k_r X_0 - \sigma t_0)} - (C_{12}^*)^2 e^{-i2(k_r X_0 - \sigma t_0)}\right] + \bar{W}_r, \qquad (6.102)$$

where

$$\bar{W}_l = \begin{cases} 0 & \text{when } t_0 < \left[-\frac{X_0}{c_\lambda}\right]_l \\ \bar{U}_l & \text{when } t_0 > \left[-\frac{X_0}{c_\lambda}\right]_l \end{cases},$$

$$\bar{W}_r = \begin{cases} 0 & \text{when } t_0 < \left[\frac{X_0}{c_\lambda}\right]_r \\ \bar{U}_r & \text{when } t_0 > \left[\frac{X_0}{c_\lambda}\right]_r \end{cases},$$

$$\bar{U}_l = \left[\frac{(EA)_l - (EA)_r}{(EA/c_\lambda)_l + (EA/c_\lambda)_r}\right] \frac{2k_l^2 k_r^2}{(k_l+k_r)^2}\left\{(A_0)^2 \frac{1}{i2\sigma}\left[1 - e^{-i2\sigma(t_0 + X_0/c_\lambda)_l}\right]\right.$$
$$\left. -(A_0^*)^2 \frac{1}{i2\sigma}\left[1 - e^{i2\sigma(t_0+X_0/c_\lambda)_l}\right] - 2A_0A_0^*\left[t_0 + \frac{X_0}{c_\lambda}\right]_l\right\}, \qquad (6.103)$$

$$\bar{U}_r = \left[\frac{(EA)_l - (EA)_r}{(EA/c_\lambda)_l + (EA/c_\lambda)_r}\right] \frac{2k_l^2 k_r^2}{(k_l+k_r)^2}\left\{(A_0)^2 \frac{1}{i2\sigma}\left[1 - e^{-i2\sigma(t_0 - X_0/c_\lambda)_r}\right]\right.$$
$$\left. -(A_0^*)^2 \frac{1}{i2\sigma}\left[1 - e^{i2\sigma(t_0-X_0/c_\lambda)_r}\right] - 2A_0A_0^*\left[t_0 - \frac{X_0}{c_\lambda}\right]_r\right\}. \qquad (6.104)$$

Chapter 7

NLS EQUATIONS

The third-order equations are used to finalize the solution. These equations are not solved, but it is important that all secular terms be eliminated to make the second-order solution uniformly valid. As a result of the third-order analysis the secular terms create three non-linear Schrödinger's (NLS) equations. The NLS equations will be solved numerically.

7.1 Third-Order Equations

The third-order equations are (6.7) and (6.8), repeated here:

$$u_{3,t_0t_0} - c_\lambda^2 u_{3,X_0X_0} = 2c_\lambda^2 u_{2,X_0X_1} - 2u_{2,t_0t_1} - c_0^2 v_{1,X_0} u_{2,X_0X_0} \\ + c_0^2 v_{1,X_0} v_{2,X_0X_0} + c_0^2 v_{2,X_0} v_{1,X_0X_0} + c_0^2 v_{1,X_1} v_{1,X_0X_0} + 2c_0^2 v_{1,X_0} v_{1,X_0X_1},$$

$$v_{3,t_0t_0} - c_\tau^2 v_{3,X_0X_0} = c_\tau^2 v_{1,X_1X_1} - v_{1,t_1t_1} + 2c_\tau^2 v_{1,X_0X_2} - 2v_{1,t_0t_2} + 2c_\tau^2 v_{2,X_0X_1} \\ - 2v_{2,t_0t_1} + c_0^2 v_{1,X_0} u_{2,X_0X_0} + c_0^2 u_{2,X_0} v_{1,X_0X_0} + \frac{3}{2} c_0^2 (v_{1,X_0})^2 v_{1,X_0X_0}.$$

Apply (6.18) and (6.37) to get

$$u_{3,t_0t_0} - c_\lambda^2 u_{3,X_0X_0} = 2c_\lambda^2 u_{2,X_0X_1} - 2u_{2,t_0t_1} - c_0^2 v_{1,X_0} u_{2,X_0X_0} \\ + c_0^2 v_{1,X_1} v_{1,X_0X_0} + 2c_0^2 v_{1,X_0} v_{1,X_0X_1}, \quad (7.1)$$

$$v_{3,t_0t_0} - c_\tau^2 v_{3,X_0X_0} = c_\tau^2 v_{1,X_1X_1} - v_{1,t_1t_1} + 2c_\tau^2 v_{1,X_0X_2} - 2v_{1,t_0t_2} \\ + c_0^2 v_{1,X_0} u_{2,X_0X_0} + c_0^2 u_{2,X_0} v_{1,X_0X_0} + \frac{3}{2} c_0^2 (v_{1,X_0})^2 v_{1,X_0X_0}. \quad (7.2)$$

Several terms contain derivatives of v_1 and u_2 with respect to X_1 or t_1. Since v_1 and u_2 are not functions of X_1 or t_1, the equations further reduce to

$$u_{3,t_0t_0} - c_\lambda^2 u_{3,X_0X_0} = -c_0^2 v_{1,X_0} u_{2,X_0X_0}, \tag{7.3}$$

$$\begin{aligned} v_{3,t_0t_0} - c_\tau^2 v_{3,X_0X_0} &= 2c_\tau^2 v_{1,X_0X_2} - 2v_{1,t_0t_2} \\ &\quad + c_0^2 v_{1,X_0} u_{2,X_0X_0} + c_0^2 u_{2,X_0} v_{1,X_0X_0} + \frac{3}{2} c_0^2 (v_{1,X_0})^2 v_{1,X_0X_0}, \end{aligned} \tag{7.4}$$

valid for both sides of the string.

7.1.1 Right Side of String

The first- and second-order solutions for the right side of the string are (6.16) and (6.102), repeated here:

$$\begin{aligned} (v_1)_r &= C_{12} e^{i(k_r X_0 - \sigma t_0)} + C_{12}^* e^{-i(k_r X_0 - \sigma t_0)}, \\ (u_2)_r &= -\frac{ik_r}{4}\left[(C_{12})^2 e^{i2(k_r X_0 - \sigma t_0)} - (C_{12}^*)^2 e^{-i2(k_r X_0 - \sigma t_0)} \right] + \bar{W}_r, \end{aligned}$$

where

$$\bar{W}_r = \begin{cases} 0 & \text{when } t_0 < \left[\frac{X_0}{c_\lambda}\right]_r \\ \bar{U}_r & \text{when } t_0 > \left[\frac{X_0}{c_\lambda}\right]_r \end{cases},$$

$$\begin{aligned} \bar{U}_r = \left[\frac{(EA)_l - (EA)_r}{(EA/c_\lambda)_l + (EA/c_\lambda)_r}\right] \frac{2k_l^2 k_r^2}{(k_l + k_r)^2} \Bigg\{ & (A_0)^2 \frac{1}{i2\sigma}\left[1 - e^{-i2\sigma(t_0 - X_0/c_\lambda)_r}\right] \\ & - (A_0^*)^2 \frac{1}{i2\sigma}\left[1 - e^{i2\sigma(t_0 - X_0/c_\lambda)_r}\right] - 2A_0 A_0^* \left[t_0 - \frac{X_0}{c_\lambda}\right]_r \Bigg\}. \end{aligned}$$

For the right side of the string (7.3) and (7.4) become

$$\begin{aligned} \left[u_{3,t_0t_0} - c_\lambda^2 u_{3,X_0X_0}\right]_r &= c_0^2 k_r^4 \left[C_{12}^3 e^{i3(k_r X_0 - \sigma t_0)} + C_{12}^{*\,3} e^{-i3(k_r X_0 - \sigma t_0)} \right] \\ &\quad - c_0^2 k_r^4 \left[C_{12}^2 C_{12}^* e^{i(k_r X_0 - \sigma t_0)} + C_{12} C_{12}^{*\,2} e^{-i(k_r X_0 - \sigma t_0)} \right] \\ &\quad - i c_0^2 k_r \left[C_{12} e^{i(k_r X_0 - \sigma t_0)} - C_{12}^* e^{-i(k_r X_0 - \sigma t_0)} \right] (\bar{W}_{X_0X_0})_r, \end{aligned} \tag{7.5}$$

where

$$(\bar{W}_{X_0X_0})_r = \begin{cases} 0 & \text{when } t_0 < \left[\frac{X_0}{c_\lambda}\right]_r \\ (\bar{U}_{X_0X_0})_r & \text{when } t_0 > \left[\frac{X_0}{c_\lambda}\right]_r \end{cases},$$

$$(\bar{U}_{X_0X_0})_r = \left[\frac{(EA)_l - (EA)_r}{(EA/c_\lambda)_l + (EA/c_\lambda)_r}\right] \frac{2k_l^2k_r^2}{(k_l+k_r)^2}\left[\frac{i2\sigma}{(c_\lambda^2)_r}\right] * \Big\{ -(A_0)^2 e^{-i2\sigma(t_0 - X_0/c_\lambda)_r} + (A_0^*)^2 e^{i2\sigma(t_0 - X_0/c_\lambda)_r} \Big\}; \quad (7.6)$$

and

$$\begin{aligned}\left[v_{3,t_0t_0} - c_\tau^2 v_{3,X_0X_0}\right]_r = & \\ & + e^{i(k_rX_0 - \sigma t_0)}\left[2ic_\tau^2 k_r \frac{\partial C_{12}}{\partial X_2} + 2ic_\tau k_r \frac{\partial C_{12}}{\partial t_2} - c_0^2 k_r^4 C_{12}^* C_{12}^2\right] \\ & - e^{-i(k_rX_0 - \sigma t_0)}\left[2ic_\tau^2 k_r \frac{\partial C_{12}^*}{\partial X_2} + 2ic_\tau k_r \frac{\partial C_{12}^*}{\partial t_2} + c_0^2 k_r^4 C_{12} {C_{12}^*}^2\right] \\ & + ic_0^2 k_r \left[C_{12} e^{i(k_rX_0 - \sigma t_0)} - C_{12}^* e^{-i(k_rX_0 - \sigma t_0)}\right](\bar{W}_{X_0X_0})_r \\ & - c_0^2 k_r^2 \left[C_{12} e^{i(k_rX_0 - \sigma t_0)} + C_{12}^* e^{-i(k_rX_0 - \sigma t_0)}\right](\bar{W}_{X_0})_r, \quad (7.7)\end{aligned}$$

where

$$(\bar{W}_{X_0})_r = \begin{cases} 0 & \text{when } t_0 < \left[\frac{X_0}{c_\lambda}\right]_r \\ (\bar{U}_{X_0})_r & \text{when } t_0 > \left[\frac{X_0}{c_\lambda}\right]_r \end{cases},$$

$$(\bar{U}_{X_0})_r = \left[\frac{(EA)_l - (EA)_r}{(EA/c_\lambda)_l + (EA/c_\lambda)_r}\right] \frac{2k_l^2k_r^2}{(k_l+k_r)^2}\left[\frac{1}{(c_\lambda)_r}\right] * \Big\{ -(A_0)^2 e^{-i2\sigma(t_0 - X_0/c_\lambda)_r} - (A_0^*)^2 e^{i2\sigma(t_0 - X_0/c_\lambda)_r} + 2A_0A_0^* \Big\}. \quad (7.8)$$

7.1.2 Left Side of String

The second-order solutions for the left side of the string are (6.35) and (6.101), repeated here:

$$(v_1)_l = A_{12}e^{i(k_lX_0 - \sigma t_0)} + A_{12}^* e^{-i(k_lX_0 - \sigma t_0)} + + B_{12}e^{i(k_lX_0 + \sigma t_0)} + B_{12}^* e^{-i(k_lX_0 + \sigma t_0)},$$

$$(u_2)_l = -\frac{ik_l}{4}\Big[(A_{12})^2 e^{i2(k_l X_0 - \sigma t_0)} - (A_{12}^*)^2 e^{-i2(k_l X_0 - \sigma t_0)} + (B_{12})^2 e^{i2(k_l X_0 + \sigma t_0)} - (B_{12}^*)^2 e^{-i2(k_l X_0 + \sigma t_0)}\Big] - \frac{ik_l}{2c_\lambda^2}\big(c_\lambda^2 - c_\tau^2\big)\Big[A_{12}B_{12}e^{i2k_l X_0} - A_{12}^* B_{12}^* e^{-i2k_l X_0}\Big] + \bar{W}_l,$$

where:

$$\bar{W}_l = \begin{cases} 0 & \text{when } t_0 < \Big[-\frac{X_0}{c_\lambda}\Big]_l \\ \bar{U}_l & \text{when } t_0 > \Big[-\frac{X_0}{(c_\lambda}\Big]_l \end{cases},$$

$$\bar{U}_l = \left[\frac{(EA)_l - (EA)_r}{(EA/c_\lambda)_l + (EA/c_\lambda)_r}\right] \frac{2k_l^2 k_r^2}{(k_l + k_r)^2}\Bigg\{(A_0)^2 \frac{1}{i2\sigma}\Big[1 - e^{-i2\sigma(t_0 + X_0/c_\lambda)_l}\Big] - (A_0^*)^2 \frac{1}{i2\sigma}\Big[1 - e^{i2\sigma(t_0 + X_0/c_\lambda)_l}\Big] - 2A_0 A_0^*\Big[t_0 + \frac{X_0}{c_\lambda}\Big]_l\Bigg\},$$

For the left side of the string (7.3) and (7.4) become

$$\begin{aligned}
&\big[u_{3,t_0t_0} - c_\lambda^2 u_{3,X_0X_0}\big]_l = \\
&+c_0^2 k_l^4\Big[A_{12}^3 e^{i3(k_l X_0 - \sigma t_0)} + {A_{12}^*}^3 e^{-i3(k_l X_0 - \sigma t_0)} + B_{12}^3 e^{i3(k_l X_0 + \sigma t_0)} + {B_{12}^*}^3 e^{-i3(k_l X_0 + \sigma t_0)}\Big] \\
&-c_0^2 k^4\Big[(A_{12}^2 A_{12}^* + 2c_1^2 A_{12}B_{12}B_{12}^*)e^{i(k_l X_0 - \sigma t_0)} + (A_{12}{A_{12}^*}^2 + 2c_1^2 A_{12}^* B_{12}B_{12}^*)e^{-i(k_l X_0 - \sigma t_0)} \\
&+(B_{12}^2 B_{12}^* + 2c_1^2 A_{12}A_{12}^* B_{12})e^{i(k_l X_0 + \sigma t_0)} + (B_{12}{B_{12}^*}^2 + 2c_1^2 A_{12}A_{12}^* B_{12}^*)e^{-i(k_l X_0 + \sigma t_0)} \\
&-(A_{12}B_{12}^2 + 2c_1^2 A_{12}B_{12}^2)e^{i(3k_l X_0 + \sigma t_0)} - (A_{12}^* {B_{12}^*}^2 + 2c_1^2 A_{12}^* {B_{12}^*}^2)e^{-i(3k_l X_0 + \sigma t_0)} \\
&-(A_{12}^2 B_{12} + 2c_1^2 A_{12}^2 B_{12})e^{i(3k_l X_0 - \sigma t_0)} - ({A_{12}^*}^2 B_{12}^* + 2c_1^2 {A_{12}^*}^2 B_{12}^*)e^{-i(3k_l X_0 - \sigma t_0)} \\
&+A_{12}^* {B_{12}}^2 e^{i(k_l X_0 + 3\sigma t_0)} + A_{12}{B_{12}^*}^2 e^{-i(k_l X_0 + 3\sigma t_0)} \\
&+A_{12}^2 B_{12}^* e^{i(k_l X_0 - 3\sigma t_0)} + {A_{12}^*}^2 B_{12} e^{-i(k_l X_0 - 3\sigma t_0)}\Big] \\
&-ic_0^2 k_l\Big[A_{12}e^{i(k_l X_0 - \sigma t_0)} - A_{12}^* e^{-i(k_l X_0 - \sigma t_0)} \\
&+B_{12}e^{i(k_l X_0 + \sigma t_0)} - B_{12}^* e^{-i(k_l X_0 + \sigma t_0)}\Big](\bar{W}_{X_0X_0})_l, \quad (7.9)
\end{aligned}$$

where

$$(\bar{W}_{X_0X_0})_l = \begin{cases} 0 & \text{when } t_0 < \left[-\frac{X_0}{c_\lambda} \right]_l \\ (\bar{U}_{X_0X_0})_l & \text{when } t_0 > \left[-\frac{X_0}{c_\lambda} \right]_l \end{cases},$$

$$(\bar{U}_{X_0X_0})_l = \left[\frac{(EA)_l - (EA)_r}{(EA/c_\lambda)_l + (EA/c_\lambda)_r} \right] \frac{2k_l^2 k_r^2}{(k_l + k_r)^2} \frac{i2\sigma}{(c_\lambda^2)_l}$$
$$* \left\{ -(A_0)^2 e^{-i2\sigma(t_0 + X_0/c_\lambda)_l} + (A_0^*)^2 e^{i2\sigma(t_0 + X_0/c_\lambda)_l} \right\}, \quad (7.10)$$

and

$$\begin{aligned}
\left[v_{3,t_0t_0} - c_\tau^2 v_{3,X_0X_0}\right]_l = &+\Bigg[i2c_\tau^2 k_l\left(\frac{\partial A_{12}}{\partial X_2}\right) + i2c_\tau k_l\left(\frac{\partial A_{12}}{\partial t_2}\right)\\
&-c_0^2k_l^4A_{12}^2A_{12}^* + c_0^2k_l^4(c_1^2-3)A_{12}B_{12}B_{12}^*\Bigg]e^{i(k_lX_0-\sigma t_0)}\\
&-\Bigg[i2c_\tau^2 k_l\left(\frac{\partial A_{12}^*}{\partial X_2}\right) + i2c_\tau k_l\left(\frac{\partial A_{12}^*}{\partial t_2}\right)\\
&+c_0^2k_l^4A_{12}{A_{12}^*}^2 - c_0^2k_l^4(c_1^2-3)A_{12}^*B_{12}B_{12}^*\Bigg]e^{-i(k_lX_0-\sigma t_0)}\\
&+\Bigg[i2c_\tau^2 k_l\left(\frac{\partial B_{12}}{\partial X_2}\right) - i2c_\tau k_l\left(\frac{\partial B_{12}}{\partial t_2}\right)\\
&-c_0^2k_l^4B_{12}^2B_{12}^* + c_0^2k_l^4(c_1^2-3)A_{12}A_{12}^*B_{12}\Bigg]e^{i(k_lX_0+\sigma t_0)}\\
&-\Bigg[i2c_\tau^2 k_l\left(\frac{\partial B_{12}^*}{\partial X_2}\right) - i2c_\tau k_l\left(\frac{\partial B_{12}^*}{\partial t_2}\right)\\
&+c_0^2k_l^4B_{12}{B_{12}^*}^2 - c_0^2k_l^4(c_1^2-3)A_{12}A_{12}^*B_{12}^*\Bigg]e^{-i(k_lX_0+\sigma t_0)}\\
&-3c_0^2k_l^4\left(c_1^2-1\right)A_{12}B_{12}^2e^{i(3k_lX_0+\sigma t_0)} - 3c_0^2k_l^4\left(c_1^2-1\right)A_{12}^*{B_{12}^*}^2e^{-i(3k_lX_0+\sigma t_0)}\\
&-3c_0^2k_l^4\left(c_1^2-1\right)A_{12}^2B_{12}e^{i(3k_lX_0-\sigma t_0)} - 3c_0^2k_l^4\left(c_1^2-1\right){A_{12}^*}^2B_{12}^*e^{-i(3k_lX_0-\sigma t_0)}\\
&-c_0^2k_l^4A_{12}^*B_{12}^2e^{i(k_lX_0+3\sigma t_0)} - c_0^2k_l^4A_{12}{B_{12}^*}^2e^{-i(k_lX_0+3\sigma t_0)}\\
&-c_0^2k_l^4A_{12}^2B_{12}^*e^{i(k_lX_0-3\sigma t_0)} - c_0^2k_l^4{A_{12}^*}^2B_{12}e^{-i(k_lX_0-3\sigma t_0)}\\
+ic_0^2k_l&\Big[A_{12}e^{i(k_lX_0-\sigma t_0)} - A_{12}^*e^{-i(k_lX_0-\sigma t_0)} + B_{12}e^{i(k_lX_0+\sigma t_0)} - B_{12}^*e^{-i(k_lX_0+\sigma t_0)}\Big](\bar{W}_{X_0X_0})_l\\
-c_0^2k_l^2&\Big[A_{12}e^{i(k_lX_0-\sigma t_0)} + A_{12}^*e^{-i(k_lX_0-\sigma t_0)} + B_{12}e^{i(k_lX_0+\sigma t_0)} + B_{12}^*e^{-i(k_lX_0+\sigma t_0)}\Big](\bar{W}_{X_0})_l,
\end{aligned} \tag{7.11}$$

where

$$(\bar{W}_{X_0})_l = \begin{cases} 0 & \text{when } t_0 < \left[-\frac{X_0}{c_\lambda}\right]_l \\ (\bar{U}_{X_0})_l & \text{when } t_0 > \left[-\frac{X_0}{c_\lambda}\right]_l \end{cases},$$

$$(\bar{U}_{X_0})_l = \left[\frac{(EA)_l - (EA)_r}{(EA/c_\lambda)_l + (EA/c_\lambda)_r}\right] \frac{2k_l^2 k_r^2}{(k_l + k_r)^2} \frac{1}{(c_\lambda)_l} \\ * \left\{ (A_0)^2 e^{-i2\sigma(t_0 + X_0/c_\lambda)_l} + (A_0^*)^2 e^{i2\sigma(t_0 + X_0/c_\lambda)_l} - 2A_0 A_0^* \right\}, \quad (7.12)$$

$$c_1^2 = \frac{c_0^2}{c_\lambda^2} = \frac{(c_\lambda^2 - c_\tau^2)}{c_\lambda^2}. \quad (7.13)$$

7.2 Secular Terms

Equations (7.5) and (7.9) produce no secular terms. Secular terms in (7.7) and (7.11) are suppressed using the relations,

$$\int_{-\pi}^{\pi} e^{imX} e^{-inX}\, dX = 0, \quad (7.14)$$

for $n \neq m$, and

$$\int_{-\pi}^{\pi} e^{imX} e^{-inX}\, dX = 2\pi, \quad (7.15)$$

for $n = m$, where m and n are integers. Multiply each equation by one of the four secular exponential factors $e^{\pm i(kX_0 \pm \sigma t_0)}$ and integrate over one period. Finally the NLS equations are

$$i2c_\tau k_l \left(\frac{\partial A_{12}}{\partial t_2}\right) + i2c_\tau^2 k_l \left(\frac{\partial A_{12}}{\partial X_2}\right) - c_0^2 k_l^4 {A_{12}}^2 A_{12}^* \\ + c_0^2 k_l^4 (c_1^2 - 3) A_{12} B_{12} B_{12}^* - c_0^2 k_l^2 A_{12} (\bar{N}_l) = 0, \quad (7.16)$$

$$i2c_\tau k_l \left(\frac{\partial B_{12}}{\partial t_2}\right) - i2c_\tau^2 k_l \left(\frac{\partial B_{12}}{\partial X_2}\right) + c_0^2 k_l^4 {B_{12}}^2 B_{12}^* \\ - c_0^2 k_l^4 (c_1^2 - 3) A_{12} A_{12}^* B_{12} + c_0^2 k_l^2 B_{12} (\bar{N}_l) = 0, \quad (7.17)$$

$$i2c_\tau k_r \left(\frac{\partial C_{12}}{\partial t_2}\right) + i2c_\tau^2 k_r \left(\frac{\partial C_{12}}{\partial X_2}\right) - c_0^2 k_r^4 C_{12}^2 C_{12}^* - c_0^2 k_r^2 C_{12} (\bar{N}_r) = 0, \quad (7.18)$$

where

$$\bar{N}_l = \begin{cases} 0 & \text{when } t_0 < \left[-\frac{X_0}{c_\lambda} \right]_l \\ \bar{M}_l & \text{when } t_0 > \left[-\frac{X_0}{c_\lambda} \right]_l \end{cases},$$

$$\bar{N}_r = \begin{cases} 0 & \text{when } t_0 < \left[\frac{X_0}{c_\lambda} \right]_r \\ \bar{M}_r & \text{when } t_0 > \left[\frac{X_0}{c_\lambda} \right]_r \end{cases},$$

with

$$\bar{M}_l = -\left[\frac{(EA)_l - (EA)_r}{(EA/c_\lambda)_l + (EA/c_\lambda)_r} \right] \frac{4k_l^2 k_r^2}{(k_l + k_r)^2} \frac{1}{(c_\lambda)_l} A_0 A_0^*, \tag{7.19}$$

$$\bar{M}_r = \left[\frac{(EA)_l - (EA)_r}{(EA/c_\lambda)_l + (EA/c_\lambda)_r} \right] \frac{4k_l^2 k_r^2}{(k_l + k_r)^2} \frac{1}{(c_\lambda)_r} A_0 A_0^*. \tag{7.20}$$

Chapter 8

SOLUTION

The equations governing the complex amplitudes of the incident, reflected, and transmitted wave packets are (7.16), (7.17), and (7.18) respectively. The interfacial conditions are given by (6.47) through (6.50). The mean longitudinal displacement due to the inhomogeneity in the interfacial conditions is governed by (6.101) through (6.104). These equations will be treated numerically. Before the numerical approximation is discussed, the equations are made dimensionless.

8.1 NLS Equations

All variables are made dimensionless using k_l and $(c_\tau)_l$:

$$\hat{A}_{12} = k_l A_{12}, \tag{8.1}$$

$$\hat{B}_{12} = k_l B_{12}, \tag{8.2}$$

$$\hat{C}_{12} = k_l C_{12}, \tag{8.3}$$

$$\hat{A}_0 = k_l A_0, \tag{8.4}$$

$$\hat{u}_2 = k_l u_2, \tag{8.5}$$

$$\hat{X}_j = k_l X_j, \tag{8.6}$$

$$\hat{t}_j = k_l (c_\tau)_l t_j, \tag{8.7}$$

where the circumflex denotes a dimensionless quantity and the subscript $j = 0, 1, 2$. Note that the dimensionless variables are defined with the string properties from the left side. The dimensionless equations are

$$\left(\frac{\partial \hat{A}_{12}}{\partial \hat{t}_2}\right) + K_0\left(\frac{\partial \hat{A}_{12}}{\partial \hat{X}_2}\right) = -\frac{i}{2}K_1\hat{A}_{12}^2\hat{A}_{12}^* + \frac{i}{2}K_2\hat{A}_{12}\hat{B}_{12}\hat{B}_{12}^* - iK_1\hat{A}_{12}\hat{N}_l, \tag{8.8}$$

$$\left(\frac{\partial \hat{B}_{12}}{\partial \hat{t}_2}\right) - K_0\left(\frac{\partial \hat{B}_{12}}{\partial \hat{X}_2}\right) = \frac{i}{2}K_1\hat{B}_{12}{}^2\hat{B}_{12}^* - \frac{i}{2}K_2\hat{A}_{12}\hat{A}_{12}^*\hat{B}_{12} + iK_1\hat{B}_{12}\hat{N}_l, \tag{8.9}$$

$$\left(\frac{\partial \hat{C}_{12}}{\partial \hat{t}_2}\right) + K_3\left(\frac{\partial \hat{C}_{12}}{\partial \hat{X}_2}\right) = -\frac{i}{2}K_4\hat{C}_{12}{}^2\hat{C}_{12}^* - iK_5\hat{C}_{12}\hat{N}_l, \tag{8.10}$$

where

$$K_0 = \frac{[c_\tau]_l}{[c_\tau]_l} = 1, \tag{8.11}$$

$$K_1 = \left[\frac{c_\lambda^2}{c_\tau^2} - 1\right]_l, \tag{8.12}$$

$$K_2 = \left[\frac{c_\tau^2}{c_\lambda^2} - 2\frac{c_\lambda^2}{c_\tau^2} + 1\right]_l, \tag{8.13}$$

$$K_3 = \frac{[c_\tau]_r}{[c_\tau]_l}, \tag{8.14}$$

$$K_4 = \left[\frac{k_r^3}{k_l^3}\right]\left[\frac{(c_\lambda^2 - c_\tau^2)_l}{(c_\tau)_r(c_\tau)_l}\right], \tag{8.15}$$

$$K_5 = \left[\frac{k_r}{k_l}\right]\left[\frac{(c_\lambda^2 - c_\tau^2)_l}{(c_\tau)_r(c_\tau)_l}\right], \tag{8.16}$$

$$\hat{N}_l = \begin{cases} 0 & \text{when } \hat{t}_0 < -\hat{X}_0\left(\frac{c_\tau}{c_\lambda}\right)_l \\ \hat{M}_l & \text{when } \hat{t}_0 > -\hat{X}_0\left(\frac{c_\tau}{c_\lambda}\right)_l \end{cases},$$

$$\hat{N}_r = \begin{cases} 0 & \text{when } \hat{t}_0 < \hat{X}_0\frac{(c_\tau)_l}{(c_\lambda)_r} \\ \hat{M}_r & \text{when } \hat{t}_0 > \hat{X}_0\frac{(c_\tau)_l}{(c_\lambda)_r} \end{cases},$$

$$\hat{M}_l = K_6\hat{A}_0\hat{A}_0^*, \tag{8.17}$$

$$\hat{M}_r = K_7\hat{A}_0\hat{A}_0^*, \tag{8.18}$$

$$K_6 = -\left[\frac{1 - \frac{(EA)_r}{(EA)_l}}{1 + \frac{(EA)_r\,(c_\lambda)_l}{(EA)_l\,(c_\lambda)_r}}\right]\frac{4\left[\frac{k_r}{k_l}\right]^2}{\left[1 + \frac{k_r}{k_l}\right]^2}, \tag{8.19}$$

$$K_7 = \left[\frac{1 - \frac{(EA)_r}{(EA)_l}}{\frac{(c_\lambda)_r}{(c_\lambda)_l} + \frac{(EA)_r}{(EA)_l}}\right]\frac{4\left[\frac{k_r}{k_l}\right]^2}{\left[1 + \frac{k_r}{k_l}\right]^2}. \tag{8.20}$$

8.2 Interface Mean Longitudinal Displacement

The mean longitudinal displacement is governed by (6.101) through (6.104). Taking the average of (6.101) and (6.102), the oscillatory terms vanish and the interfacial mean longitudinal displacement terms remain. The equations become

$$\bar{u}_2(X_0,t_0)_l = -\frac{ik_l}{2}\left(1-\frac{c_\tau^2}{c_\lambda^2}\right)_l\left[ABe^{i2k_lX_0} - A^*B^*e^{-i2k_lX_0}\right] + \bar{\bar{W}}_l, \tag{8.21}$$

$$\bar{u}_2(X_0,t_0)_r = \bar{\bar{W}}_r, \tag{8.22}$$

where

$$\bar{\bar{W}}_l = \begin{cases} 0 & \text{when } t_0 < \left[-\frac{X_0}{c_\lambda}\right]_l \\ \bar{U}_l & \text{when } t_0 > \left[-\frac{X_0}{c_\lambda}\right]_l \end{cases},$$

$$\bar{\bar{W}}_r = \begin{cases} 0 & \text{when } t_0 < \left[\frac{X_0}{c_\lambda}\right]_r \\ \bar{U}_r & \text{when } t_0 > \left[\frac{X_0}{c_\lambda}\right]_r \end{cases}.$$

Apply (8.1) through (8.7) as before to get the dimensionless equations:

$$\hat{u}_l = -\frac{i}{2}K_8\left[\hat{A}\hat{B}e^{i2\hat{X}} - \hat{A}^*\hat{B}^*e^{-i2\hat{X}}\right] + \hat{W}_l, \tag{8.23}$$

$$\hat{u}_r = \hat{W}_r, \tag{8.24}$$

where

$$K_8 = \left(1-\frac{c_\tau^2}{c_\lambda^2}\right)_l, \tag{8.25}$$

$$\hat{W}_l = \begin{cases} 0 & \text{when } \hat{t} < -\hat{X}\left(\frac{c_\tau}{c_\lambda}\right)_l \\ \hat{U}_l & \text{when } \hat{t} > -\hat{X}\left(\frac{c_\tau}{c_\lambda}\right)_l \end{cases},$$

$$\hat{W}_r = \begin{cases} 0 & \text{when } \hat{t} < \hat{X}\frac{(c_\tau)_l}{(c_\lambda)_r} \\ \hat{U}_r & \text{when } \hat{t} > \hat{X}\frac{(c_\tau)_l}{(c_\lambda)_r} \end{cases},$$

$$\hat{U}_l = K_9 \Bigg\{ (\hat{A}_0^*)^2 \frac{i}{2} \left[1 - e^{i2\left[\hat{t}+\hat{X}(c_\tau/c_\lambda)_l\right]} \right] - (\hat{A}_0)^2 \frac{i}{2} \left[1 - e^{-i2\left[\hat{t}+\hat{X}(c_\tau/c_\lambda)_l\right]} \right] - 2\hat{A}_0\hat{A}_0^* \left[\hat{t} + \hat{X} \left(\frac{c_\tau}{c_\lambda} \right)_l \right] \Bigg\}, \quad (8.26)$$

$$\hat{U}_r = K_9 \Bigg\{ (\hat{A}_0^*)^2 \frac{i}{2} \left[1 - e^{i2\left[\hat{t}-\hat{X}(c_\tau)_l/(c_\lambda)_r\right]} \right] - (\hat{A}_0)^2 \frac{i}{2} \left[1 - e^{-i2\left[\hat{t}-\hat{X}(c_\tau)_l/(c_\lambda)_r\right]} \right] - 2\hat{A}_0\hat{A}_0^* \left[\hat{t} - \hat{X} \frac{(c_\tau)_l}{(c_\lambda)_r} \right] \Bigg\}, \quad (8.27)$$

$$K_9 = \left[\frac{1 - \frac{(EA)_r}{(EA)_l}}{\left[\frac{c_\tau}{c_\lambda}\right]_l + \frac{(EA)_r}{(EA)_l}\frac{(c_\tau)_l}{(c_\lambda)_r}} \right] \frac{2\left[\frac{k_r}{k_l}\right]^2}{\left[1 + \frac{k_r}{k_l}\right]^2}. \quad (8.28)$$

8.3 Parameters

There are four dimensional parameters for each side of the string related to the string properties: the density ρ, the elastic modulus E, the cross section area A, and the initial tension T_0. For the string to be continuous at the interface, the initial tension must be the same on both sides of the string. Furthermore, E and A only appear together as the product EA, and hence may be treated as a single parameter. This leaves five free parameters. In addition, the initial conditions that create the incident wave packet introduce wave number, amplitude, and packet length, as well as the packet shape.

After non-dimesionalization, the material properties are reduced to three dimensionless parameters: the wave speed ratio c_n^2, the density ratio ρ_n, and the elastic-area product ratio $(EA)_n$. These parameter ratios are defined as

$$c_n^2 = \left[\frac{c_\lambda^2}{c_\tau^2} \right]_l, \quad (8.29)$$

$$\rho_n = \frac{\rho_r}{\rho_l}, \tag{8.30}$$

$$(EA)_n = \frac{(EA)_r}{(EA)_l}. \tag{8.31}$$

The wave speed ratio (8.29) relates the longitudinal and transverse wave speeds for the left side of the string where the incident wave packet begins. When the wave speed ratio is unity, the coefficient of the non-linear terms in governing equations, (2.26) and (2.27), is zero. The non-linear terms vanish for the left side of the string.

The wave speed ratio is equal to the reciprocal of the initial strain in the string, since

$$c_n^2 = \frac{c_\lambda^2}{c_\tau^2} = \frac{EA}{T_0}, \tag{8.32}$$

which is found using (2.20) and (2.21). Furthermore,

$$\frac{\delta}{L} = \frac{T_0}{EA} = \frac{1}{c_n^2}, \tag{8.33}$$

where δ is the change in length and L is the initial length of the string. Hence when the wave speed ratio is unity, the string's stretched length would be twice the affected initial length, see Morse [8]. Therefore

$$c_n^2 > 1. \tag{8.34}$$

With the use of (2.21) and (4.9), the density ratio can be related to the wave number ratio by

$$\frac{k_r}{k_l} = \left[\frac{\rho_r}{\rho_l}\right]^{1/2}. \tag{8.35}$$

This allows the reflection and transmission coefficients (4.19) and (4.20) to be written as

$$\hat{\mathcal{R}} = \left[\frac{1 - \frac{k_r}{k_l}}{1 + \frac{k_r}{k_l}}\right], \tag{8.36}$$

$$\hat{\mathcal{T}} = \left[\frac{2}{1 + \frac{k_r}{k_l}}\right]. \tag{8.37}$$

If the density ratio and wave number ratio are equal to zero, then the right side of the string has zero density. This would require that the interface be rigidly fixed. The elastic-area product ratio can only be equal to zero under the circumstance where either the elastic modulus or the cross-sectional area of the right side of the string is zero. Therefore, both ρ_n and $(EA)_n$ must be positive,

$$\rho_n > 0, \tag{8.38}$$

$$(EA)_n > 0. \tag{8.39}$$

All three parameter ratios appear in the coefficients of both the NLS and mean longitudinal displacement equations in various combinations. How the values of these parameters affect the behavior of the equations will be discussed further in the results section.

8.4 Numerical Techniques

For numerical computation, the complex amplitudes $\hat{A}$, $\hat{B}$, and $\hat{C}$ are converted into magnitude and phase using

$$\hat{A} = Re^{i\phi}, \tag{8.40}$$

$$\hat{B} = Se^{i\theta}, \tag{8.41}$$

$$\hat{C} = Pe^{i\psi}. \tag{8.42}$$

Apply (8.40) through (8.42) to (8.8) through (8.10), expand, simplify, and separate into real and imaginary parts to get

$$R_t + K_0 R_X = 0, \tag{8.43}$$

$$S_t - K_0 S_X = 0, \tag{8.44}$$

$$P_t + K_3 P_X = 0, \tag{8.45}$$

$$\phi_t + K_0 \phi_X = -\frac{1}{2} K_1 R^2 + \frac{1}{2} K_2 S^2 - K_1 \tilde{N}_l, \tag{8.46}$$

$$\theta_t - K_0 \theta_X = \frac{1}{2} K_1 R^2 - \frac{1}{2} K_2 S^2 + K_1 \tilde{N}_l, \tag{8.47}$$

$$\psi_t + K_3 \psi_X = -\frac{1}{2} K_4 P^2 - K_3 \tilde{N}_r, \tag{8.48}$$

where

$$\tilde{N}_l = \begin{cases} 0 & \text{when } \hat{t} < -\hat{X}\left(\frac{c_\tau}{c_\lambda}\right)_l \\ \tilde{M}_l & \text{when } \hat{t} > -\hat{X}\left(\frac{c_\tau}{c_\lambda}\right)_l \end{cases},$$

$$\tilde{N}_r = \begin{cases} 0 & \text{when } \hat{t} < \hat{X}\frac{(c_\tau)_l}{(c_\lambda)_r} \\ \tilde{M}_r & \text{when } \hat{t} > \hat{X}\frac{(c_\tau)_l}{(c_\lambda)_r} \end{cases},$$

$$\tilde{M}_l = K_6 R_0^2, \tag{8.49}$$

$$\tilde{M}_r = K_7 R_0^2. \tag{8.50}$$

Use (6.55) and (6.57) to get the relationship between R, S, and P,

$$S = \left[\frac{k_l - k_r}{k_l + k_r}\right] R e^{-i(\phi+\theta)}, \tag{8.51}$$

$$P = \left[\frac{2k_l}{k_l + k_r}\right] R e^{i(\phi-\psi)}. \tag{8.52}$$

Use (8.40) through (8.42) in (8.23), (8.24), (8.26), and (8.27) to obtain

$$\hat{u}_l = K_8 R S \, sin(\phi + \theta + 2\hat{X}) + \hat{W}_l, \tag{8.53}$$

$$\hat{u}_r = \hat{W}_r, \tag{8.54}$$

where

$$\hat{W}_l = \begin{cases} 0 & \text{when } \hat{t} < -\hat{X}\left(\frac{c_\tau}{c_\lambda}\right)_l \\ \hat{U}_l & \text{when } \hat{t} > -\hat{X}\left(\frac{c_\tau}{c_\lambda}\right)_l \end{cases},$$

$$\hat{W}_r = \begin{cases} 0 & \text{when } \hat{t} < \hat{X}\frac{(c_\tau)_l}{(c_\lambda)_r} \\ \hat{U}_r & \text{when } \hat{t} > \hat{X}\frac{(c_\tau)_l}{(c_\lambda)_r} \end{cases},$$

$$\hat{U}_l = K_9\left[R_0^2\left(sin(2\phi_0) + sin\Big[2\big(\hat{t} + \hat{X}(c_\tau/c_\lambda)_l - \phi_0\big)\Big]\right) - 2R_0^2\left[\hat{t} + \hat{X}\left(\frac{c_\tau}{c_\lambda}\right)_l\right]\right], \tag{8.55}$$

$$\hat{U}_r = K_9\left[R_0^2\left(sin(2\phi_0) + sin\Big[2\big(\hat{t} - \hat{X}(c_\tau)_l/(c_\lambda)_r - \phi_0\big)\Big]\right) - 2R_0^2\left[\hat{t} - \hat{X}\frac{(c_\tau)_l}{(c_\lambda)_r}\right]\right], \tag{8.56}$$

where subsrpcipt 0 again refers to the value at $X = 0$.

Equations (8.43) through (8.48) are solved using a two-step Lax Wendroff method, see Ames [18], for linear terms and the third-order Adams Bashforth method, see Gear [19], for non-linear terms. All interior points are treated with a central difference scheme, for example (8.43) and (8.46) are discretized as

$$R_{i,\,j+1} = R_{i,\,j} - \frac{1}{2}K_0\frac{\Delta t}{\Delta x}\big(R_{i+1,\,j} - R_{i-1,\,j}\big) + \frac{1}{2}\left(K_0\frac{\Delta t}{\Delta x}\right)^2\big(R_{i+1,\,j} - 2R_{i,\,j} + R_{i-1,\,j}\big), \tag{8.57}$$

$$\begin{aligned}\phi_{i,\,j+1} = \phi_{i,\,j} - \frac{1}{2}K - 0\frac{\Delta t}{\Delta x}(\phi_{i+1,\,j} - \phi_{i-1,\,j}) \\ + \frac{1}{2}\left(K_0\frac{\Delta t}{\Delta x}\right)^2\big(\phi_{i+1,\,j} - 2\phi_{i,\,j} + \phi_{i-1,\,j}\big) \\ - \frac{\Delta t}{48}K_1\big(55R_{i,\,j}^2 - 59R_{i,\,j-1}^2 + 37R_{i,\,j-2}^2 - 9R_{i,\,j-3}^2\big) \\ + \frac{\Delta t}{48}K_2\big(55S_{i,\,j}^2 - 59S_{i,\,j-1}^2 + 37S_{i,\,j-2}^2 - 9S_{i,\,j-3}^2\big),\end{aligned} \tag{8.58}$$

where $i,\ j$ are the space and time grid points, respectively.

At the interface (the right boundary point) an upwind scheme was used, for example (8.43) and (8.46) are discretized as

$$R_{i,\,j+1} = R_{i,\,j} - \frac{1}{2}K_0\frac{\Delta t}{\Delta x}\big(R_{i,\,j} - R_{i-1,\,j}\big) + \frac{1}{2}\left(K_0\frac{\Delta t}{\Delta x}\right)^2\big(R_{i,\,j} - 2R_{i-1,\,j} + R_{i-2,\,j}\big), \quad (8.59)$$

$$\begin{aligned}\phi_{i,\,j+1} = \phi_{i,\,j} - \frac{1}{2}K - 0\frac{\Delta t}{\Delta x}(\phi_{i,\,j} - \phi_{i-1,\,j}) \\ + \frac{1}{2}\left(K_0\frac{\Delta t}{\Delta x}\right)^2\big(\phi_{i,\,j} - 2\phi_{i-1,\,j} + \phi_{i-2,\,j}\big) \\ - \frac{\Delta t}{48}K_1\big(55R^2_{i,\,j} - 59R^2_{i,\,j-1} + 37R^2_{i,\,j-2} - 9R^2_{i,\,j-3}\big) \\ + \frac{\Delta t}{48}K_2\big(55S^2_{i,\,j} - 59S^2_{i,\,j-1} + 37S^2_{i,\,j-2} - 9S^2_{i,\,j-3}\big). \quad (8.60)\end{aligned}$$

Simulations use 2000 spatial points on each side of the string with $\Delta X = 0.01$. The time step chosen is $\Delta t = .005$. A raised cosine curve is used for the incident wave packet. The wave packet consists of 8 individual waves, see Figure 8.1.

8.5 Strain

The strain in the string can be directly calculated using (2.9) repeated here

$$\epsilon = \left[(1 + u_X)^2 + v_X^2\right]^{1/2} - 1.$$

Use the binomial series expansion and retaining up to cubic terms for the fractional exponent gives

$$\epsilon = u_X + \frac{1}{2}v_X^2 - \frac{1}{2}u_X v_X^2 + \cdots. \quad (8.61)$$

As before expand the displacements using the slow scales (5.1) and (5.2) to get

$$u = \varepsilon u_1 + \varepsilon^2 u_2 + \varepsilon^3 u_3 + \cdots, \quad (8.62)$$

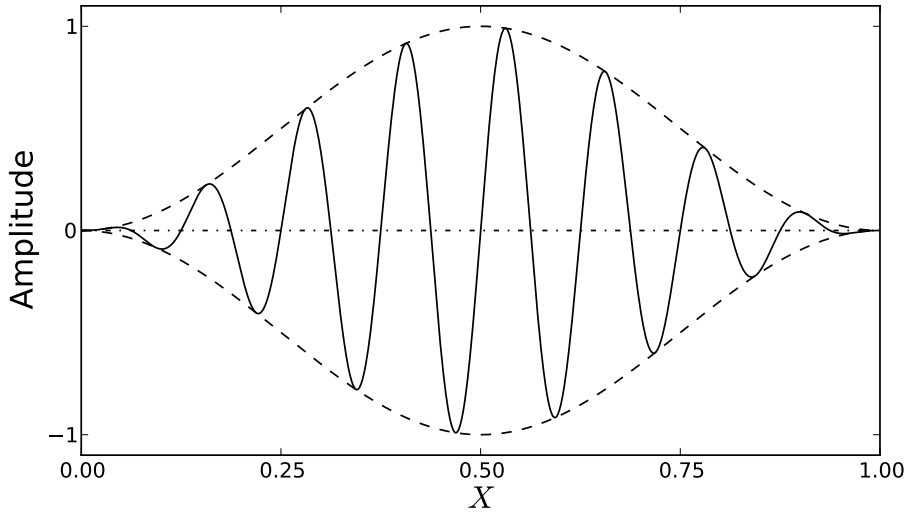

Figure 8.1: Wave packet showing raised cosine envelope (dashed line) and individual waves (solid line).

$$v = \varepsilon v_1 + \varepsilon^2 v_2 + \varepsilon^3 v_3 + \cdots. \tag{8.63}$$

Take the derivatives and group by powers of ε gives

$$u_X = \varepsilon u_{1,X_0} + \varepsilon^2(u_{2,X_0} + u_{1,X_1}) + \varepsilon^3(u_{3,X_0} + u_{2,X_1} + u_{1,X_2}) + \cdots, \tag{8.64}$$

$$v_X = \varepsilon v_{1,X_0} + \varepsilon^2(v_{2,X_0} + v_{1,X_1}) + \varepsilon^3(v_{3,X_0} + v_{2,X_1} + v_{1,X_2}) + \cdots. \tag{8.65}$$

For both sides of the string it was determined that

$$u_1 = 0, \tag{8.66}$$

$$v_2 = 0. \tag{8.67}$$

and it was also determined that u_2 and v_2 are not functions of X_1 and since the third-order solution u_3 and v_3 is not sought, the strain can be simplified as

$$\epsilon = \varepsilon^2\left(\frac{1}{2}v_{1,X_0}^2 + u_{2,X_0}\right). \tag{8.68}$$

Non-dimensionalize and separate the wave amplitudes coefficents A, B, and C into magnitude and phase components gives the following expressions

$$(v_{1,X_0})_l^2 = -\Big[2R^2 cos\big(2\phi + 2(X_0 - t_0)\big) + 2S^2 cos\big(2\theta + 2(X_0 + t_0)\big) + RScos\big(\phi + \theta + 2X_0\big) + RScos\big(\phi - \theta - 2t_0\big) - 2R^2 - 2S^2\Big], \quad (8.69)$$

$$(u_{2,X_0})_l = \Big[R^2 cos\big(2\phi + 2(X_0 - t_0)\big) + S^2 cos\big(2\theta + 2(X_0 - t_0)\big) + K_8\Big[2RScos(\phi + \theta + 2X_0)\Big] + (\hat{W}_{X_0})_l. \quad (8.70)$$

Chapter 9

RESULTS

Three free dimensionless parameters emerge from the non-dimensional equations: the wave speed ratio c_n^2, the density ratio ρ_n, and the elastic-area product ratio $(EA)_n$. While these parameters are present in several of the coefficients in the governing equations, each parameter can be connected to a physical process that it approximately controls. The wave speed ratio c_n^2 primarily sets the relationship between the transverse waves and the longitudinal interfacial mean longitudinal displacement. The density ratio ρ_n has the major effect upon the magnitudes of the reflected and transmitted waves. The elastic-area product ratio $(EA)_n$ has the major effect upon the mean longitudinal displacement when incident, reflected, and transmitted waves are acting near the interface.

A choice of unity for any of the three dimensionless parameters have unique consequences for the results. For example, when c_n^2 is unity many coefficients vanish, causing the non-linear terms in the NLS equations to vanish, see (8.12), (8.13), (8.15), and (8.16). When ρ_n is unity, the reflection coefficient is zero and the transmission coefficient is unity, see (4.19) and (4.20). As a result, there is no reflected wave and the transmitted wave is identical to the incident wave in shape and amplitude; the incident wave passes through the interface unchanged. When $(EA)_n$ is unity, the interfacial part of the mean longitudinal displacement becomes zero. Hence careful choice of the parameters can be used to select particular cases.

9.1 A Typical Case (Case T1)

Choose

$$c_n^2 = 16.0, \tag{9.1}$$

$$\rho_n = 0.4, \tag{9.2}$$

$$(EA)_n = 0.5. \tag{9.3}$$

This is called Case T1. For this case both ρ_n and $(EA)_n$ on the left side of the string are greater than the corresponding values on the right side. Thus the left side is more dense and stiffer.

The results for this case are shown in Figures 9.1, 9.2, and 9.3. Figure 9.1 has three sub-figures, each representing a single time. Figure 9.1a corresponds to a time prior to the incident wave reaching the interface, Figure 9.1b corresponds to a time when the incident wave is transiting the interface, and Figure 9.1c corresponds to a time when the reflected and transmitted waves have disengaged fully from the interface.

Each sub-figure has three panels. The top panel shows the wave magnitude versus horizontal position. The incident wave (solid line) and reflected wave (dashed line) are shown on the left side of the string and the transmitted wave (solid line) is shown on the right side of the string. The second or middle panel shows the wave phase versus horizontal position. The third or bottom panel shows the mean longitudinal displacement. Note that the mean displacement is a *longitudinal* displacement, despite being plotted vertically. The interface is shown as a vertical dash-dot line in the center of each panel. This same combination of time values and panels will be used again for other cases.

The mean longitudinal displacement is zero before the incident wave packet has reached the interface, and after the incident waves have disappeared and been con-

verted into reflected and transmitted waves, as shown in the third panel of Figures 9.1a and 9.1c. This mean longitudinal displacement is only nonzero when the wave packet is interacting with the interface, as shown in Figure 9.1b.

This result may also be inferred directly from equations (6.101) and (6.102). The mean longitudinal displacement for the left side of the string is given by (6.101) and has two components. One component is proportional to $e^{i2k_l X_0}$, and this component depends on the presence of both the incident and reflected waves acting simultaneously. This oscillatory mean longitudinal displacement is a result of direct interaction between the incident and reflected waves. If either the incident wave or reflected wave packets do not exist, then this component is zero. The oscillatory component of the mean is evident in Figure 9.1b for $\bar{X} < 0$ as very fine-scale oscillations. The wavelength of this oscillation is always half the wavelength of the incident waves (or twice the wave number).

The other component is $\bar{W}_l$, which is the mean longitudinal displacement due to the inhomogeneity in the interfacial conditions. The right side only has one component $\bar{W}_r$ (no oscillatory part), also due to this interfacial effect. This interfacial mean longitudinal displacement is only nonzero when the incident waves are exciting the interface, e.g. when $A_0 \neq 0$.

Figure 9.2 shows the development with time of the mean longitudinal displacement. Given in Figure 9.2 are mean longitudinal displacement profiles at a sequence of times, each profile shifted by a fixed value merely for display purposes. It is evident in Figure 9.2 that this mean longitudinal displacement expands outward from the interface as the incident wave begins to interact with the interface. The extent of this mean longitudinal displacement is therefore not the same as the incident wave packet length, as in many other nonlinear wave systems. The mean longitudinal displacement length is related to the incident wave packet length only in the sense

of the time associated with the incident wave packet to interact with the interface. This mean longitudinal displacement length or span of longitudinal influence directed outward in both directions from the interface is determined by this time along with the longitudinal wave speed, c_λ.

The interfacial component of the mean longitudinal displacement appears to be comprised of two parts, clearly evident in Figure 9.2. One part is the broad shape that continues to grow with time. The other part is a narrower effect that results in a peaked shape at the interface. These two parts can be clearly distinguished in the expressions for $\bar{W}$ in (8.26) and (8.27). Both effects are due to the quadratic contributions of v_1^2 for both sides of the string. Since $(v_1)_l$ is the sum of the incident and reflected waves (and their complex conjugates), then $(v_1^2)_l$ consists of squares of the amplitudes of the incident and reflected waves A_0^2 and A_0^{*2}, and cross terms $2A_0A_0^*$. The A_0^2 and A_0^{*2} terms are responsible for the oscillatory part of the interfacial mean longitudinal displacement, and the frequency of oscillation is twice the incident wave frequency. The cross product $A_0A_0^*$ contributes a linear variation with position (as an increase on the left side). Both contributions have compact support. Note in Figure 9.2 that combination of oscillatory and linear components of the interfacial mean longitudinal displacement results in a relatively large displacement of the interface.

There are two curves in Figure 9.3. A solid line shows the maximum mean longitudinal displacement versus time. A dashed line shows the mean longitudinal displacement at the interface position. Figure 9.3 shows that overall, the largest mean longitudinal displacements occur when the incident wave packet is nearly centered at the interface. Also the fluctuations are slightly smaller at the interface (dashed line), e.g. the interface is not the location of the maximum mean longitudinal displacement.

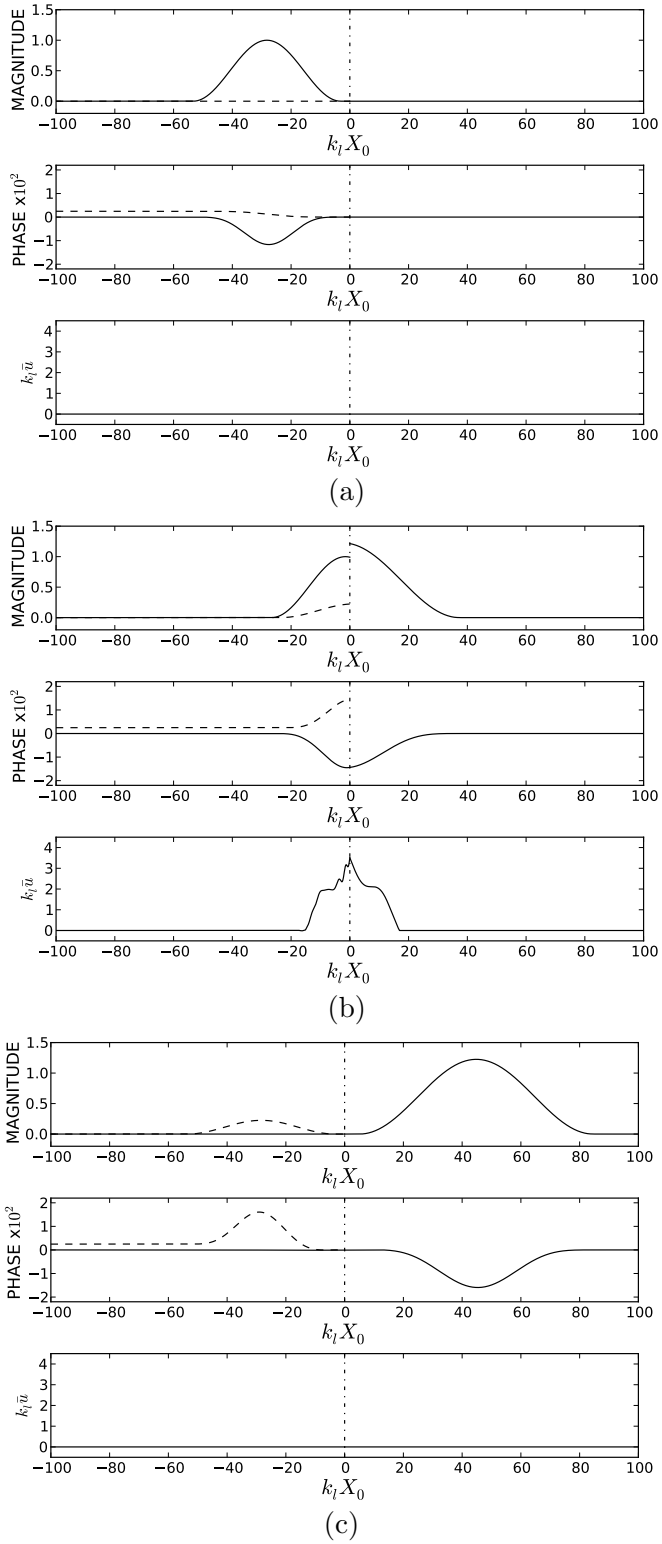

Figure 9.1: Case T1: Results with parameter settings of $\rho_n = 0.4$, $(EA)_n = 0.5$, and $c_n^2 = 16.0$, at times of (a) $\hat{t} = 3.10$, (b) $\hat{t} = 3.82$, and (c) $\hat{t} = 4.54$.

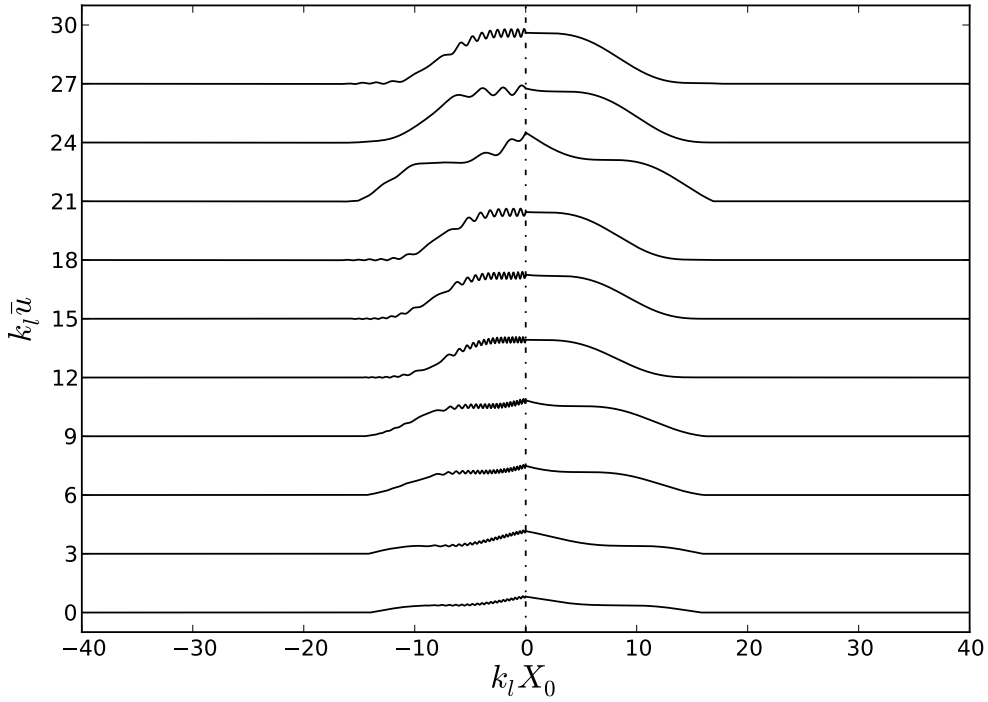

Figure 9.2: Case T1: Mean longitudinal displacement evolution versus time from $\hat{t} = 3.10$ (bottom) through $\hat{t} = 3.90$ (top) in increments of $\Delta\hat{t} = 0.08$ each separated by 3.0 units vertically.

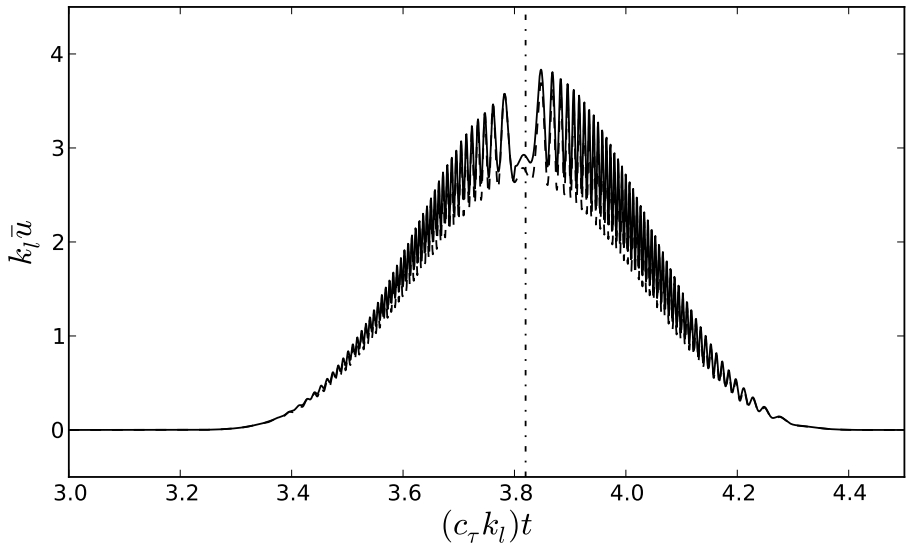

Figure 9.3: Case T1: Mean maximum vs. time plot - solid line is maximum mean longitudinal displacement and dashed line is the mean longitudinal displacement at the interface location.

9.2 $\rho_n = (EA)_n = 1$ (Case 1)

Now choose

$$\rho_n = 1.0, \tag{9.4}$$

$$(EA)_n = 1.0, \tag{9.5}$$

but allow c_n^2 to have a sequence of values. This is called Case 1. Table 9.1 lists the parameters for this sequence. Results for Case 1 are shown in Figures 9.4 through 9.7.

When ρ_n is unity, the reflection coefficient is zero and the transmission coefficient is unity. Therefore there are no reflected waves for Case 1 and the transmitted wave packet has the same magnitude and shape as the incident wave packet. Since $(EA)_n$ is also chosen to be unity, this becomes a special case where the material properties for both sides of the string are the same and the incident wave passes through the interface with no change. The mean longitudinal displacement for this case is also zero.

Table 9.1: Parameter Test Case 1

Case	ρ_n	$(EA)_n$	c_n^2	$\hat{u}_2$ max.
1a	1.0	1.0	1.0	0
1b	1.0	1.0	4.0	0
1c	1.0	1.0	9.0	0
1d	1.0	1.0	16.0	0

If c_n^2 is also chosen to be unity, then the nonlinear terms are zero (Case 1a), and this case is shown in Figure 9.4. This is equivalent to the linear case for a string with constant properties everywhere. Figure 9.4 shows results at three time values,

as before. The third panel for each time shows the mean longitudinal displacement, which is zero for this case. The first and second panels show the magnitude and phase. Clearly for this case the wave packet moves to the right with the transverse wave speed c_τ and no other change, as expected.

Figures 9.5 through 9.7 (Cases 1b and 1c) show results with $c_n^2 \neq 1$. Since ρ_n and $(EA)_n$ are unity, there is still no reflected wave packet and the mean longitudinal displacement is zero. However, with $c_n^2 \neq 1$, the nonlinear effects are nonzero. Figures 9.5 through 9.7 show that the magnitude of the wave packet is unaffected by the nonlinearity for these sub-cases, and the only difference between the linear and nonlinear cases is the phase, which now develops a variation within the wave packet, and this variation becomes increasingly rapid with time. A larger value of c_n^2 means the rate of increase of this variation is faster, as can be seen by contrasting Figures 9.5 through 9.7. This result can be inferred directly from (8.43) through (8.48).

9.3 $(EA)_n = 1, c_n^2 = 4$ (Case 2)

Now choose

$$(EA)_n = 1.0, \tag{9.6}$$

$$c_n^2 = 4.0, \tag{9.7}$$

along with a sequence of values of ρ_n, and call this Case 2. The choice of $c_n^2 = 4$ is merely for convenience, as the phase for this choice is less congested. Table 9.2 shows the parameter values for Case 2, and results are shown in Figures 9.8 through 9.19.

For Cases 2a and 2b, ρ_n is less than one which makes the right side of the string less dense than the left. This causes the reflected waves to be smaller and the transmitted waves to be larger in magnitude than the incident waves, as can

Table 9.2: Parameter Test Case 2

Case	ρ_n	$(EA)_n$	c_n^2	$\hat{u}_2$ max.
2a	0.25	1.0	4.0	0.24
2b	0.75	1.0	4.0	0.05
2c	1.5	1.0	4.0	0.07
2d	2.0	1.0	4.0	0.13

be seen in the top panels of sub-figures in Figure 9.8. The third panel in Figure 9.8b shows that the mean longitudinal displacement is weak but non-zero. Figure 9.9 gives more profiles of this mean longitudinal displacement. The interfacial part of the mean longitudinal displacement with $(EA)_n = 1$ is zero, hence the mean longitudinal displacement shown in Figures 9.8 and 9.9 contains only the direct interaction between the incident and reflected waves on the left side. This feature makes Case 2 a special case.

Figure 9.10 shows the maximum displacement with time as the packet interacts with the interface. There is a maximum in the displacement that occurs when the packet is centered near the interface. However when the packet is very nearly centered on the interface, the mean longitudinal displacement decreases briefly. This brief effect is due to the symmetry that exists only when the incident wave packet is centered, nearly cancelling this part of the mean longitudinal displacement.

Case 2b, shown in Figures 9.11 through 9.13, only differs in the value of ρ_n, now larger but still less than unity. Figures 9.11 through 9.13 show that the results closely match the results of case 2a in Figures 9.8 through 9.10. The significant differences are that the reflected wave is much weaker for case 2b, and as a result the mean longitudinal displacement is also much weaker, but otherwise has the same character. Thus as ρ_n approaches unity, the result quickly approach the behavior

shown in Case 1.

For Cases 2c and 2d, see Figures 9.14 and 9.17, ρ_n is greater than one, which now makes the right side of the string more dense than the left and causes the reflected wave and the transmitted wave to be smaller in magnitude than the incident wave. As ρ_n increases from unity, the mean longitudinal displacement oscillations on the left side of the string grow larger. Reflected and transmitted waves are present and both reflected and transmitted wave magnitudes are smaller than the incident wave.

Three conclusions can be drawn from the results of the ρ_n variation in this case and from the data in Table 9.3.

1. For $\rho_n > 1$: The left side of string is more dense than the right. The incident wave upon reaching the interface causes both reflected and transmitted waves. In the limit as $\rho_n \to \infty$, the magnitude of the reflected wave approaches unity at 180° out of phase and the magnitude of the transmitted wave approaches zero.

2. For $\rho_n = 1$: Both sides of the string have the same density. The incident wave upon reaching the interface continues to pass through with no change in magnitude or shape and there is no reflected wave created.

3. For $\rho_n < 1$: The right side of string is more dense than the left. The incident wave upon reaching the interface causes both reflected and transmitted waves. In the limit as $\rho_n \to 0$, the magnitude of the reflected wave approaches unity and the magnitude of the transmitted wave approaches a value twice that of the incident wave.

Table 9.3: Density and Wave Number Ratio Comparison

Density Ratio	Wave Number Ratio	Reflection Coefficient	Transmission Coefficient
$(\rho_r/\rho_l)^{1/2}$	k_r/k_l	$\mathcal{R}$	$\mathcal{T}$
0	0	1.0	2.0
.25	0.5	0.3333	1.3333
.50	0.7071	0.1716	1.1716
.75	0.8667	0.0718	1.0718
1.0	1.0	0	1.0
1.25	1.1180	-0.0557	0.9443
1.50	1.2247	-0.1010	0.8990
1.75	1.3229	-0.1390	0.8610
2.0	1.4142	-0.1716	0.8284
10	3.1623	-0.5195	0.4805
100	10	-0.8182	0.1818
1000	31.6228	-0.9387	0.0613
1000000	1000	-0.9980	0.0020
$+\infty$	$+\infty$	-1.0	0

9.4 $\rho = 1, c_n^2 = 4$ (Case 3)

Choose

$$\rho_n = 1.0, \tag{9.8}$$

$$c_n^2 = 4.0, \tag{9.9}$$

along with a sequence of values of $(EA)_n$. This is called Case 3. Once again the choice of $c_n^2 = 4$ is made for convenience, so that the phase is less congested. Table 9.4 shows the parameter values for Case 3. This table also includes the span of influence lengths on both sides of the interface of the mean longitudinal displacement under the columns ($\hat{X}$ min.) and ($\hat{X}$ max.). Results are shown in Figures 9.20 through 9.31.

With the choice $\rho_n = 1$ the reflection coefficient is zero and there are no reflected waves. Since there is no reflected waves, the magnitude of the incident waves are unchanged by interaction with the interface. This is seen for Case 3a in Figure 9.20. The top panels of each sub-figure of Figure 9.20 show that the wave packet merely moves to the right without any significant evolution is shape. However, the mean longitudinal displacement is not zero as the wave packet interacts with the interface, as can be seen in the third panel of Figure 9.20b. More profiles of the mean longitudinal displacement are shown together in Figure 9.21, as before. This mean longitudinal displacement is purely due to the interfacial inhomogeneity, but does show both parts, including the oscillatory component. Figure 9.22 shows the maximum of the mean longitudinal displacement, indicating again that the maximum mean longitudinal displacement occurs when the packet is nearly centered on the interface. Case 3a has $(EA)_n < 1$. With such values, the coefficient of the mean longitudinal displacement K_9 is positive, and the mean longitudinal displacement is positive on both sides of the interface. This corresponds to a nonuniform shift to the right of the region near the interface.

Case 3b only differs from Case 3a in its value for $(EA)_n$, now being $(EA)_n = 0.75$, closer to unity. The results for Case 3b are shown in Figures 9.23 through 9.25, and are generally the same as Case 3a, except now the mean longitudinal displacement is weaker. As with Case 3a, $(EA)_n < 1$ and the mean longitudinal displacement is

positive everywhere, as shown in Figure 9.25. As $(EA)_n \to 1$, the mean longitudinal displacement gets progressively weaker, being zero with $(EA)_n = 1$, as discussed above.

With $(EA)_n > 1$, the value of K_9 is negative and the mean longitudinal displacement is also negative. For example, Case 3c has $(EA)_n = 1.5$ and results are shown in Figures 9.26 through 9.28. Figure 9.26 shows that the wave packet still propagates to the right with no significant changes, other than an increase in the oscillations in phase. However the mean longitudinal displacement in Figure 9.26b, also shown in Figure 9.28, is everywhere negative. This negative mean longitudinal displacement is a shift to the left. Thus in general, when the stiffness increases across the interface, the mean longitudinal displacement is negative, indicating a shift toward the source of the waves. Case 3d shows similar results to Case 3c, as $(EA)_n$ grows larger away from unity, the mean longitudinal displacement becomes greater in the negative direction, see Figures 9.29 through 9.31.

Table 9.4: Parameter Test Case 3

Case	ρ_n	$(EA)_n$	c_n^2	$\hat{u}_2$ max/min.	$\hat{X}$ min.	$\hat{X}$ max.
3a	1.0	0.25	4.0	4.44	-7.8	3.6
3b	1.0	0.75	4.0	1.16	-7.8	6.7
3c	1.0	1.5	4.0	-1.91	-7.8	8.9
3d	1.0	2.0	4.0	-3.69	-7.8	10.6

9.5 $\rho \neq 1, (EA)_n \neq 1, c_n^2 = 4$ (Cases 4, 5, and 6)

Cases 4, 5, and 6 treat values of ρ_n and $(EA)_n$ that are not unity. Again $c_n^2 = 4$ for convenience.

Table 9.5: Parameter Test Case 4, 5, 6

Case	ρ_n	$(EA)_n$	c_n^2	$\hat{u}_2$ max/min.	$\hat{X}$ min.	$\hat{X}$ max.
4a	0.3	0.3	4.0	2.33	-11.0	7.8
4b	0.3	0.7	4.0	0.99	-11.0	11.0
4c	0.7	0.3	4.0	3.51	-7.8	4.8
4d	0.7	0.7	4.0	1.26	-7.8	7.8
5a	1.3	0.4	4.0	3.49	-7.8	4.4
5b	1.8	0.7	4.0	1.61	-7.8	5.0
5c	0.4	1.3	4.0	-0.90	-8.8	13.3
5d	0.7	1.8	4.0	-2.78	-7.8	12.2
6a	1.3	1.3	4.0	-1.19	-7.8	7.8
6b	1.3	1.8	4.0	-3.20	-7.8	8.8
6c	1.8	1.3	4.0	-1.30	-7.8	6.6
6d	1.8	1.8	4.0	-3.34	-7.8	7.8

Case 4 has both ρ_n and $(EA)_n$ less than unity, making the left side of the string more dense and stiffer than the right side. Results are shown in Figures 9.32 through 9.43. This case has reflected and transmitted waves, as well as nonzero mean longitudinal displacement. As before, since $\rho_n < 1$, the transmitted wave is larger than the incident wave while the reflected wave is smaller. Also, the mean longitudinal displacement due to the direct interaction is not zero, and since $(EA)_n < 1$, the interfacial mean longitudinal displacement is positive. Case 4a has $\rho_n = (EA)_n = 0.3$ and results are shown in Figures 9.32 through 9.34. Overall the results agree with the previous cases that isolated the effects of the parameters. However the mean longitudinal displacement now includes all components and is therefore more complex,

as shown in Figure 9.36. Furthermore, the maximum mean longitudinal displacement shown in Figure 9.37 indicates that the oscillations in the mean longitudinal displacement are larger after the wave packet has passed the time when it would be centered on the interface.

Cases 4b, 4c, and 4d are shown in Figures 9.35 through 9.43, all with values of ρ_n and $(EA)_n$ that are less than unity. The results are similar to Case 4a, and indicate that as these parameters approach unity, the mean longitudinal displacement becomes weaker. Some combinations of parameters produce unusual patterns in the mean longitudinal displacement, for example Case 4c with $\rho_n = 0.7$ and $(EA)_n = 0.3$, results shown in Figure 9.38, indicates a very narrow region at the interface where the mean longitudinal displacement is quite large, and an even narrow peak at the interface location.

Case 6 has both ρ_n and $(EA)_n$ greater than unity, making the left side of the string less dense and less stiff than the right side. Results are shown in Figures 9.56 through 9.67. Here $(EA)_n > 1$ causes the mean longitudinal displacement to be negative, as before. The transmitted waves are larger than the incident waves, and the reflected wave is small. This makes the oscillatory part of the mean longitudinal displacement very small and difficult to discern in Figures 9.56 through 9.67.

Finally, Case 5 uses a combination of values ρ_n and $(EA)_n$, with one greater and the other less than unity. In all these cases, the value of $(EA)_n$ controlled the sign of the mean longitudinal displacement, despite a value of ρ_n that was greater or less than unity, see Figures 9.44 through 9.55.

9.6 A sequence of c_n^2 values (Case 7)

Now choose

$$\rho_n = 0.25, \tag{9.10}$$

$$(EA)_n = 0.5, \tag{9.11}$$

this being a typical case with the left side of the string more dense and stiff than the right side. The c_n^2 value is allowed to be varied, this is called Case 7. Table 9.6 gives the parameter values and a summary of the results of mean longitudinal displacement and strain. The mean longitudinal displacement along with the transverse displacement create an associated strain in the string. The strain is calculated directly from (2.9) using values of $\hat{u}_2$ and $\hat{v}_1$ for each time step in the numerical program.

The results for Case 7 are shown in Figures 9.68 through 9.87. As $\rho_n < 1$, then the transmitted wave is larger than the incident wave and the reflected wave is smaller. The mean longitudinal displacement has all parts non-zero. This can be seen in Figures 9.68 through 9.70 for Case 7a. The strain for this case is shown in Figures 9.71 and 9.72. Figure 9.71 indicates that the largest values of strain for this case occur on the left of the interface, and are due to the fine-scale oscillations that result when the incident and transmitted waves exist simultaneously. The effect of the mean longitudinal displacement is relatively small for Case 7a.

Case 7b has $c_n^2 = 9$, larger than Case 7a, and results for this case are shown in Figures 9.73 through 9.77. The behavior of the wave packet is not significantly different here, but the strain is larger, as shown in Figures 9.72 and 9.77.

Figure 9.76 shows that the fine-scale oscillations are still responsible for the largest values of the strain, despite a significant larger contribution from the mean longitudinal displacement as shown in Figure 9.74. It seems in general true that the largest

Table 9.6: Parameter Test Case 7

Case	ρ_n	$(EA)_n$	c_n^2	$\hat{u}_2$ max/min.	$\hat{X}$ min.	$\hat{X}$ max.	Strain max.
7a	.25	.5	4.0	1.49	-7.8	11.0	15.3
7b	.25	.5	9.0	2.39	-13.3	15.5	46.6
7c	.25	.5	16.0	3.17	-15.5	21.7	91.8
7d	.25	.5	25.0	3.93	-18.9	26.7	151.0

strains are due not to the interfacial part of the mean longitudinal displacement, but to these fine-scale oscillations in the mean longitudinal displacement. Also note in Figure 9.77 that largest overall values of the strain occur after the center of the wave packet has passed through the interface. Cases 7c and 7d, with even larger values of c_n^2, shows the same general trends in the strain and of the mean longitudinal displacement. In general it may be concluded that as the wave speed increases, the mean longitudinal displacement and the strain also increase. It can also be concluded that as seen in the Case 7 set of graphs and in Table 9.6 the span of influence to the left and right of the interface also increases with larger values of c_n^2.

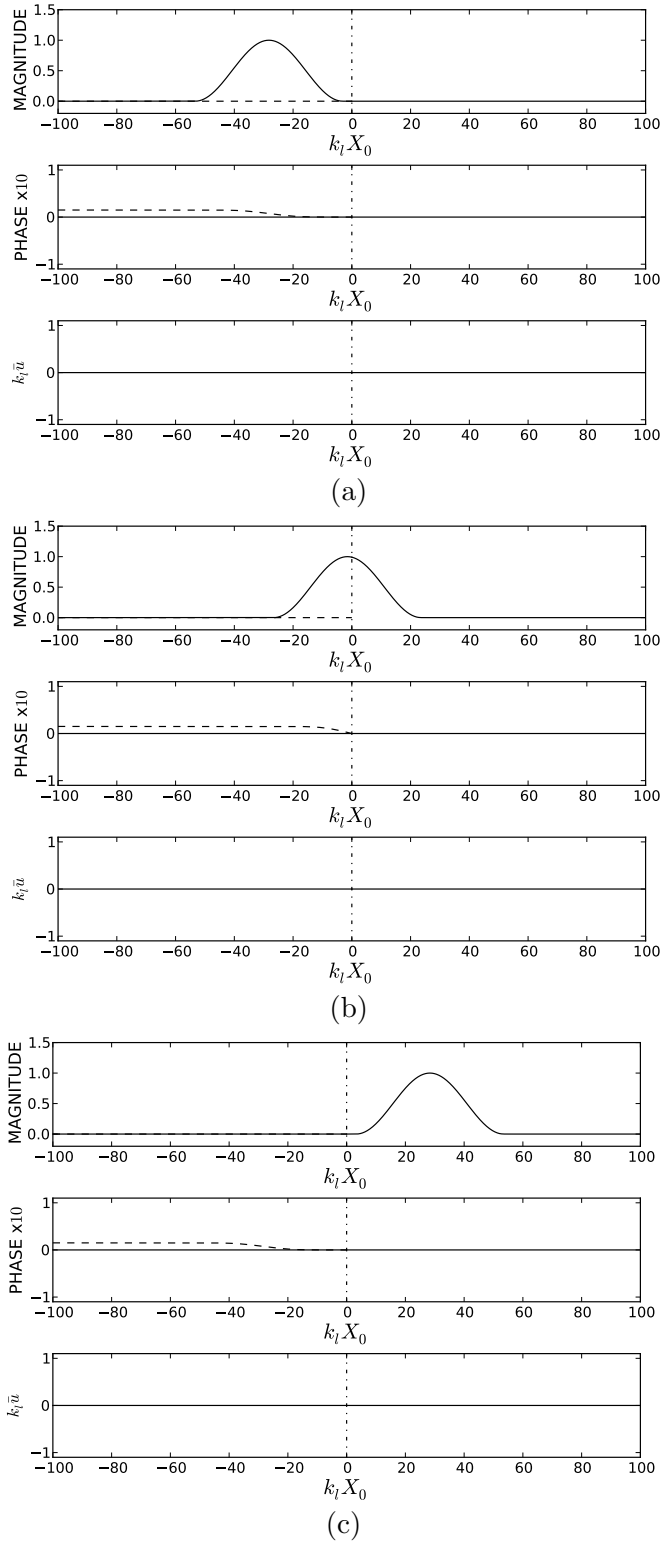

Figure 9.4: Case 1a: Results with parameter settings of $\rho_n = 1.0$, $(EA)_n = 1.0$, and $c_n^2 = 1.0$, at time of (a) $\hat{t} = 3.10$, (b) $\hat{t} = 3.78$, and (c) $\hat{t} = 4.54$.

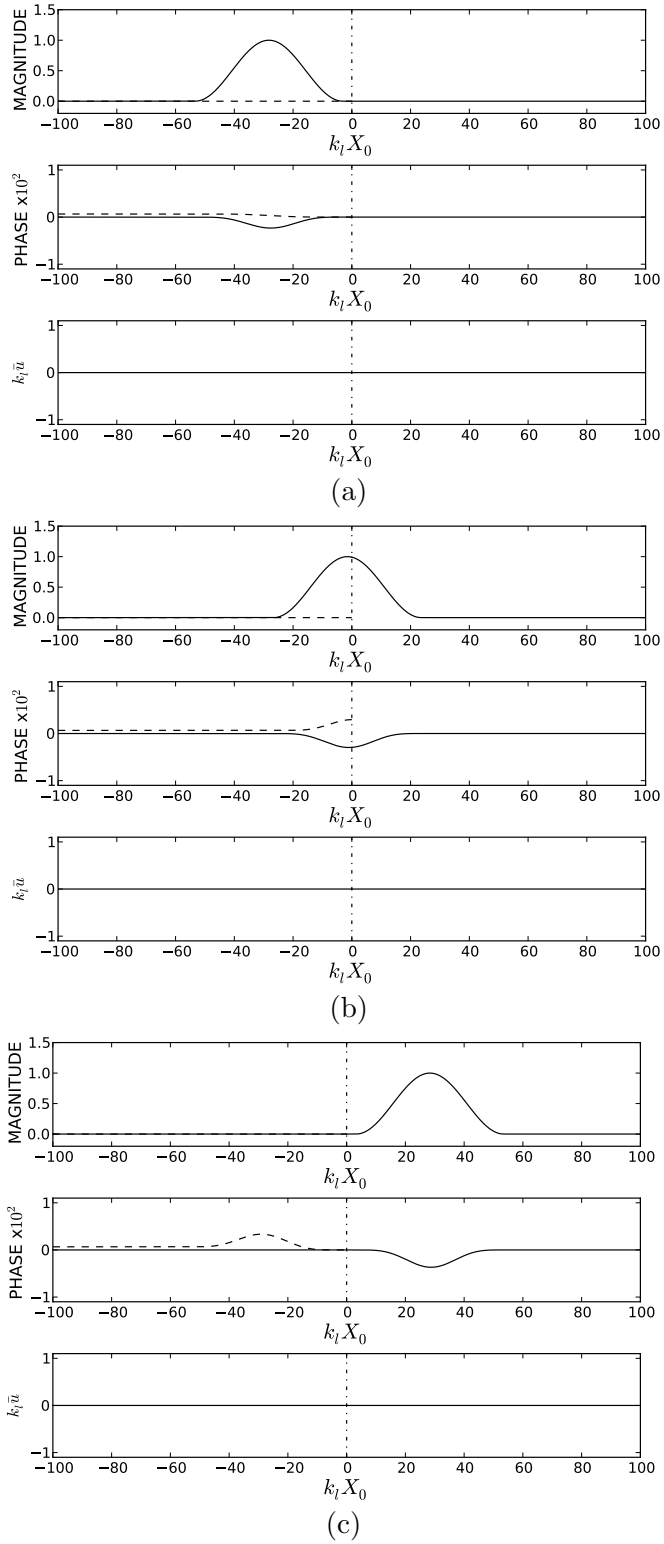

Figure 9.5: Case 1b: Results with parameter settings of $\rho_n = 1.0$, $(EA)_n = 1.0$, and $c_n^2 = 4.0$, at time of (a) $\hat{t} = 3.10$, (b) $\hat{t} = 3.78$, and (c) $\hat{t} = 4.54$.

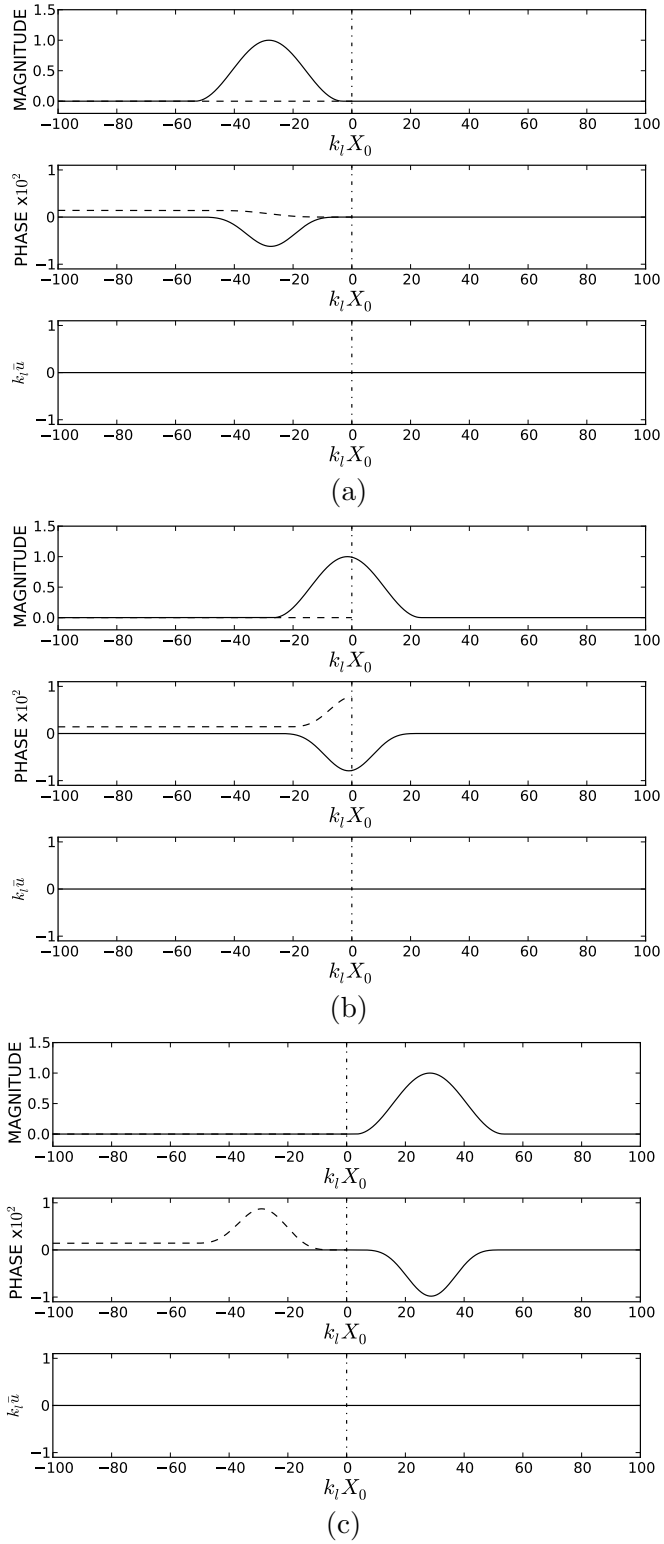

Figure 9.6: Case 1c: Results with parameter settings of $\rho_n = 1.0$, $(EA)_n = 1.0$, and $c_n^2 = 9.0$, at time of (a) $\hat{t} = 3.10$, (b) $\hat{t} = 3.78$, and (c) $\hat{t} = 4.54$.

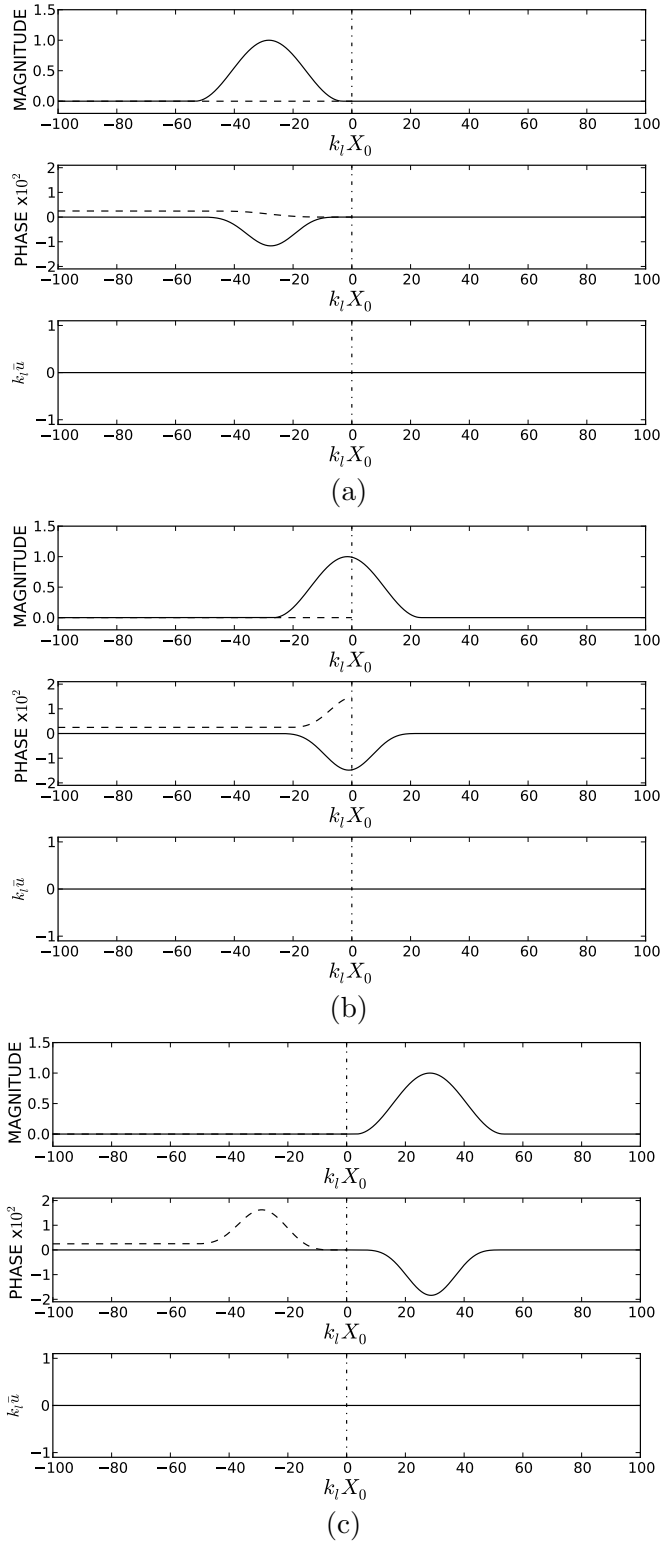

Figure 9.7: Case 1d: Results with parameter settings of $\rho_n = 1.0$, $(EA)_n = 1.0$, and $c_n^2 = 16.0$, at time of (a) $\hat{t} = 3.10$, (b) $\hat{t} = 3.78$, and (c) $\hat{t} = 4.54$.

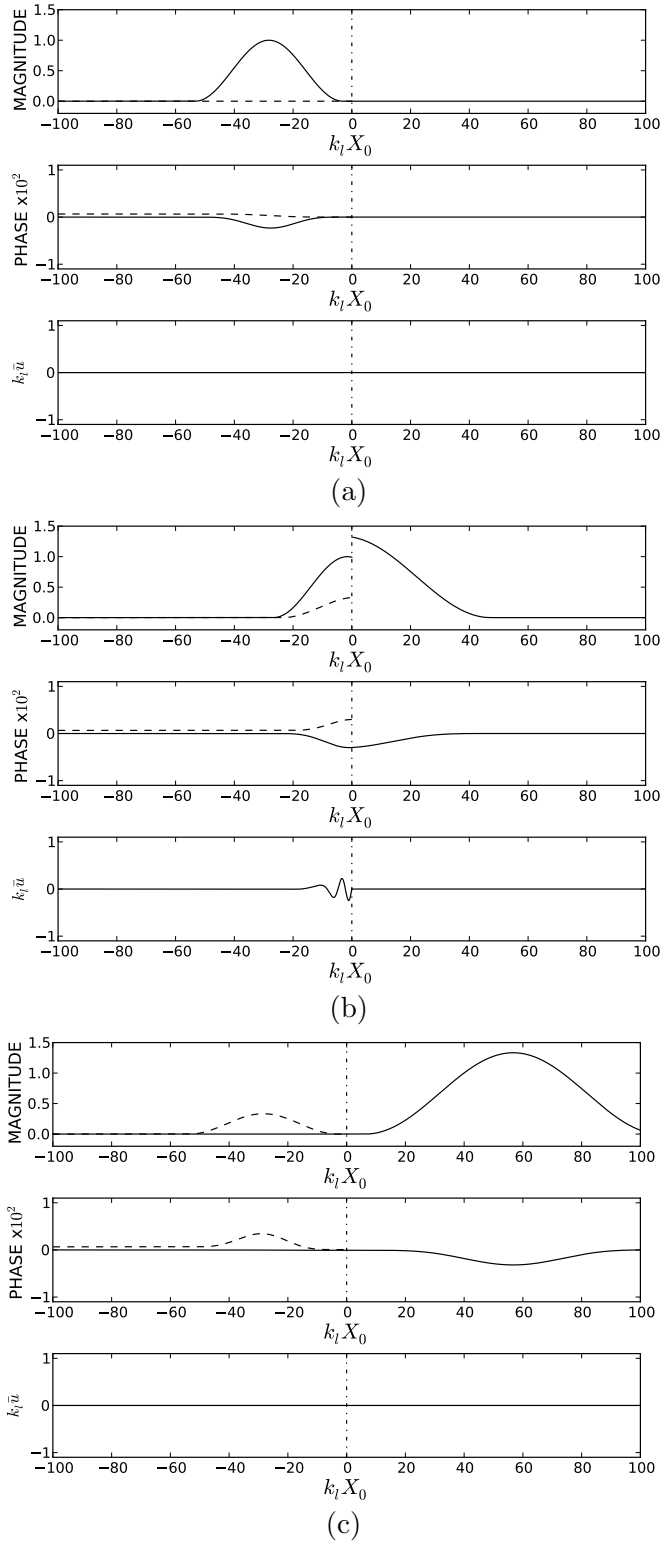

Figure 9.8: Case 2a: Results with parameter settings of $\rho_n = 0.25$, $(EA)_n = 1.0$, and $c_n^2 = 4.0$, at time of (a) $\hat{t} = 3.10$, (b) $\hat{t} = 3.78$, and (c) $\hat{t} = 4.54$.

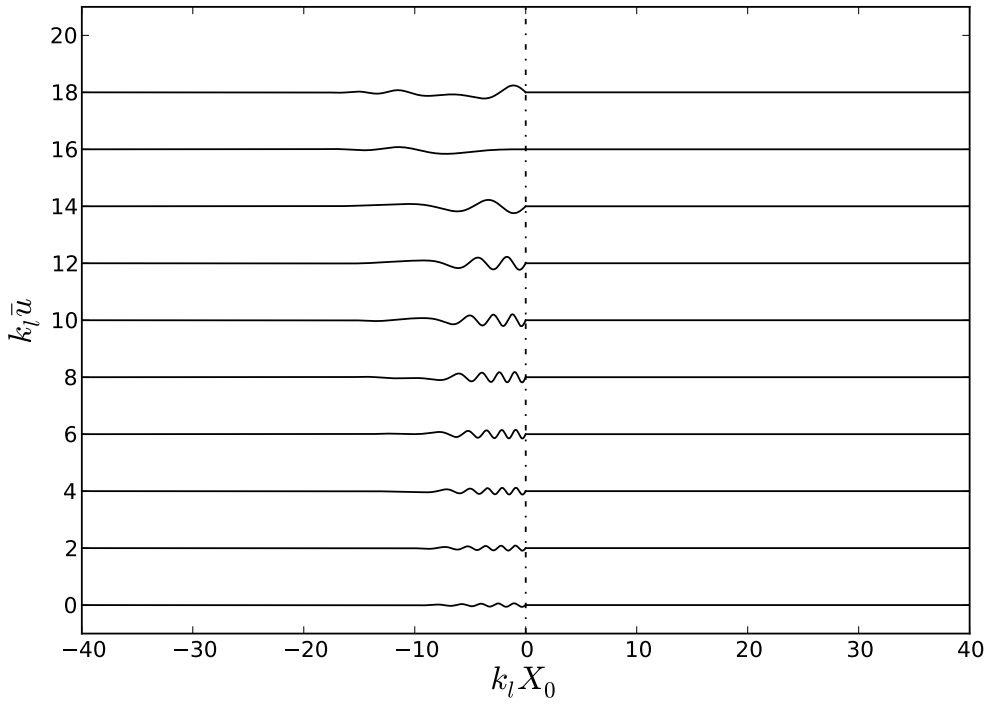

Figure 9.9: Case 2a: Mean longitudinal displacement evolution versus time from $\hat{t} = 3.10$ (bottom) through $\hat{t} = 3.90$ (top) in increments of $\Delta\hat{t} = 0.08$ each separated by 2.0 units vertically.

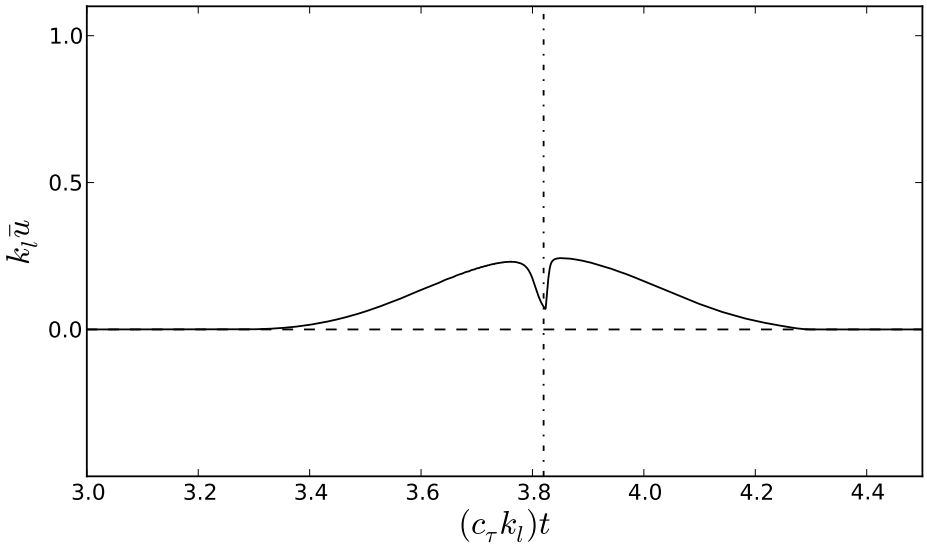

Figure 9.10: Case 2a: Mean longitudinal displacement maximum versus time plot - solid line is mean maximum and dashed line is mean at the interface.

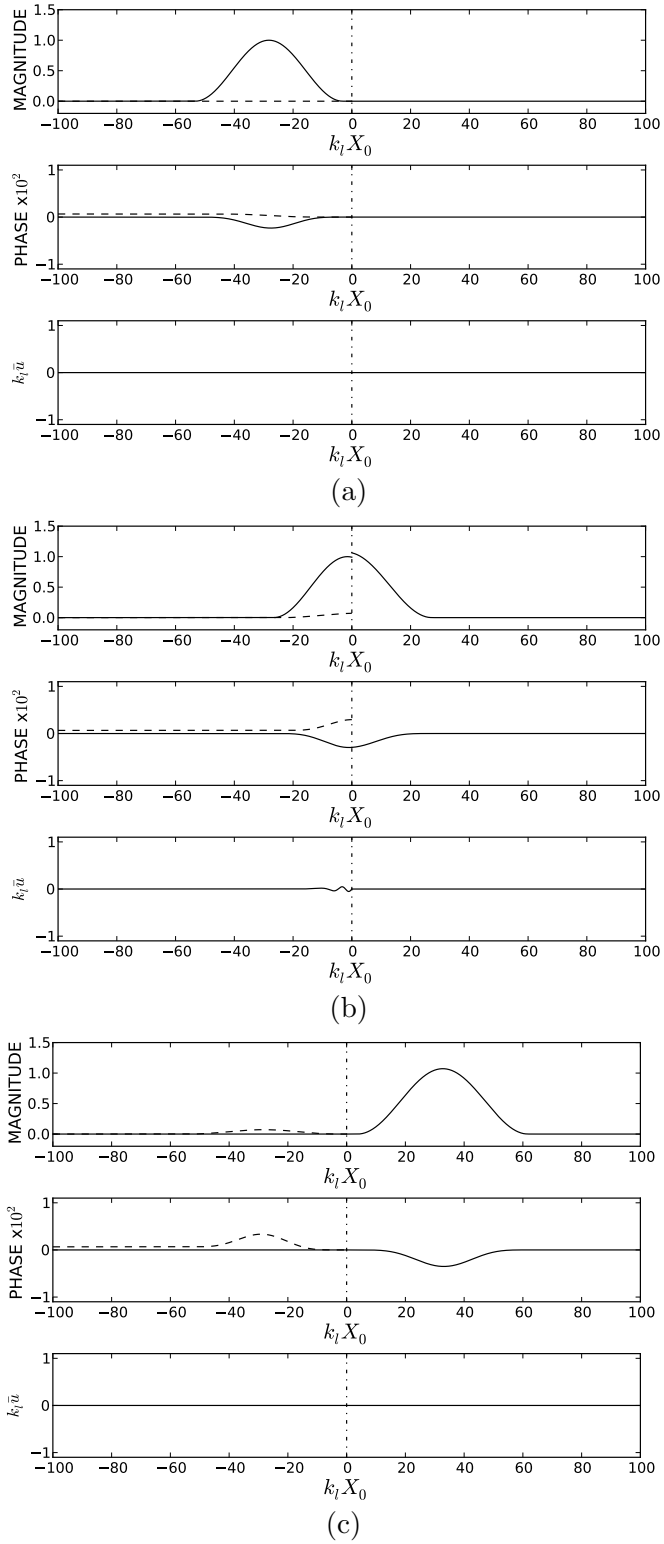

Figure 9.11: Case 2b: Results with parameter settings of $\rho_n = 0.75$, $(EA)_n = 1.0$, and $c_n^2 = 4.0$, at time of (a) $\hat{t} = 3.10$, (b) $\hat{t} = 3.78$, and (c) $\hat{t} = 4.54$.

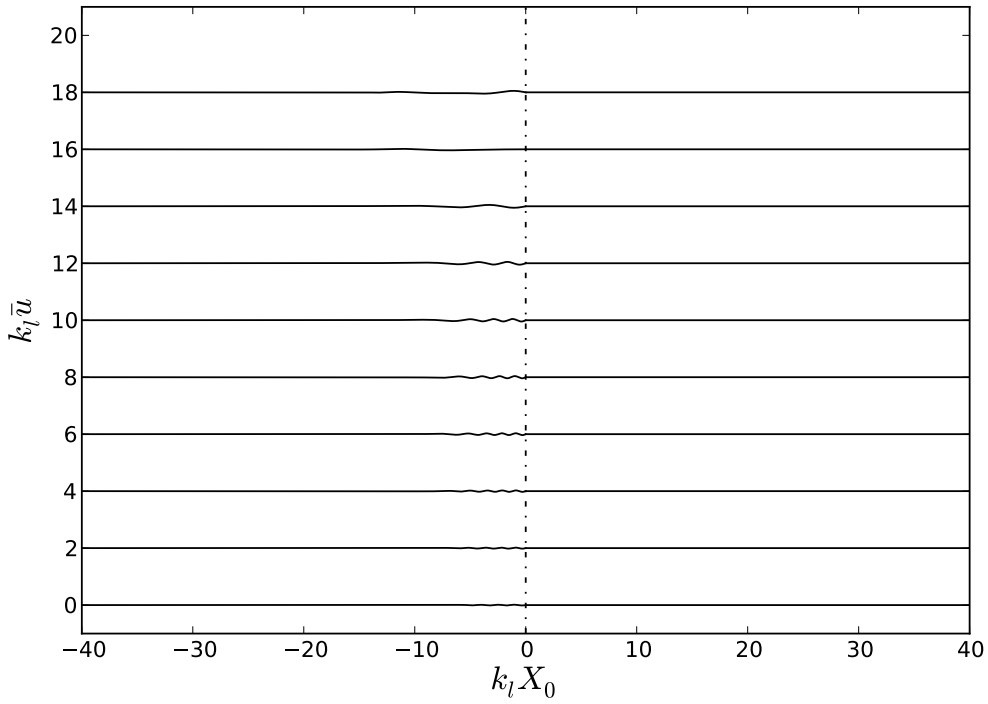

Figure 9.12: Case 2b: Mean longitudinal displacement evolution versus time from $\hat{t} = 3.10$ (bottom) through $\hat{t} = 3.90$ (top) in increments of $\Delta\hat{t} = 0.08$ each separated by 2.0 units vertically.

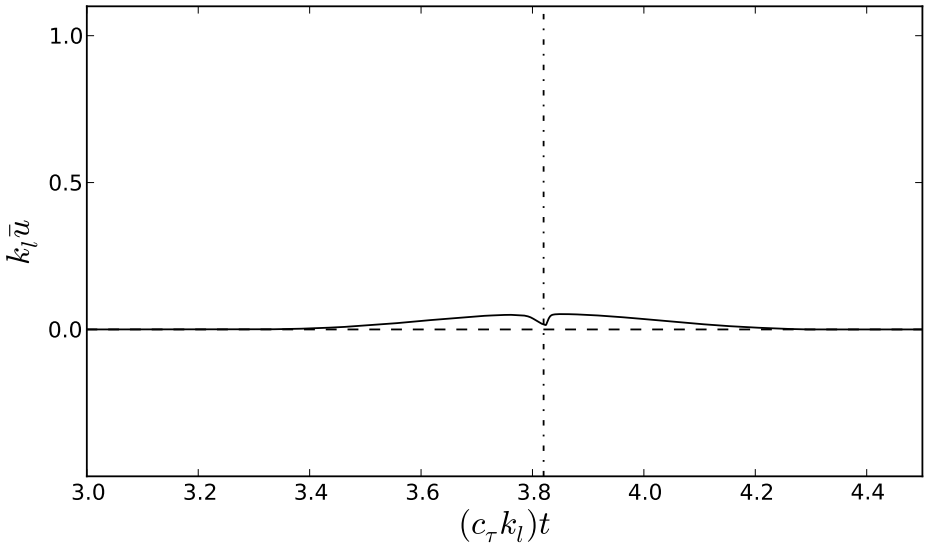

Figure 9.13: Case 2b: Mean longitudinal displacement maximum versus time plot - solid line is mean maximum and dashed line is mean at the interface.

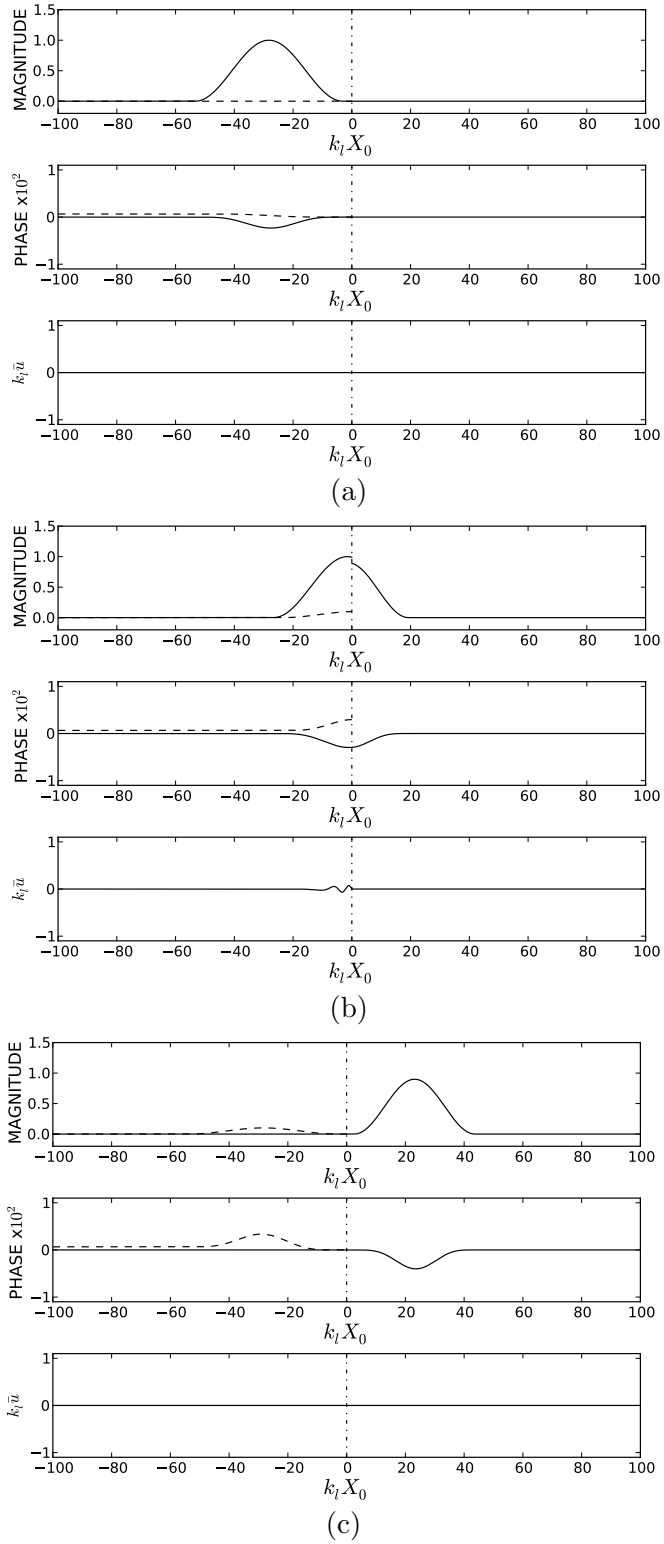

Figure 9.14: Case 2c: Results with parameter settings of $\rho_n = 1.5$, $(EA)_n = 1.0$, and $c_n^2 = 4.0$, at time of (a) $\hat{t} = 3.10$, (b) $\hat{t} = 3.78$, and (c) $\hat{t} = 4.54$.

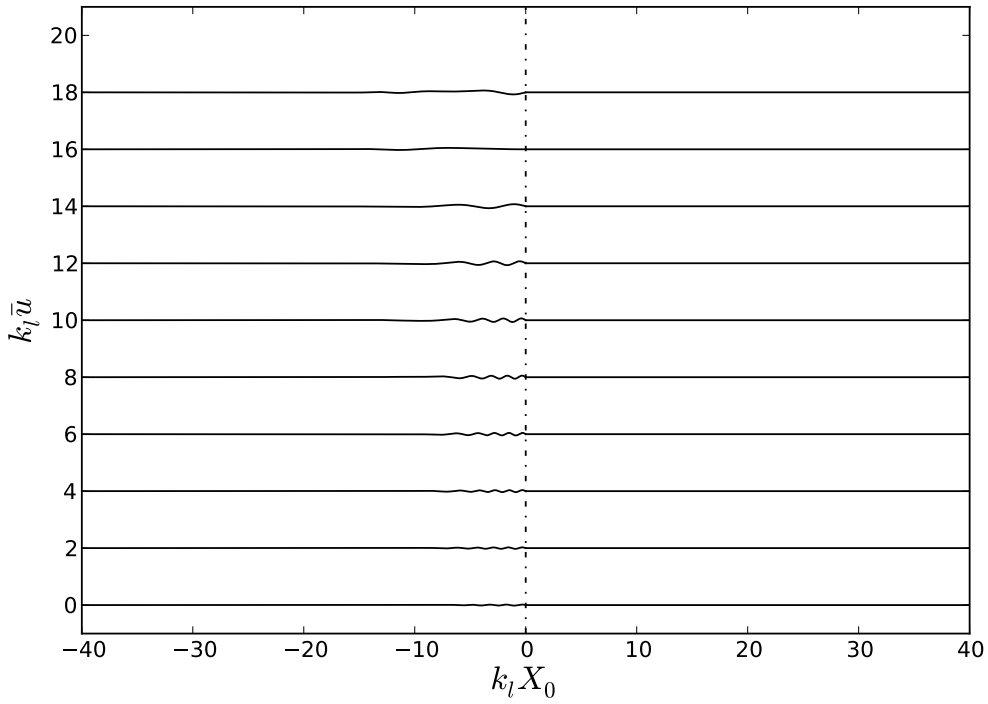

Figure 9.15: Case 2c: Mean longitudinal displacement evolution versus time from $\hat{t} = 3.10$ (bottom) through $\hat{t} = 3.90$ (top) in increments of $\Delta\hat{t} = 0.08$ each separated by 2.0 units vertically.

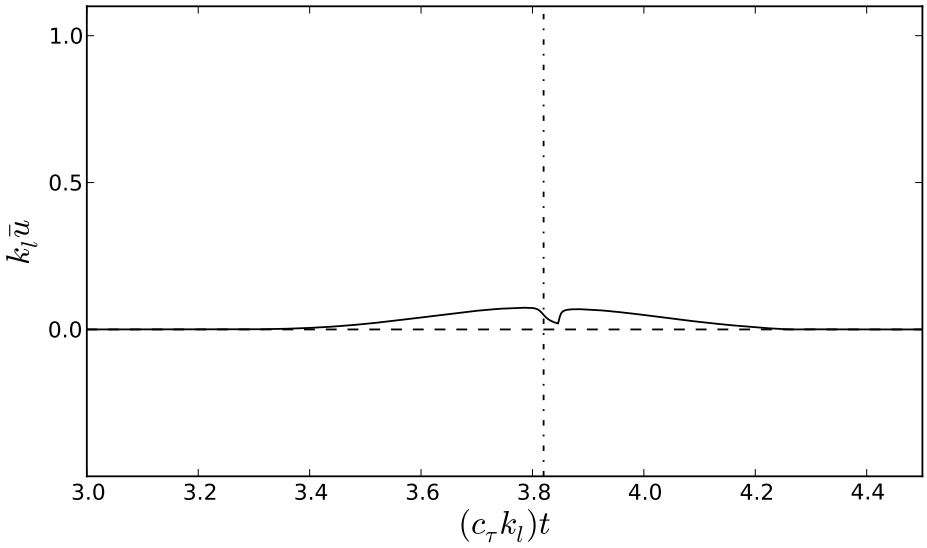

Figure 9.16: Case 2c: Mean longitudinal displacement maximum versus time plot - solid line is mean maximum and dashed line is mean at the interface.

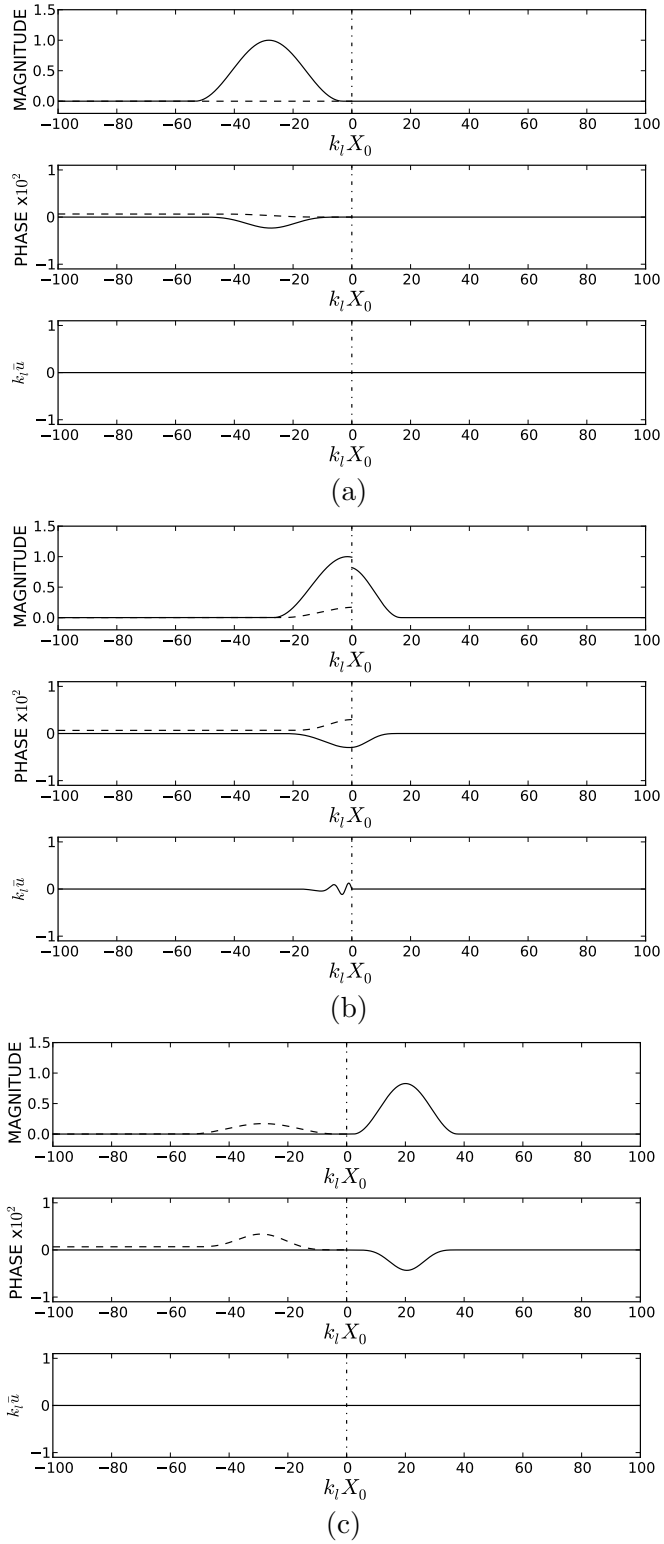

Figure 9.17: Case 2d: Results with parameter settings of $\rho_n = 2.0$, $(EA)_n = 1.0$, and $c_n^2 = 4.0$, at time of (a) $\hat{t} = 3.10$, (b) $\hat{t} = 3.78$, and (c) $\hat{t} = 4.54$.

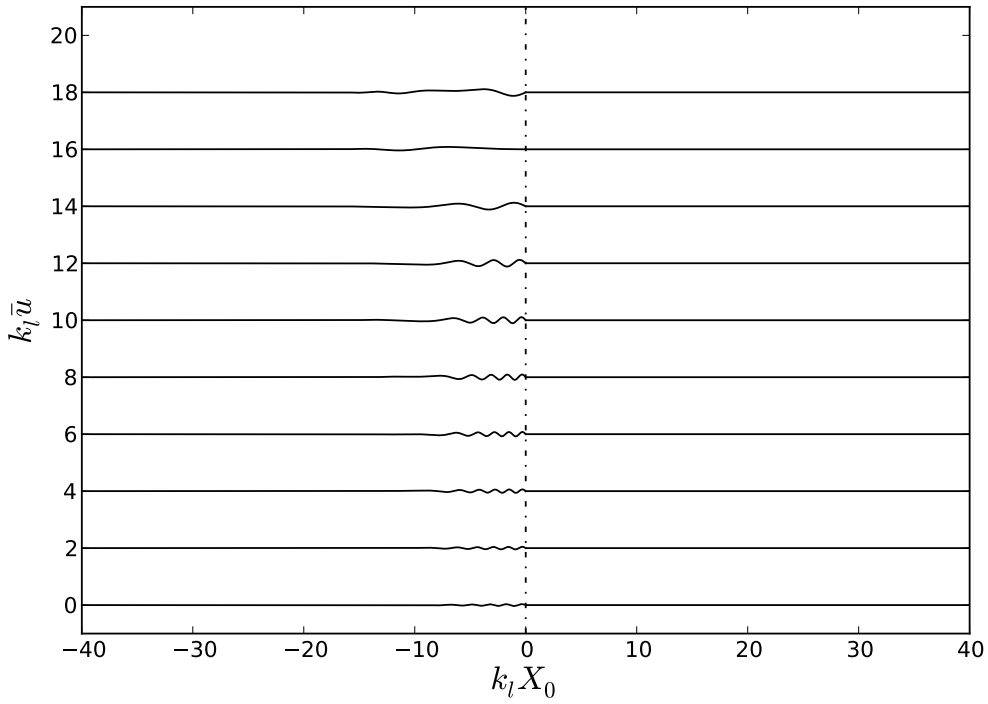

Figure 9.18: Case 2d: Mean longitudinal displacement evolution versus time from $\hat{t} = 3.10$ (bottom) through $\hat{t} = 3.90$ (top) in increments of $\Delta\hat{t} = 0.08$ each separated by 2.0 units vertically.

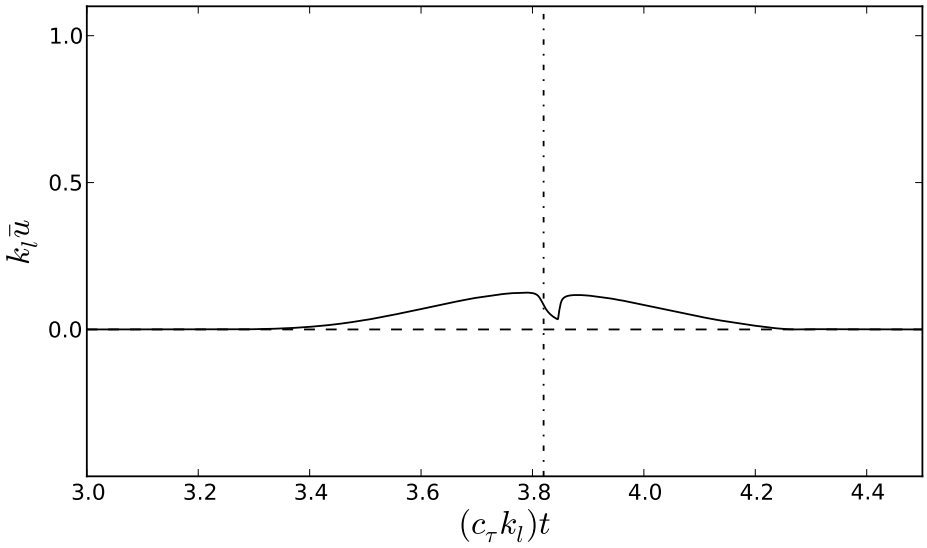

Figure 9.19: Case 2d: Mean longitudinal displacement maximum versus time plot - solid line is mean maximum and dashed line is mean at the interface.

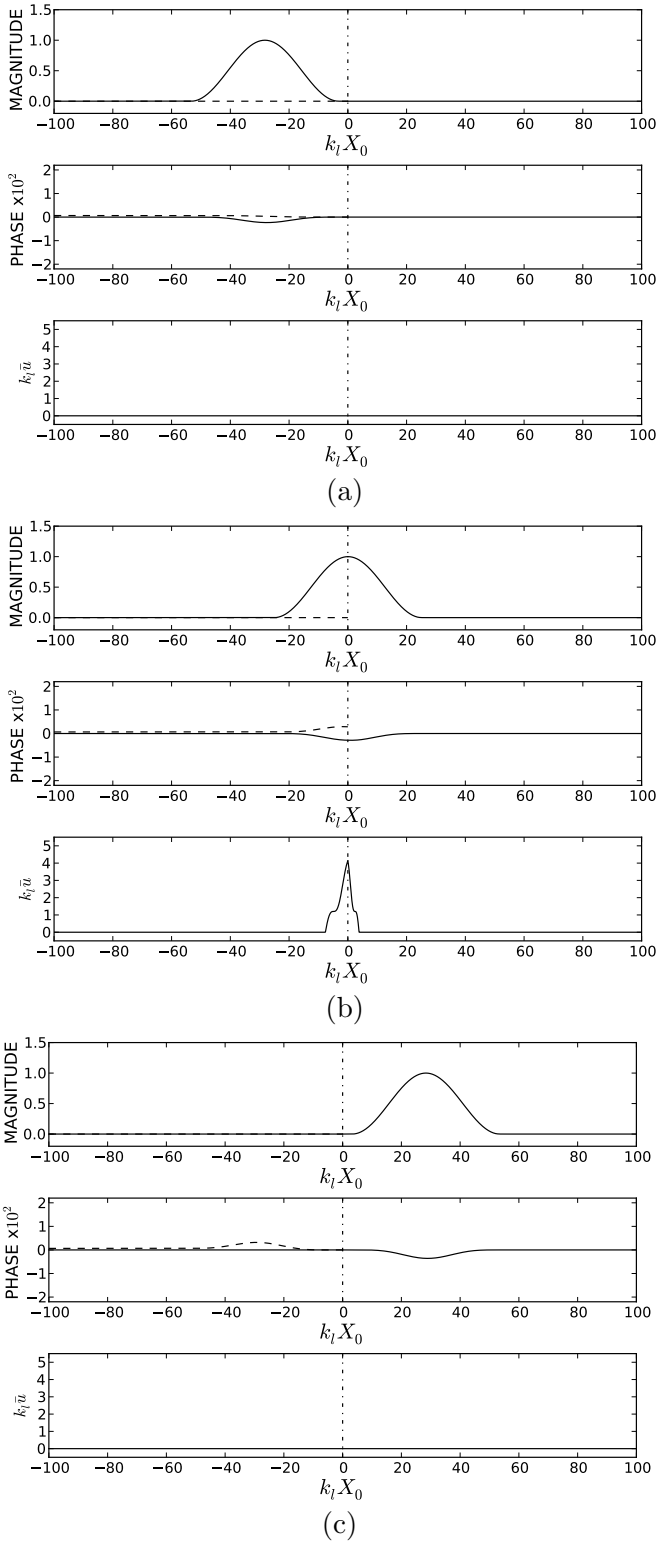

Figure 9.20: Case 3a: Results with parameter settings of $\rho_n = 1.0$, $(EA)_n = 0.25$, and $c_n^2 = 4.0$, at time of (a) $\hat{t} = 3.10$, (b) $\hat{t} = 3.78$, and (c) $\hat{t} = 4.54$.

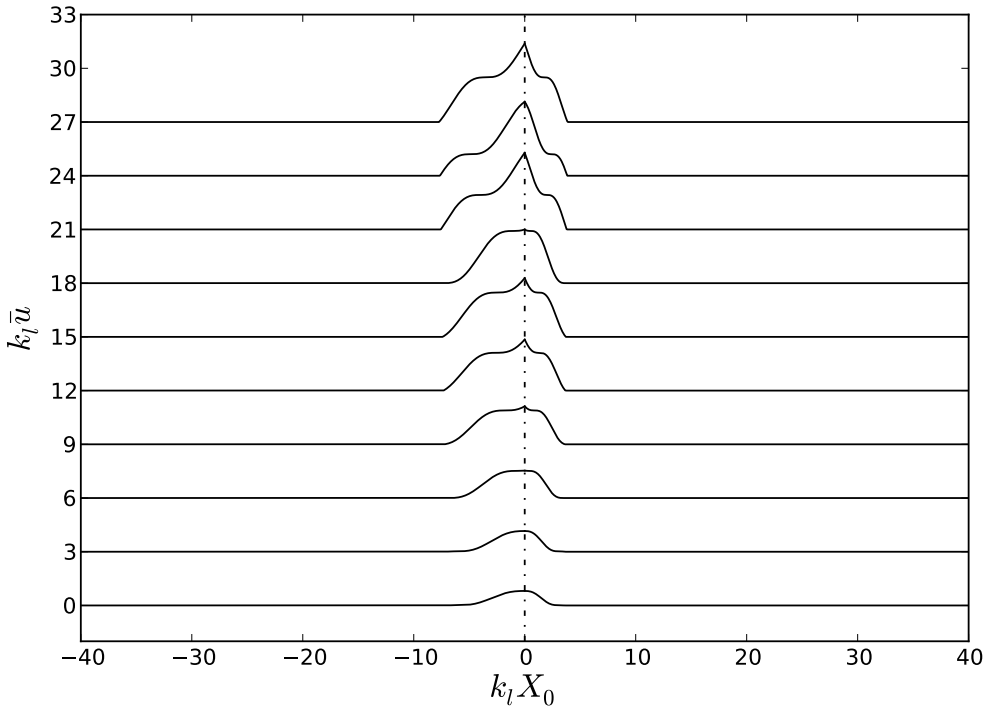

Figure 9.21: Case 3a: Mean longitudinal displacement evolution versus time from $\hat{t} = 3.10$ (bottom) through $\hat{t} = 3.90$ (top) in increments of $\Delta\hat{t} = 0.08$ each separated by 3.0 units vertically.

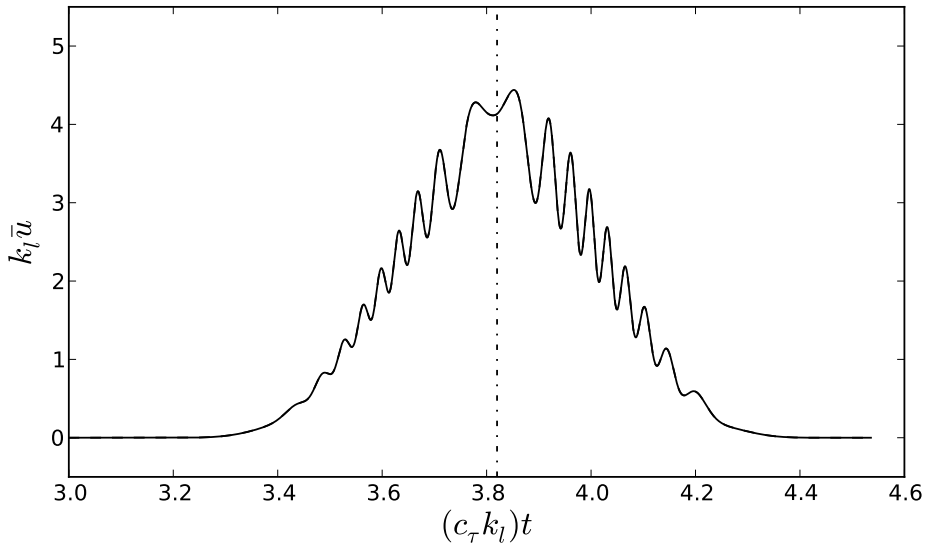

Figure 9.22: Case 3a: Mean longitudinal displacement maximum versus time plot - solid line is mean maximum and dashed line is mean at the interface.

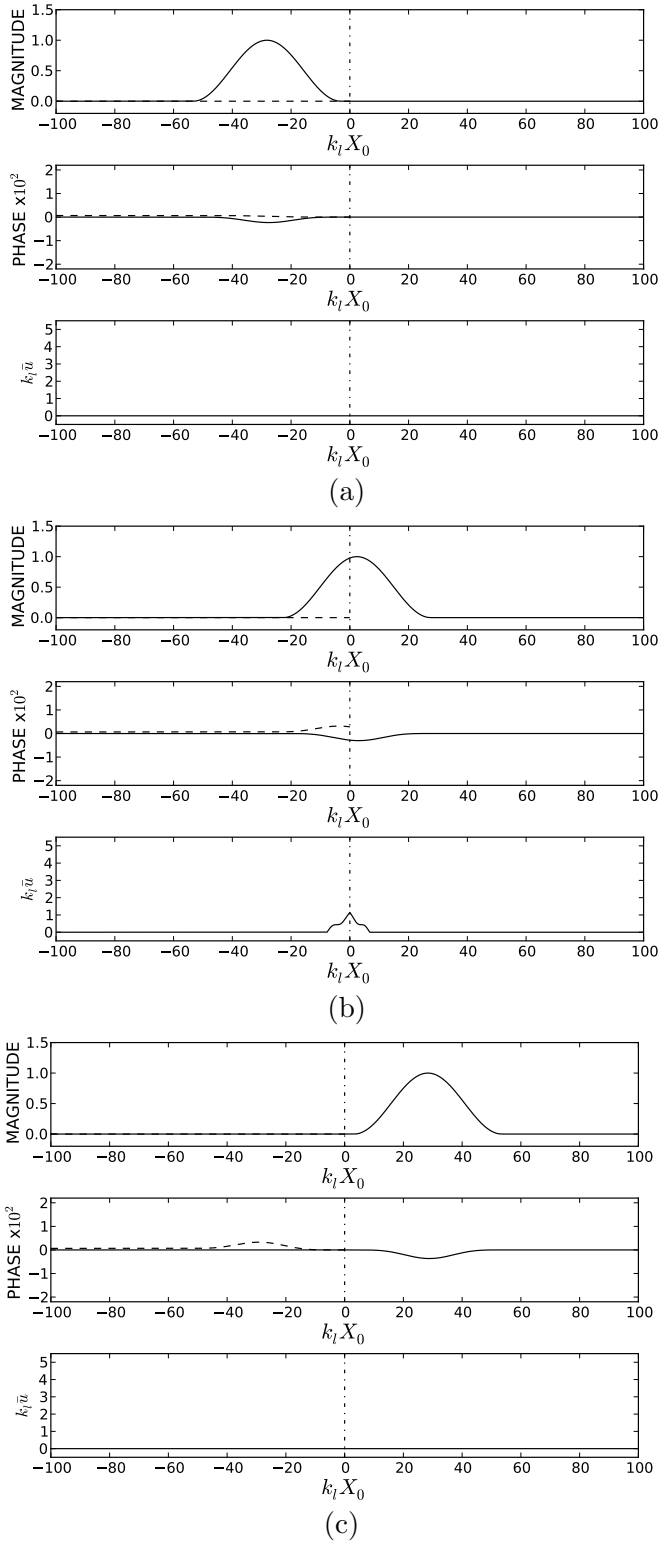

Figure 9.23: Case 3b: Results with parameter settings of $\rho_n = 1.0$, $(EA)_n = 0.75$, and $c_n^2 = 4.0$, at time of (a) $\hat{t} = 3.10$, (b) $\hat{t} = 3.78$, and (c) $\hat{t} = 4.54$.

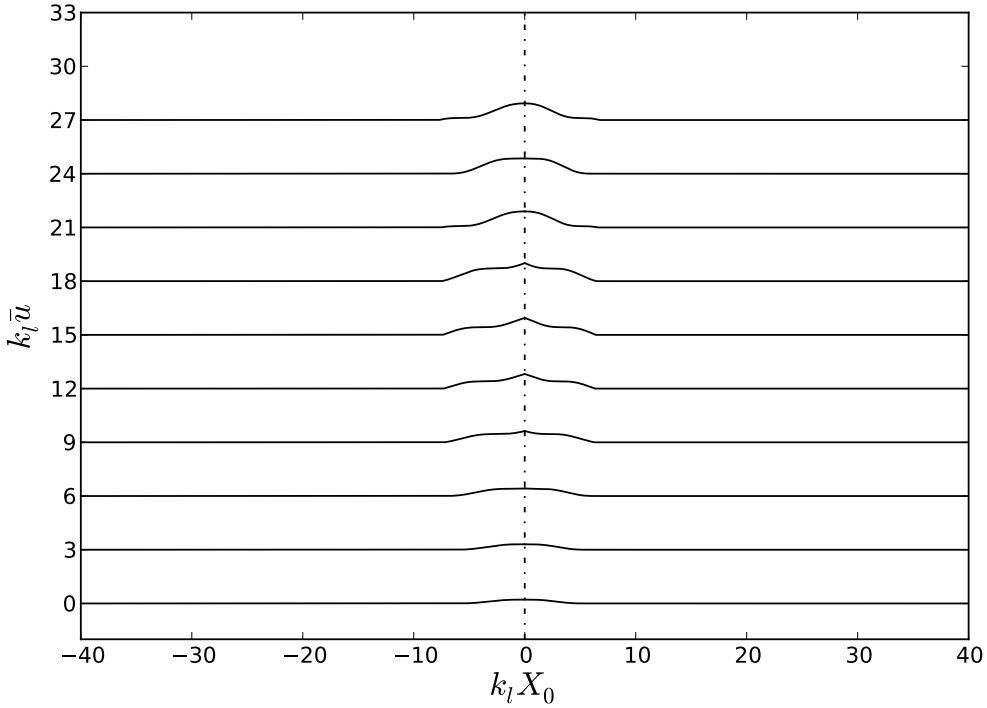

Figure 9.24: Case 3b: Mean longitudinal displacement evolution versus time from $\hat{t} = 3.10$ (bottom) through $\hat{t} = 3.90$ (top) in increments of $\Delta\hat{t} = 0.08$ each separated by 3.0 units vertically.

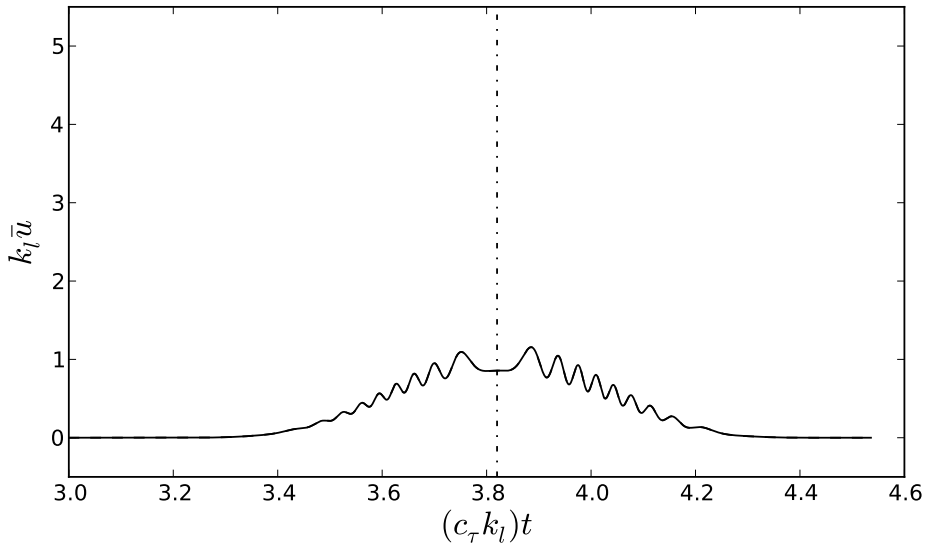

Figure 9.25: Case 3b: Mean longitudinal displacement maximum versus time plot - solid line is mean maximum and dashed line is mean at the interface.

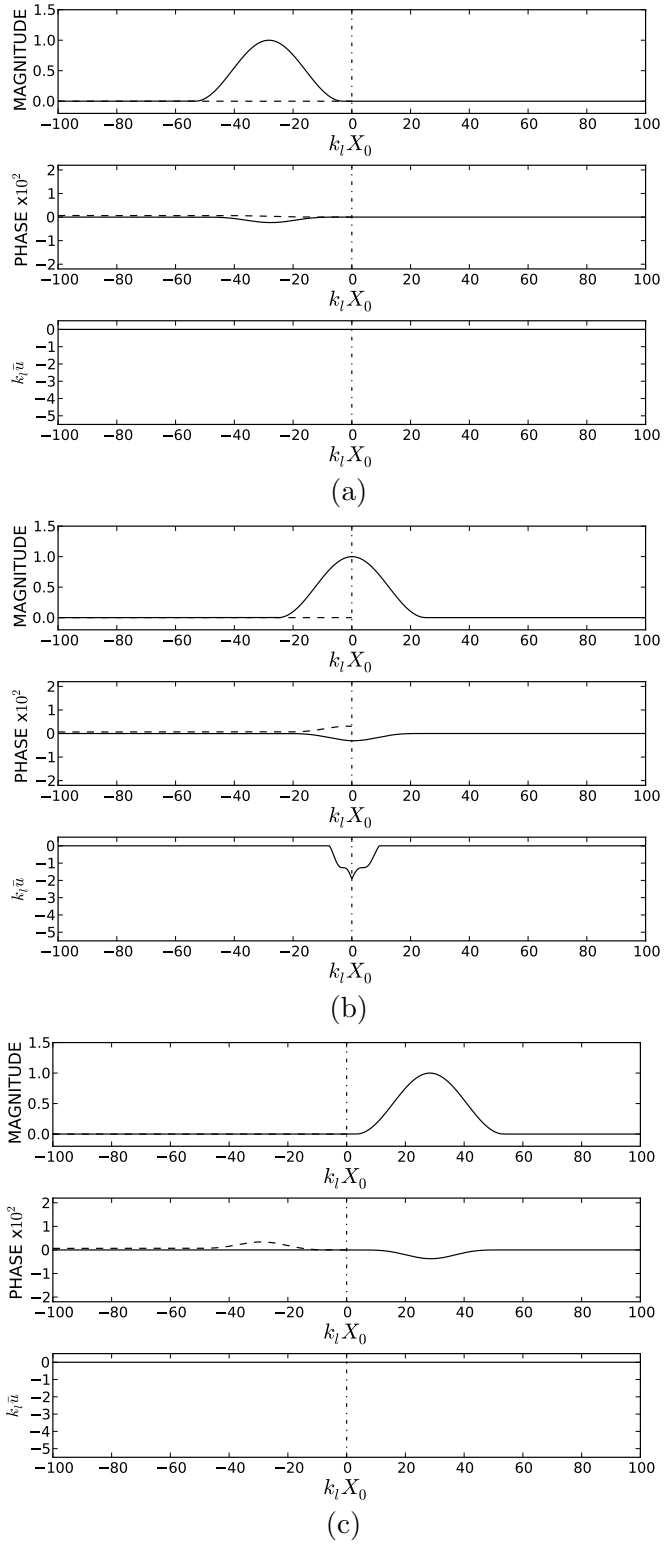

Figure 9.26: Case 3c: Results with parameter settings of $\rho_n = 1.0$, $(EA)_n = 1.5$, and $c_n^2 = 4.0$, at time of (a) $\hat{t} = 3.10$, (b) $\hat{t} = 3.78$, and (c) $\hat{t} = 4.54$.

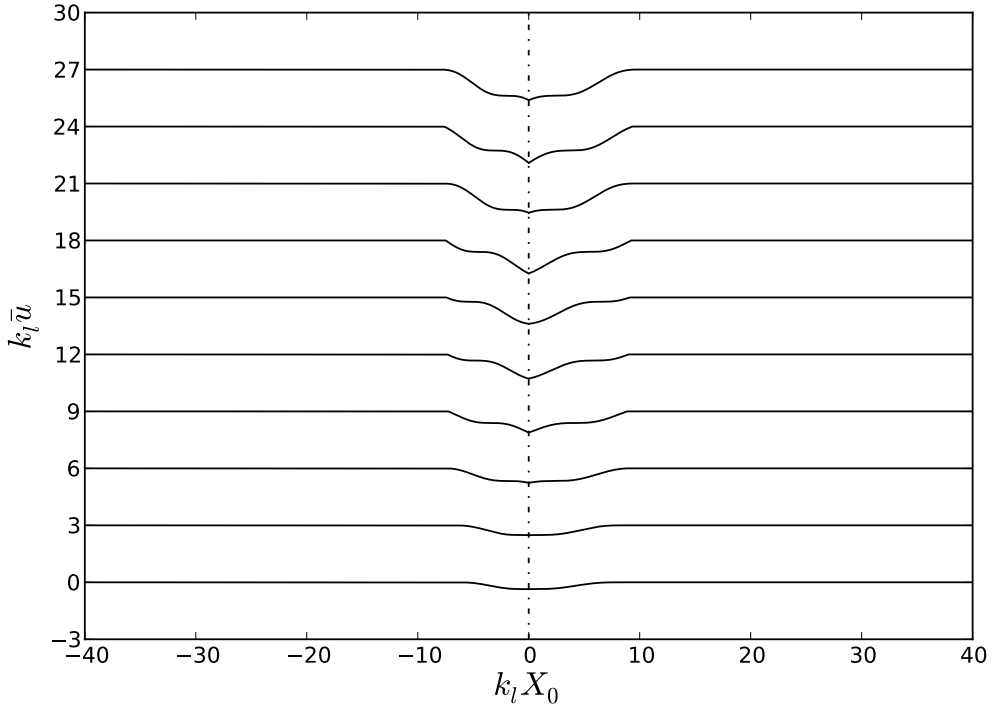

Figure 9.27: Case 3c: Mean longitudinal displacement evolution versus time from $\hat{t} = 3.10$ (bottom) through $\hat{t} = 3.90$ (top) in increments of $\Delta\hat{t} = 0.08$ each separated by 3.0 units vertically.

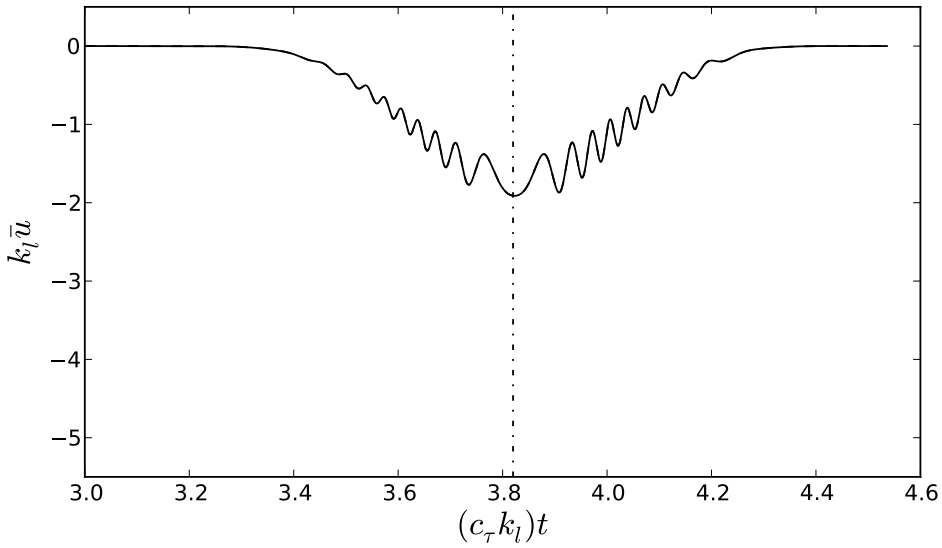

Figure 9.28: Case 3c: Mean longitudinal displacement maximum versus time plot - solid line is mean maximum and dashed line is mean at the interface.

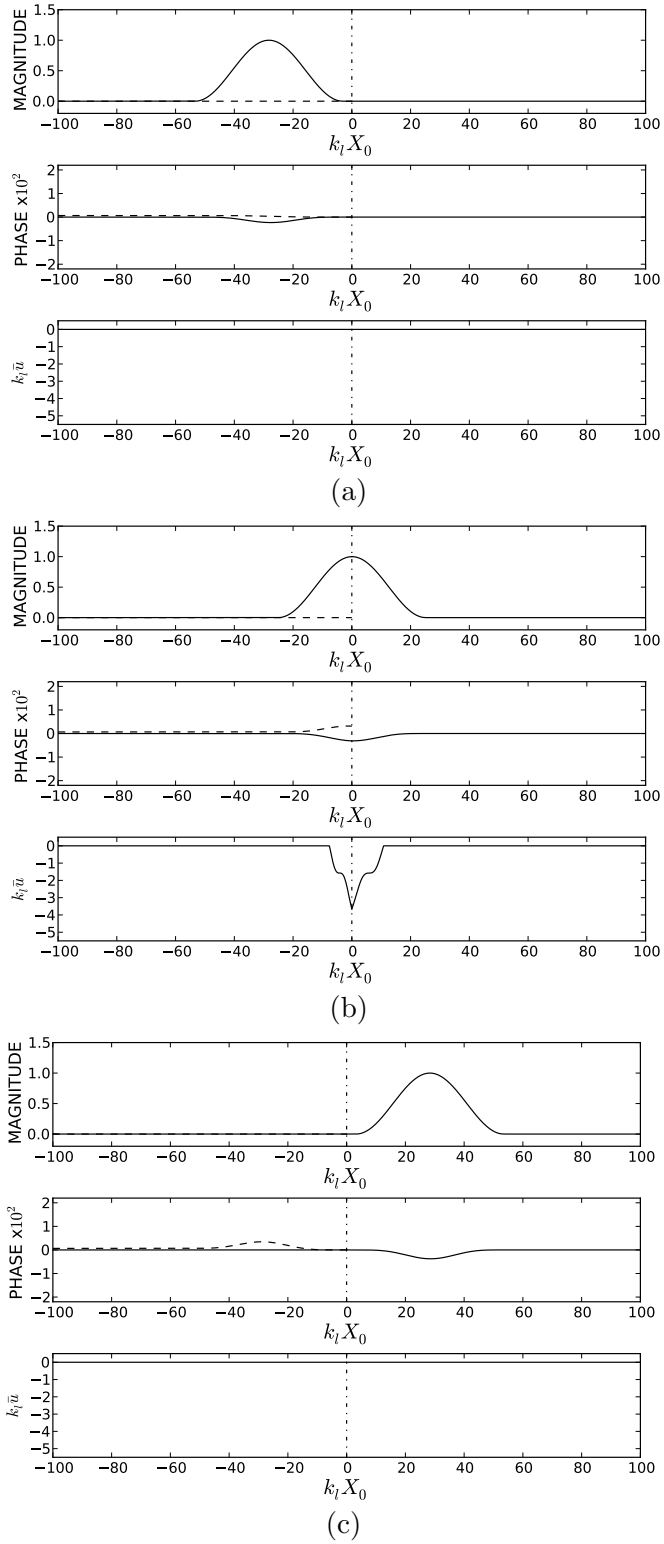

Figure 9.29: Case 3d: Results with parameter settings of $\rho_n = 1.0$, $(EA)_n = 2.0$, and $c_n^2 = 4.0$, at time of (a) $\hat{t} = 3.10$, (b) $\hat{t} = 3.78$, and (c) $\hat{t} = 4.54$.

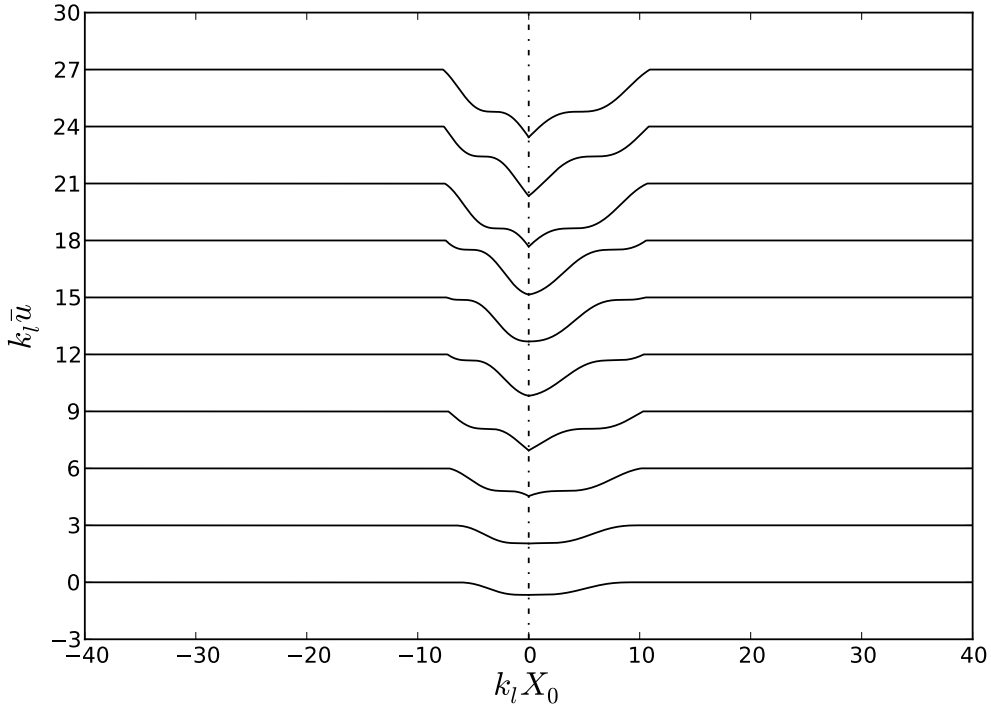

Figure 9.30: Case 3d: Mean longitudinal displacement evolution versus time from $\hat{t} = 3.10$ (bottom) through $\hat{t} = 3.90$ (top) in increments of $\Delta\hat{t} = 0.08$ each separated by 3.0 units vertically.

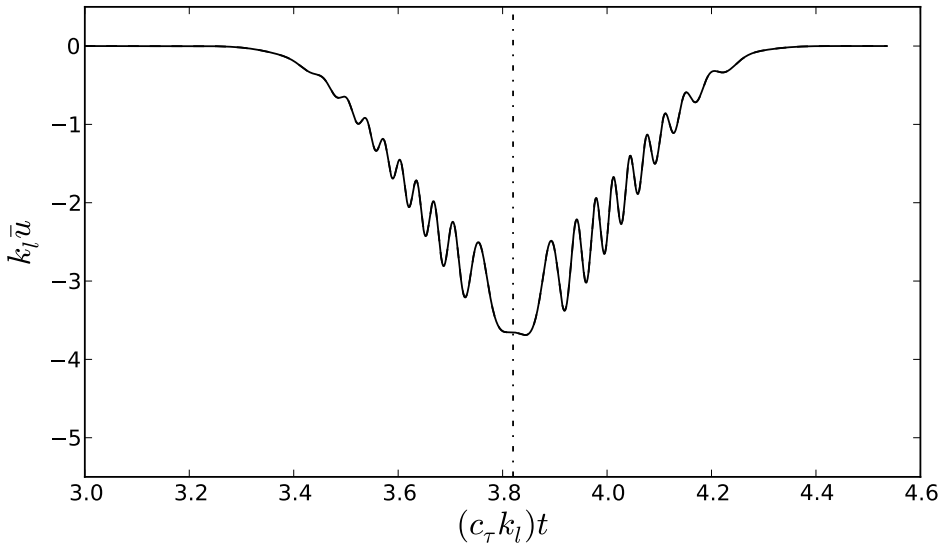

Figure 9.31: Case 3d: Mean longitudinal displacement maximum versus time plot - solid line is mean maximum and dashed line is mean at the interface.

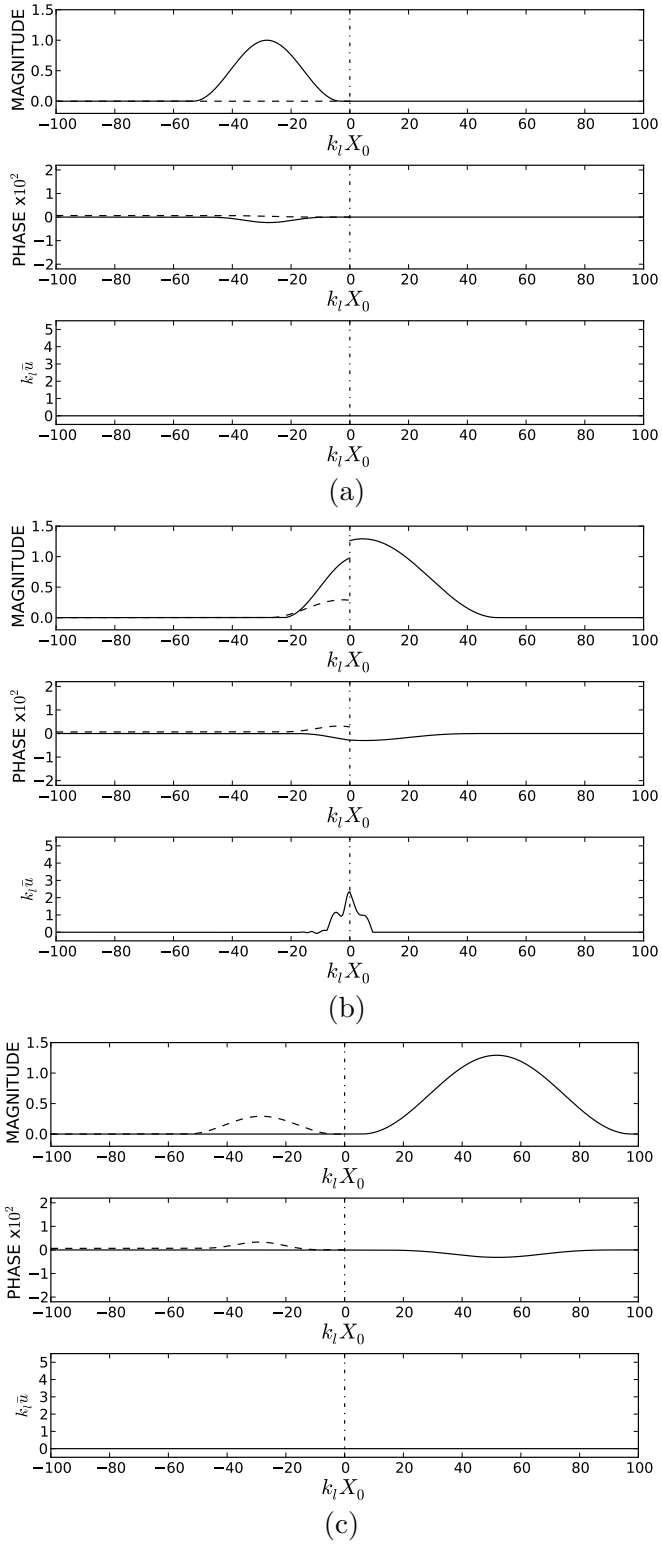

Figure 9.32: Case 4a: Results with parameter settings of $\rho_n = 0.3$, $(EA)_n = 0.3$, and $c_n^2 = 4.0$, at time of (a) $\hat{t} = 3.10$, (b) $\hat{t} = 3.78$, and (c) $\hat{t} = 4.54$.

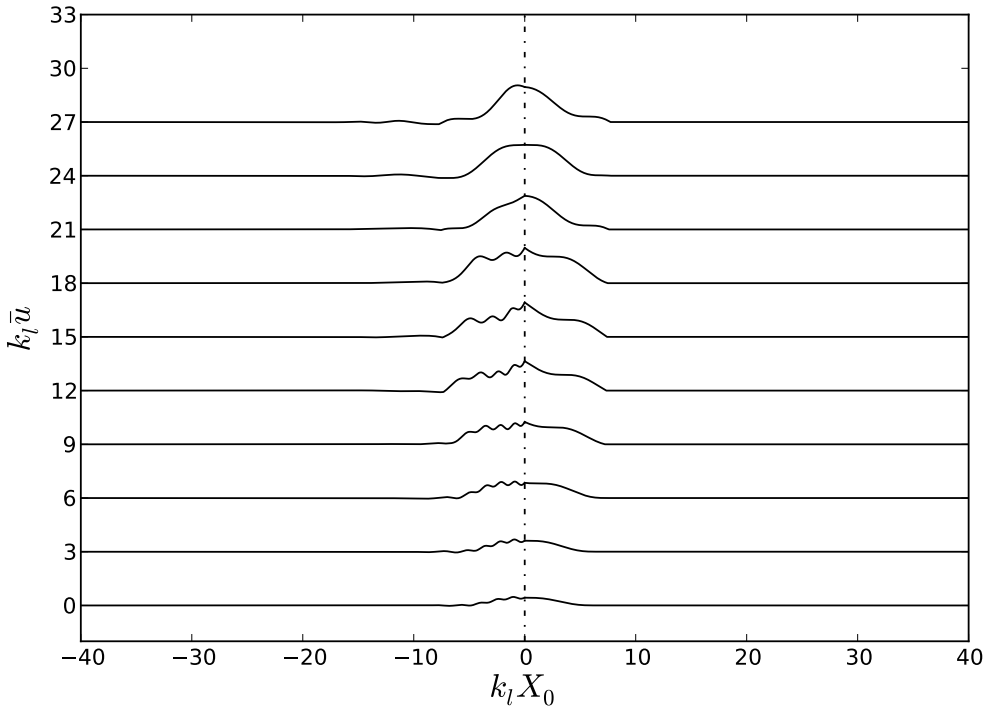

Figure 9.33: Case 4a: Mean longitudinal displacement evolution versus time from $\hat{t} = 3.10$ (bottom) through $\hat{t} = 3.90$ (top) in increments of $\Delta\hat{t} = 0.08$ each separated by 3.0 units vertically.

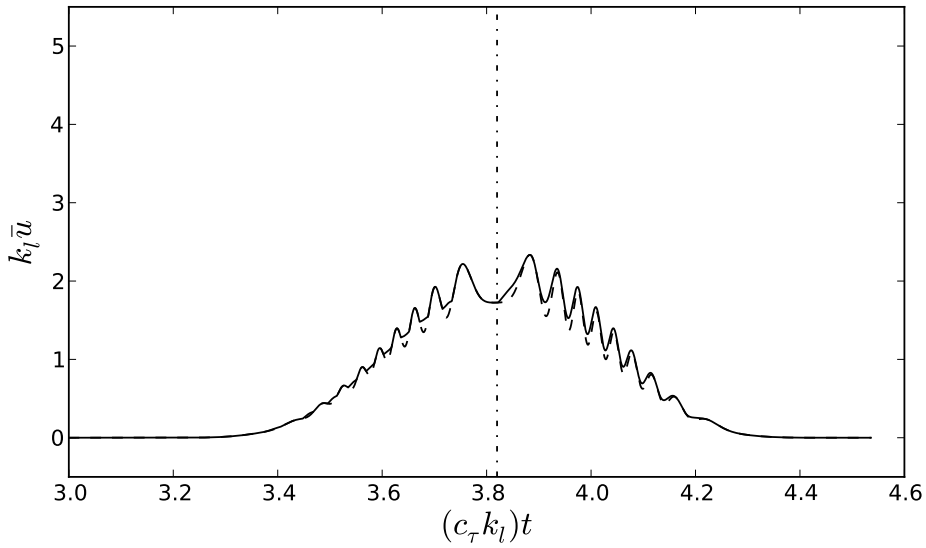

Figure 9.34: Case 4a: Mean longitudinal displacement maximum versus time plot - solid line is mean maximum and dashed line is mean at the interface.

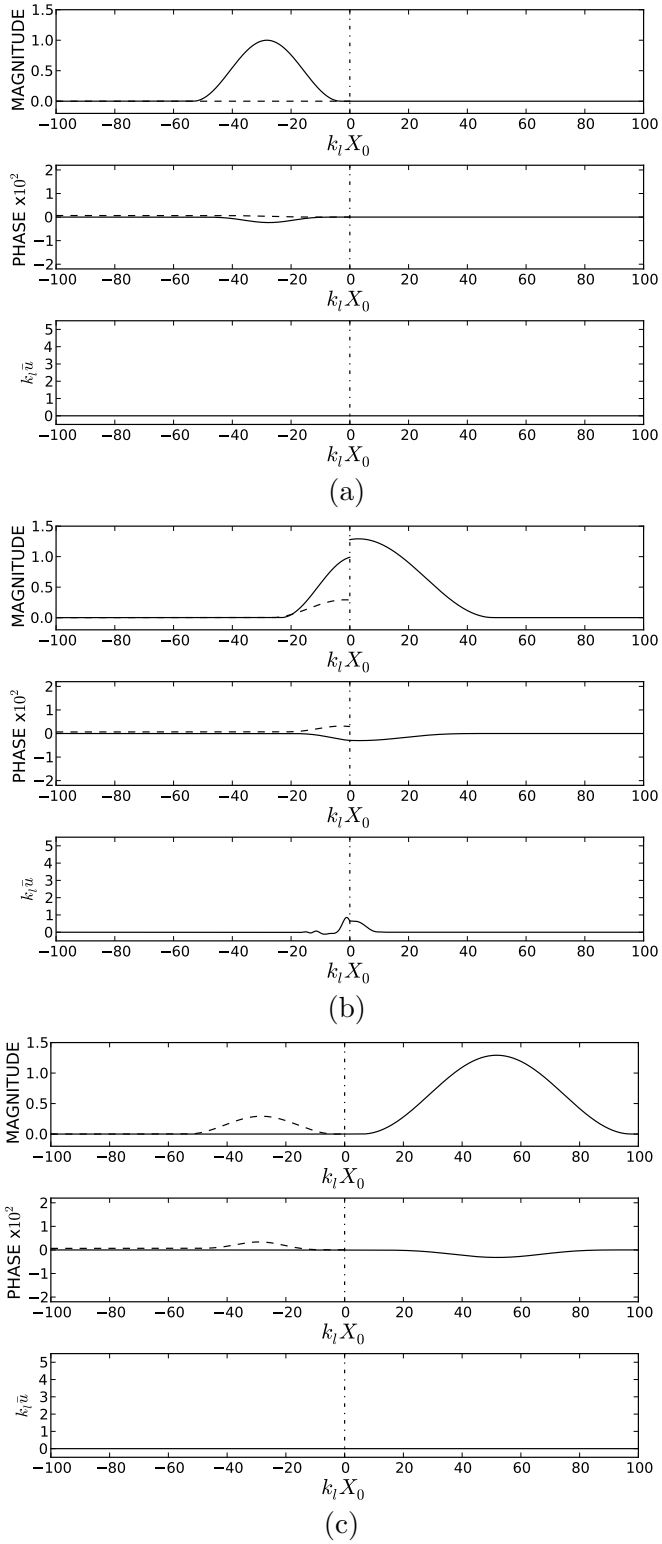

Figure 9.35: Case 4b: Results with $\rho_n = 0.3$, $(EA)_n = 0.7$, and $c_n^2 = 4.0$, at time of (a) $\hat{t} = 3.10$, (b) $\hat{t} = 3.78$, and (c) $\hat{t} = 4.54$.

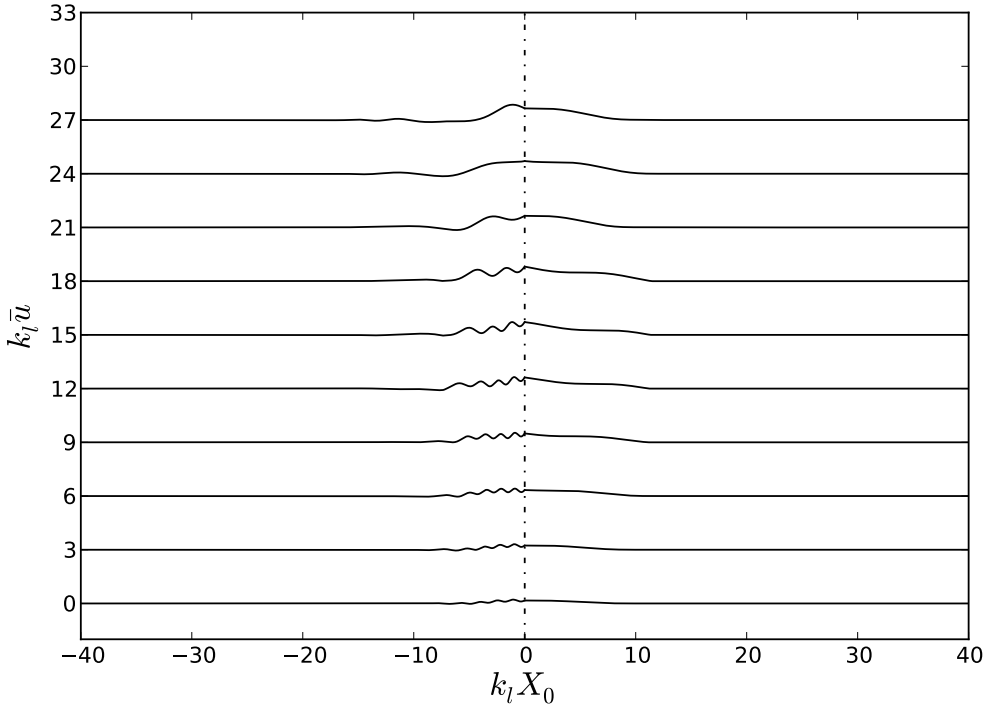

Figure 9.36: Case 4b: Mean longitudinal displacement evolution versus time from $\hat{t} = 3.10$ (bottom) through $\hat{t} = 3.90$ (top) in increments of $\Delta\hat{t} = 0.08$ each separated by 3.0 units vertically.

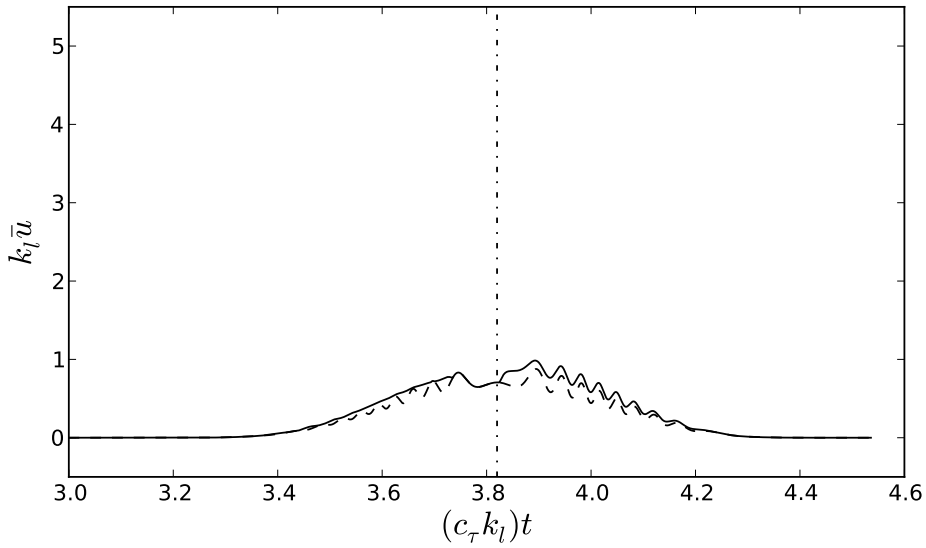

Figure 9.37: Case 4b: Mean longitudinal displacement maximum versus time plot - solid line is mean maximum and dashed line is mean at the interface.

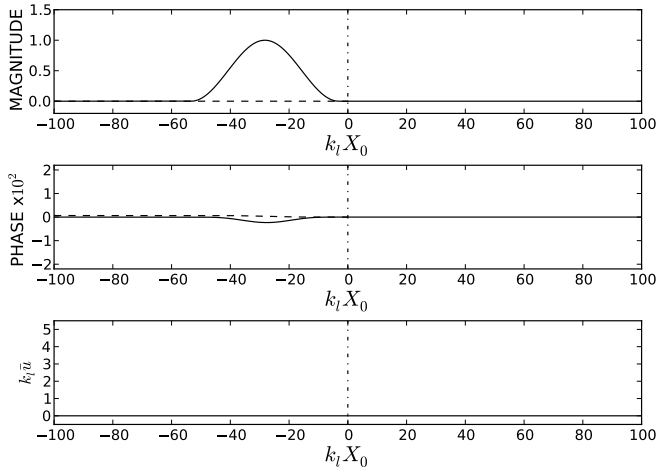

(a)

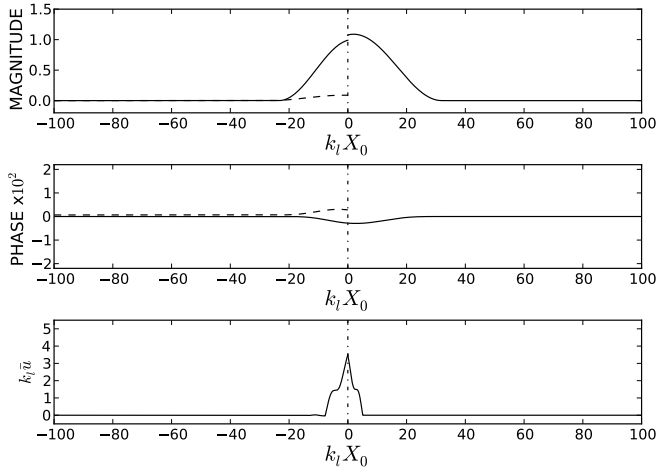

(b)

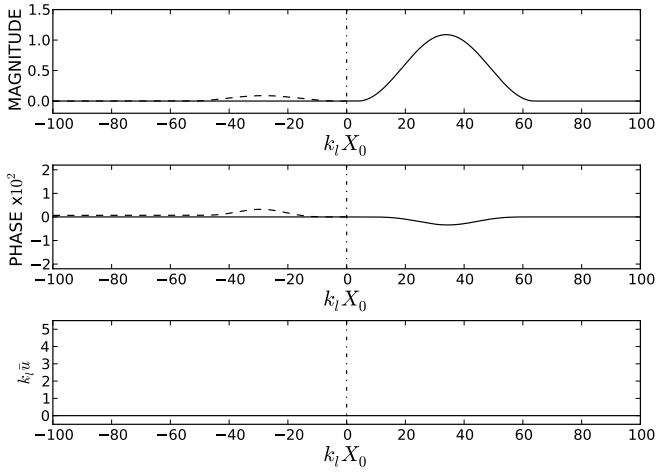

(c)

Figure 9.38: Case 4c: Results with $\rho_n = 0.7$, $(EA)_n = 0.3$, and $c_n^2 = 4.0$, at time of (a) $\hat{t} = 3.10$, (b) $\hat{t} = 3.78$, and (c) $\hat{t} = 4.54$.

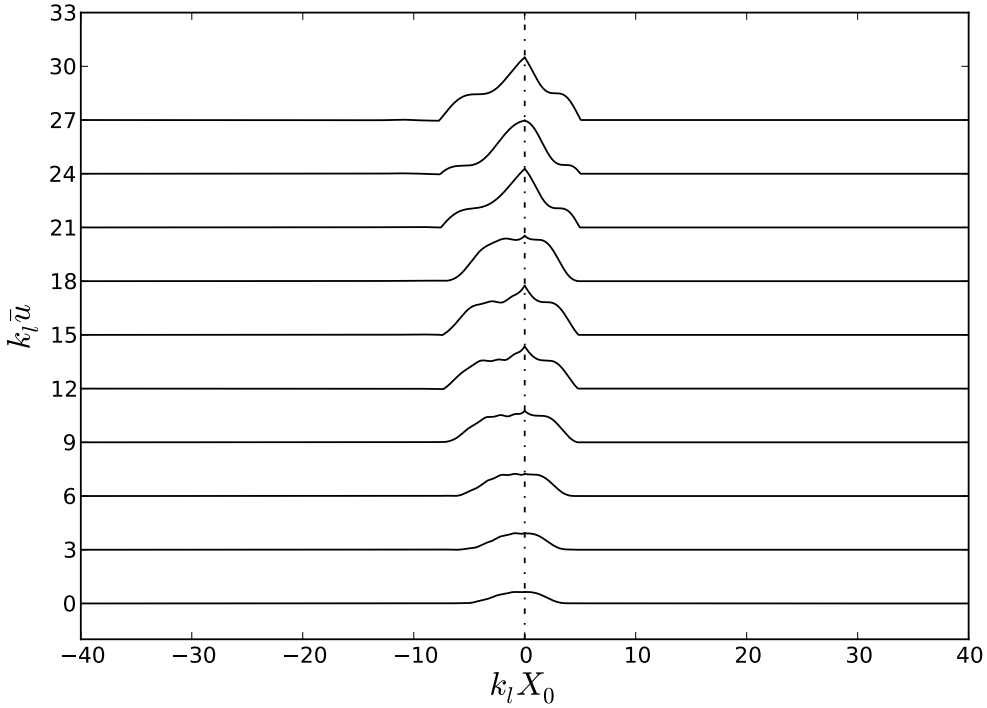

Figure 9.39: Case 4c: Mean longitudinal displacement evolution versus time from $\hat{t} = 3.10$ (bottom) through $\hat{t} = 3.90$ (top) in increments of $\Delta\hat{t} = 0.08$ each separated by 3.0 units vertically.

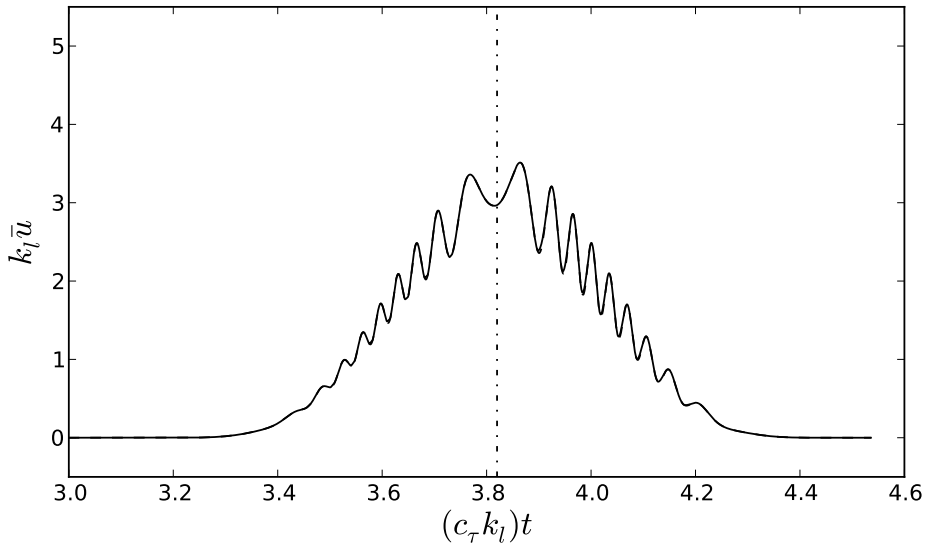

Figure 9.40: Case 4c: Mean longitudinal displacement maximum versus time plot - solid line is mean maximum and dashed line is mean at the interface.

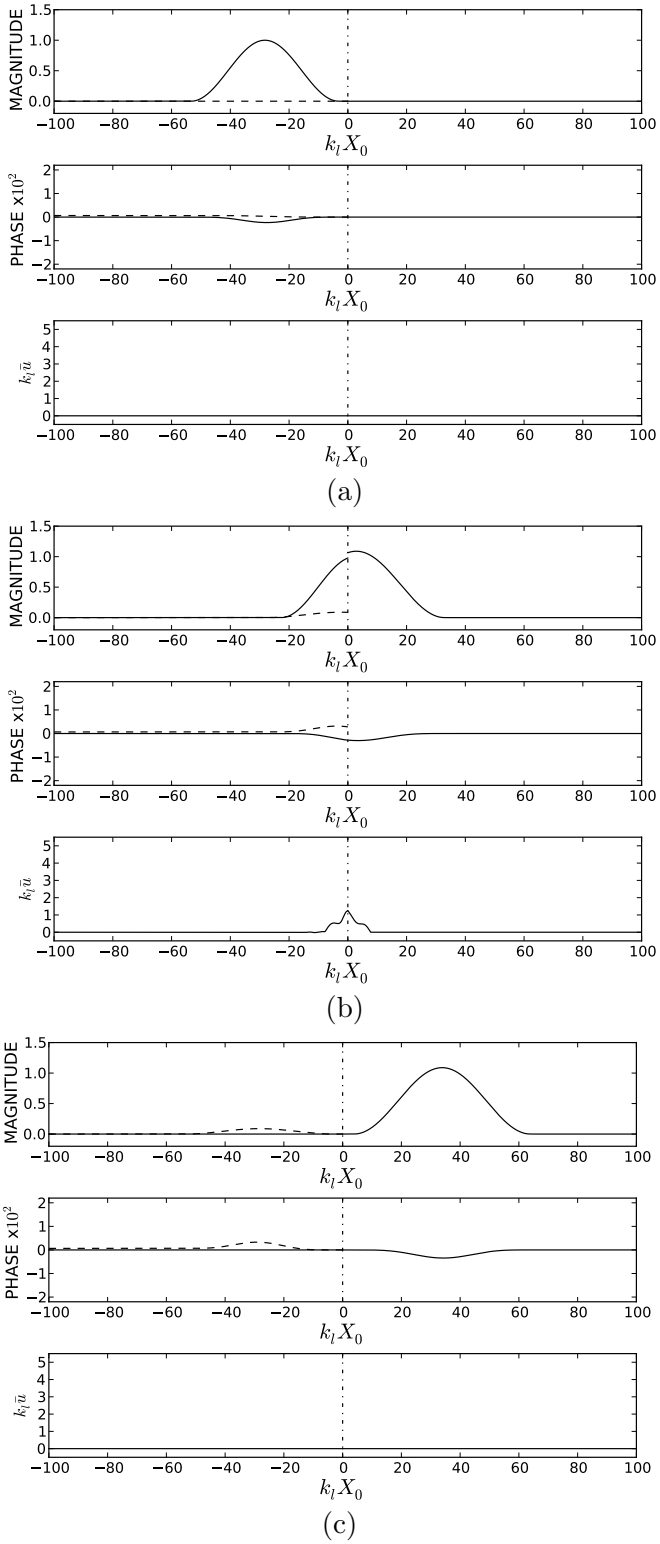

Figure 9.41: Case 4d: Results with $\rho_n = 0.7$, $(EA)_n = 0.7$, and $c_n^2 = 4.0$, at time of (a) $\hat{t} = 3.10$, (b) $\hat{t} = 3.78$, and (c) $\hat{t} = 4.54$.

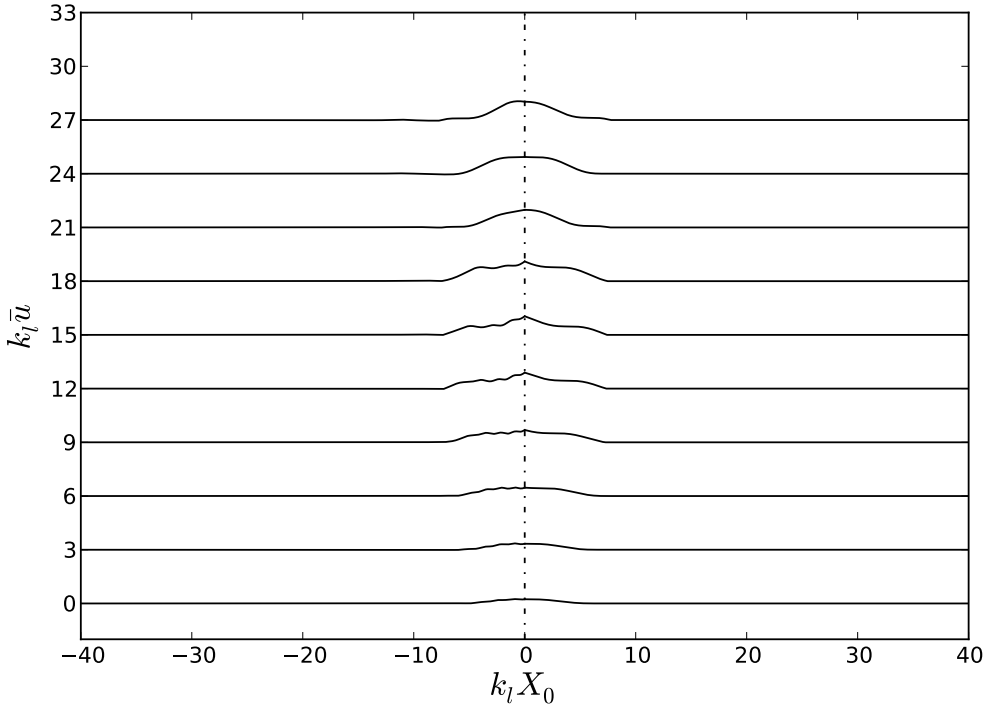

Figure 9.42: Case 4d: Mean longitudinal displacement evolution versus time from $\hat{t} = 3.10$ (bottom) through $\hat{t} = 3.90$ (top) in increments of $\Delta\hat{t} = 0.08$ each separated by 3.0 units vertically.

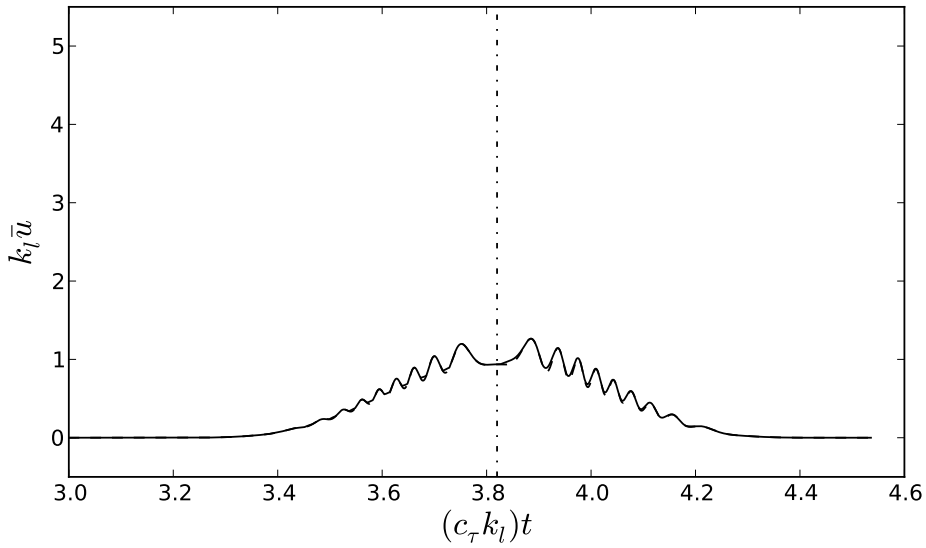

Figure 9.43: Case 4d: Mean longitudinal displacement maximum versus time plot - solid line is mean maximum and dashed line is mean at the interface.

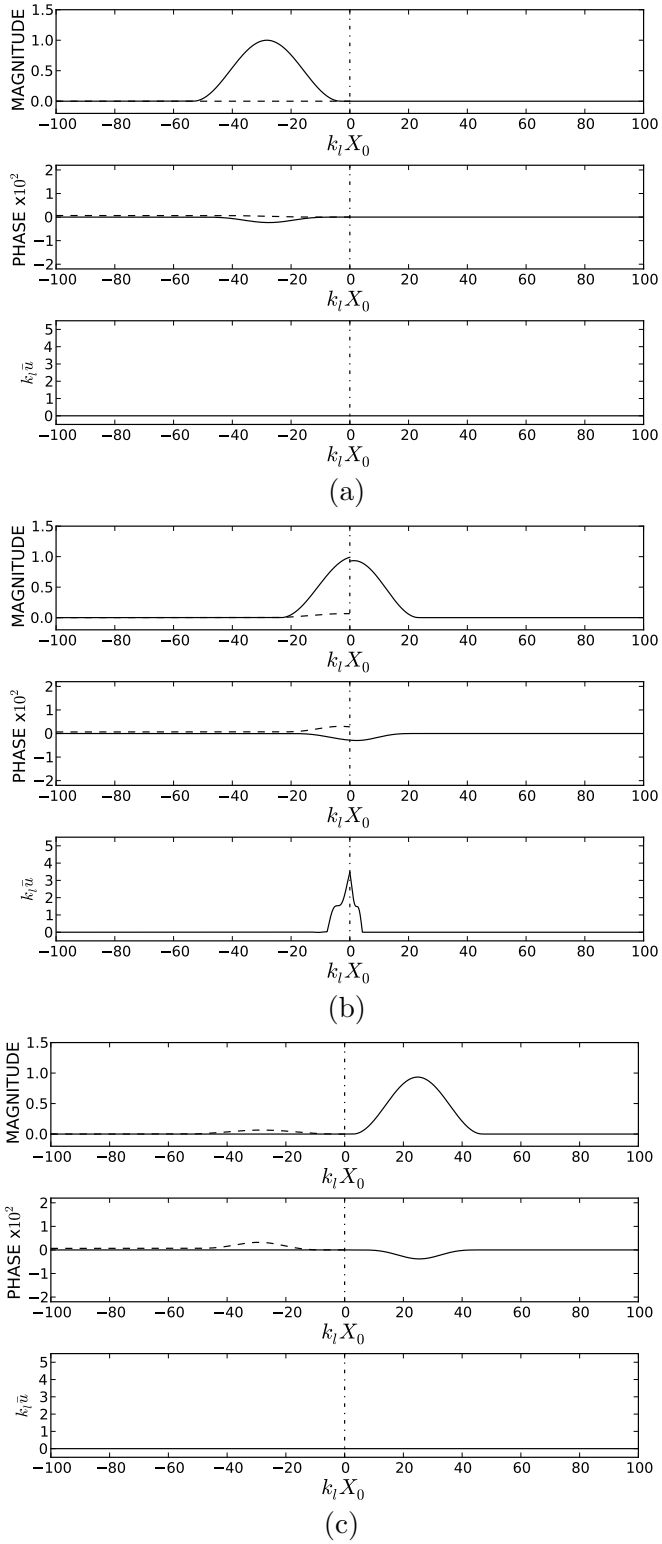

Figure 9.44: Case 5a: Results with $\rho_n = 1.3$, $(EA)_n = 0.4$, and $c_n^2 = 4.0$, at time of (a) $\hat{t} = 3.10$, (b) $\hat{t} = 3.78$, and (c) $\hat{t} = 4.54$.

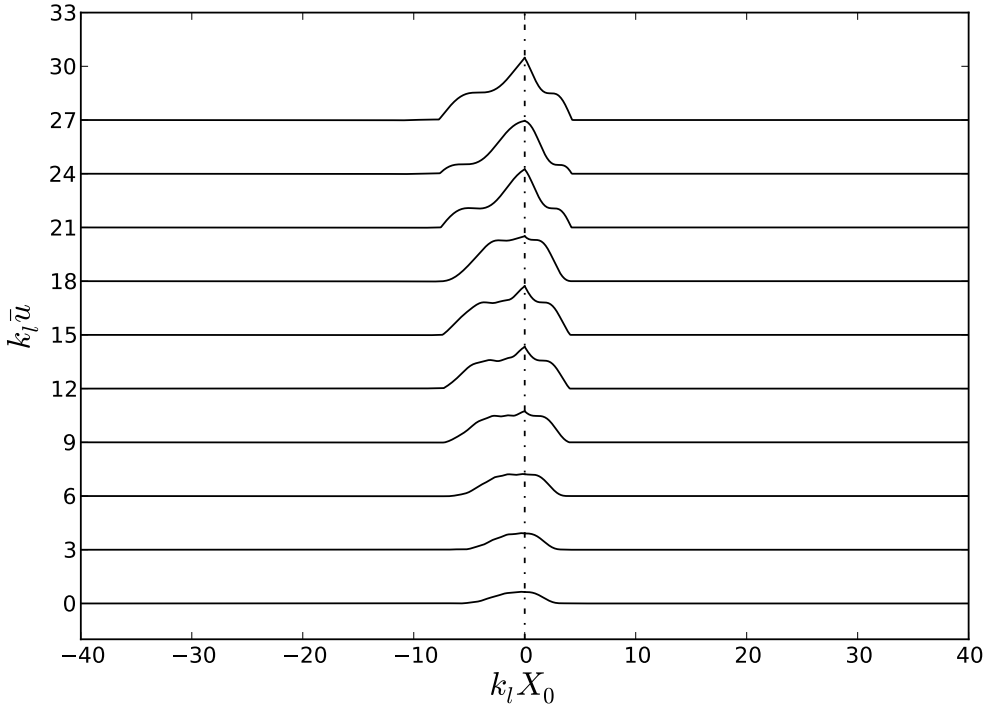

Figure 9.45: Case 5a: Mean longitudinal displacement evolution versus time from $\hat{t} = 3.10$ (bottom) through $\hat{t} = 3.90$ (top) in increments of $\Delta\hat{t} = 0.08$ each separated by 3.0 units vertically.

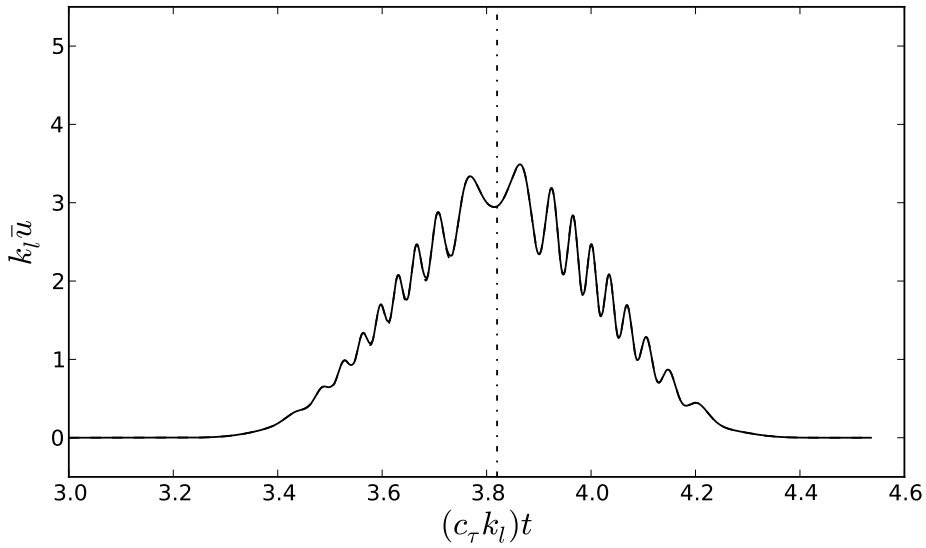

Figure 9.46: Case 5a: Mean longitudinal displacement maximum versus time plot - solid line is mean maximum and dashed line is mean at the interface.

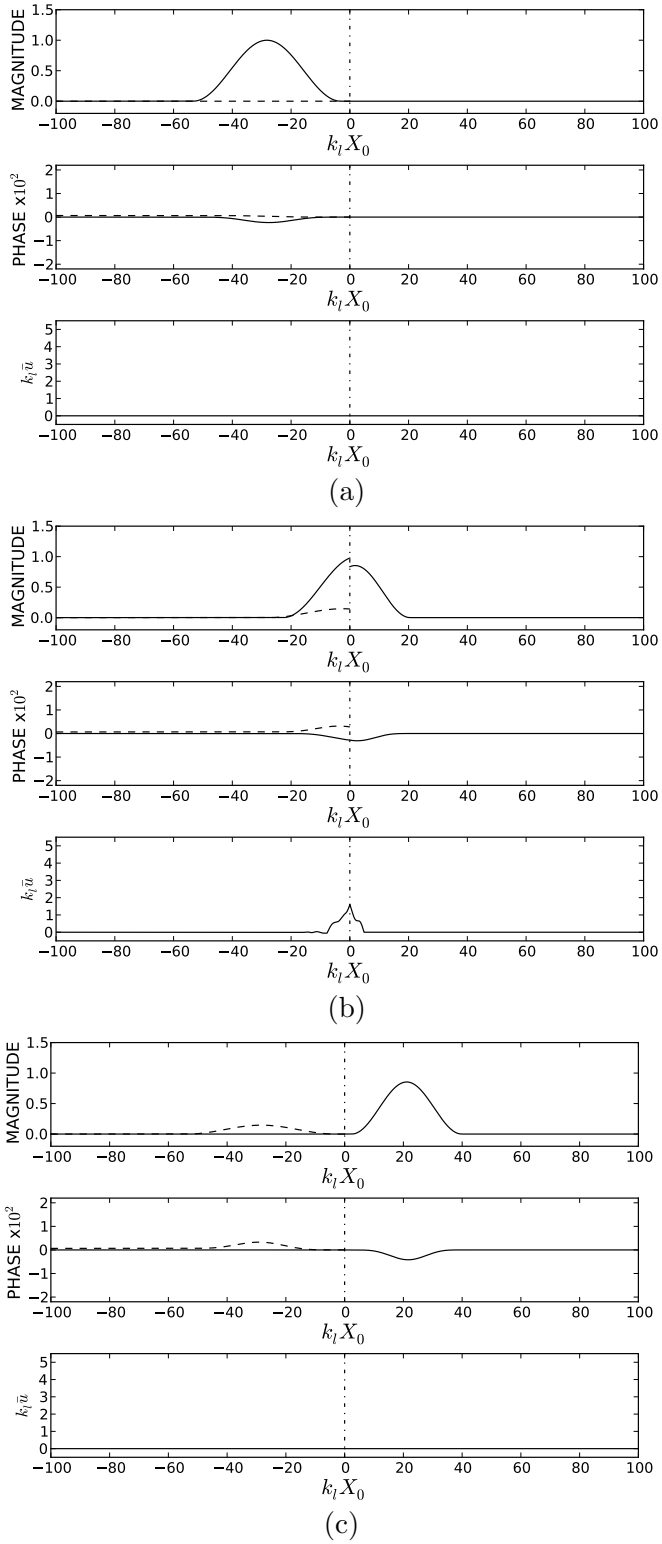

Figure 9.47: Case 5b: Results with $\rho_n = 1.8$, $(EA)_n = 0.7$, and $c_n^2 = 4.0$, at time of (a) $\hat{t} = 3.10$, (b) $\hat{t} = 3.78$, and (c) $\hat{t} = 4.54$.

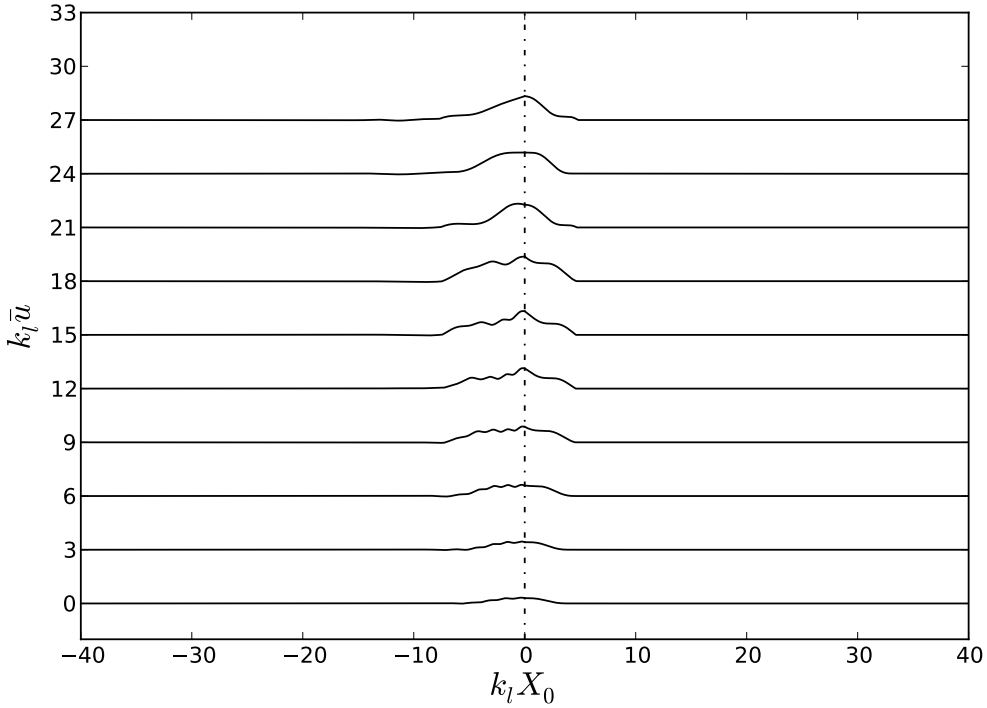

Figure 9.48: Case 5b: Mean longitudinal displacement evolution versus time from $\hat{t} = 3.10$ (bottom) through $\hat{t} = 3.90$ (top) in increments of $\Delta\hat{t} = 0.08$ each separated by 3.0 units vertically.

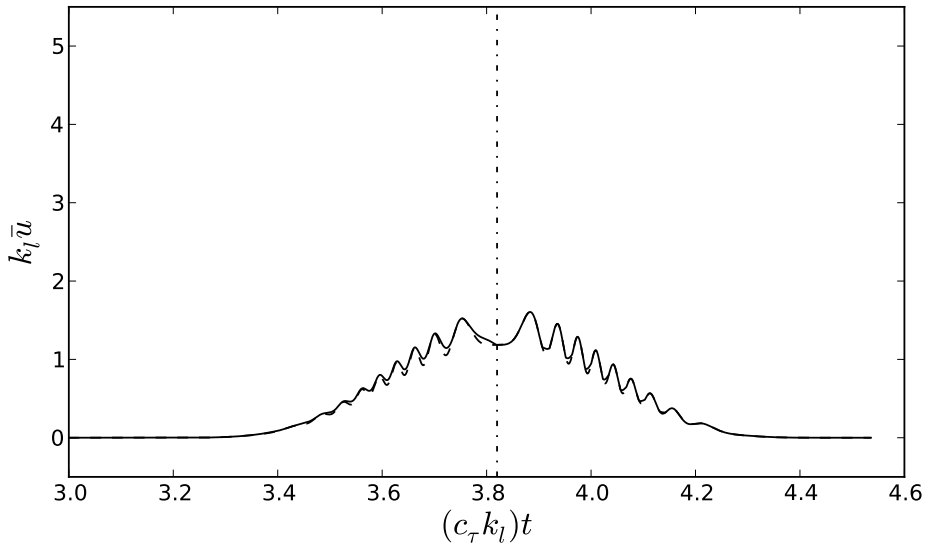

Figure 9.49: Case 5b: Mean longitudinal displacement maximum versus time plot - solid line is mean maximum and dashed line is mean at the interface.

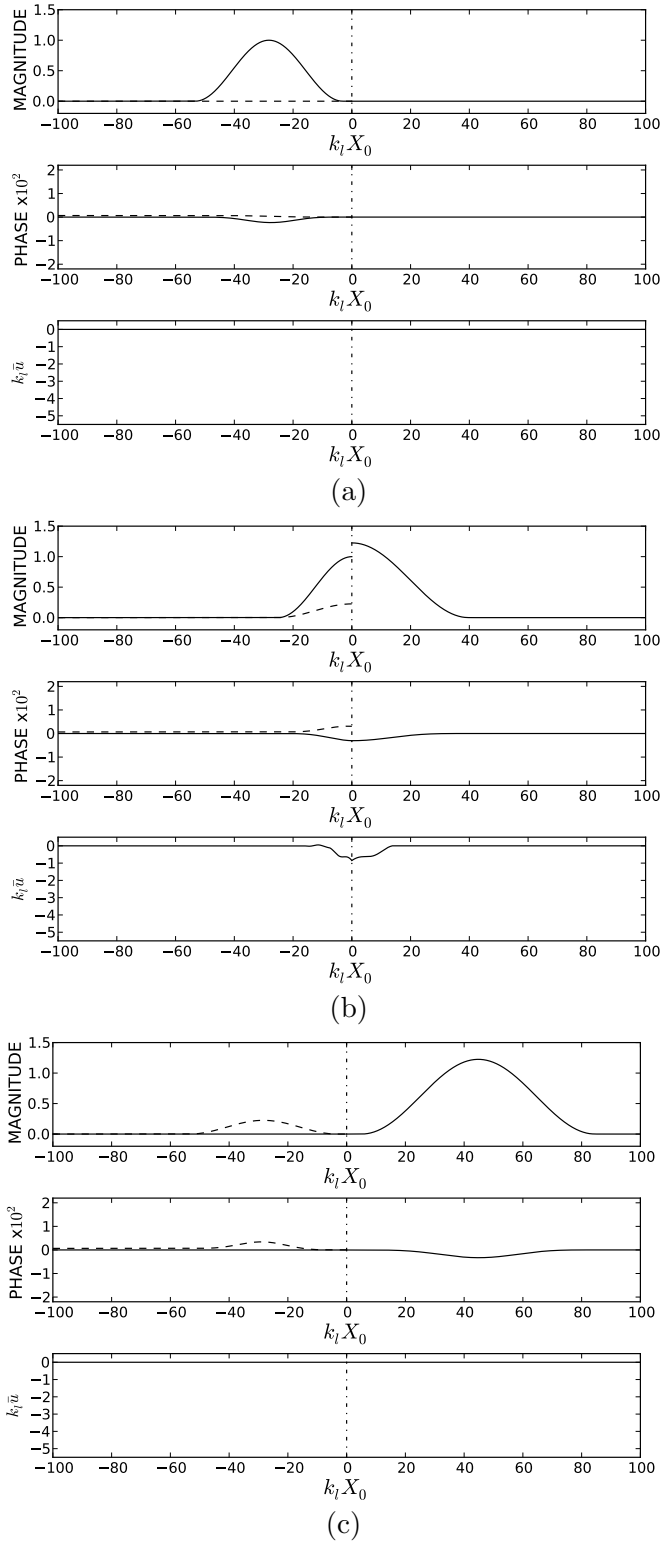

Figure 9.50: Case 5c: Results with $\rho_n = 0.4$, $(EA)_n = 1.3$, and $c_n^2 = 4.0$, at time of (a) $\hat{t} = 3.10$, (b) $\hat{t} = 3.78$, and (c) $\hat{t} = 4.54$.

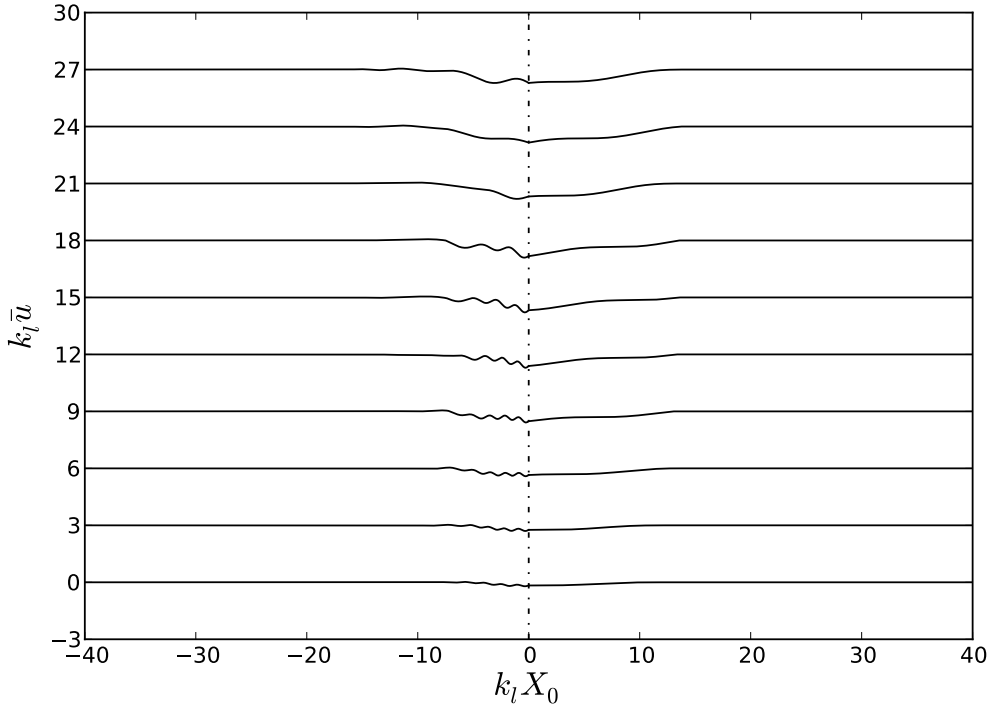

Figure 9.51: Case 5c: Mean longitudinal displacement evolution versus time from $\hat{t} = 3.10$ (bottom) through $\hat{t} = 3.90$ (top) in increments of $\Delta\hat{t} = 0.08$ each separated by 3.0 units vertically.

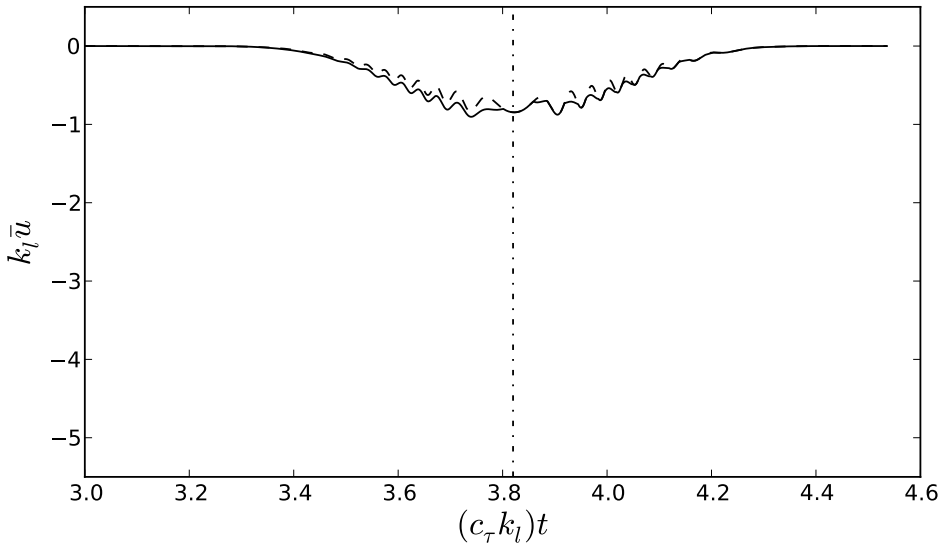

Figure 9.52: Case 5c: Mean longitudinal displacement maximum versus time plot - solid line is mean maximum and dashed line is mean at the interface.

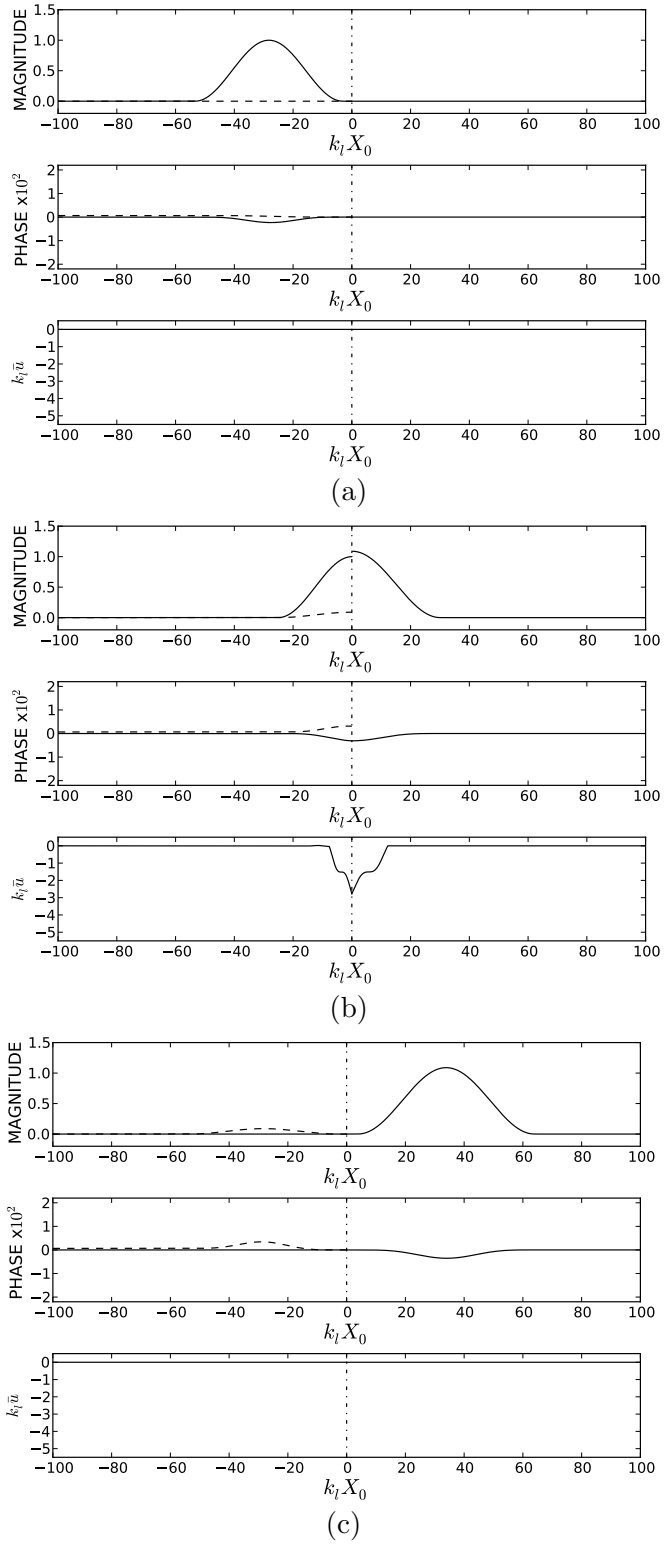

Figure 9.53: Case 5d: Results with $\rho_n = 0.7$, $(EA)_n = 1.8$, and $c_n^2 = 4.0$, at time of (a) $\hat{t} = 3.10$, (b) $\hat{t} = 3.78$, and (c) $\hat{t} = 4.54$.

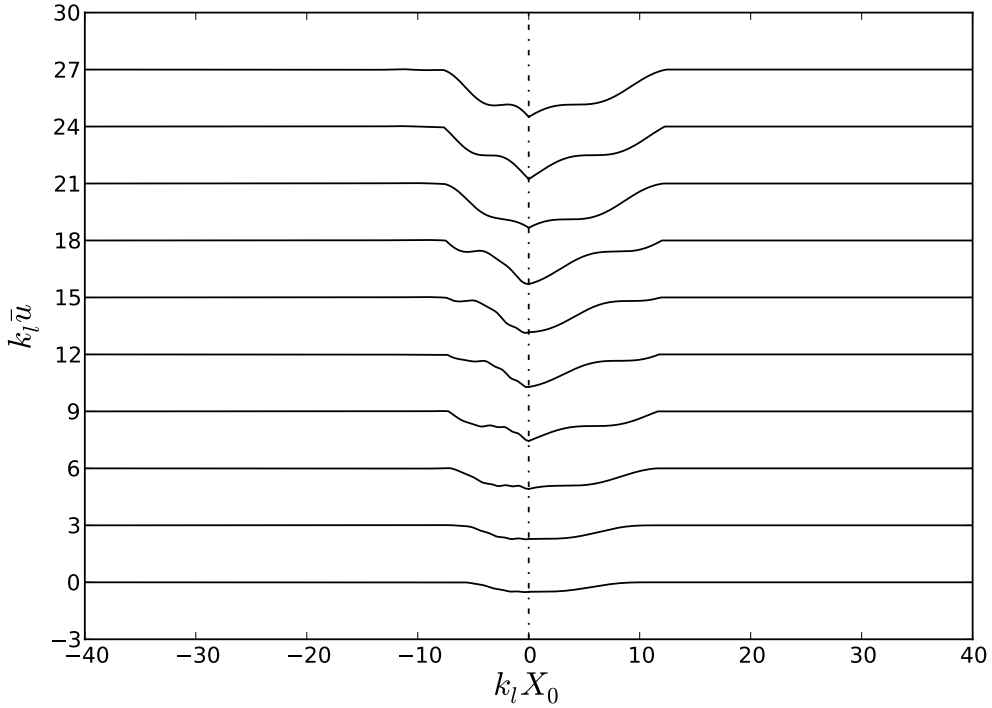

Figure 9.54: Case 5d: Mean longitudinal displacement evolution versus time from $\hat{t} = 3.10$ (bottom) through $\hat{t} = 3.90$ (top) in increments of $\Delta\hat{t} = 0.08$ each separated by 3.0 units vertically.

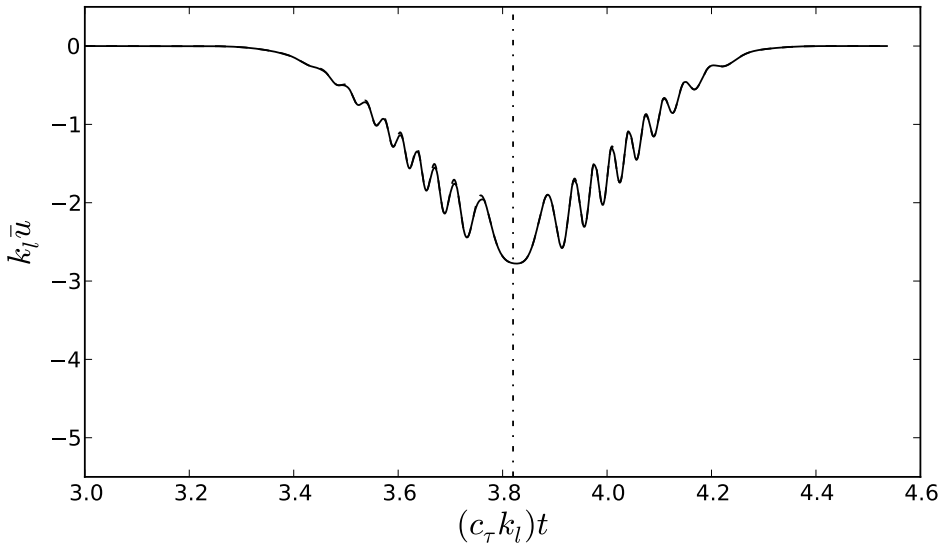

Figure 9.55: Case 5d: Mean longitudinal displacement maximum versus time plot - solid line is mean maximum and dashed line is mean at the interface.

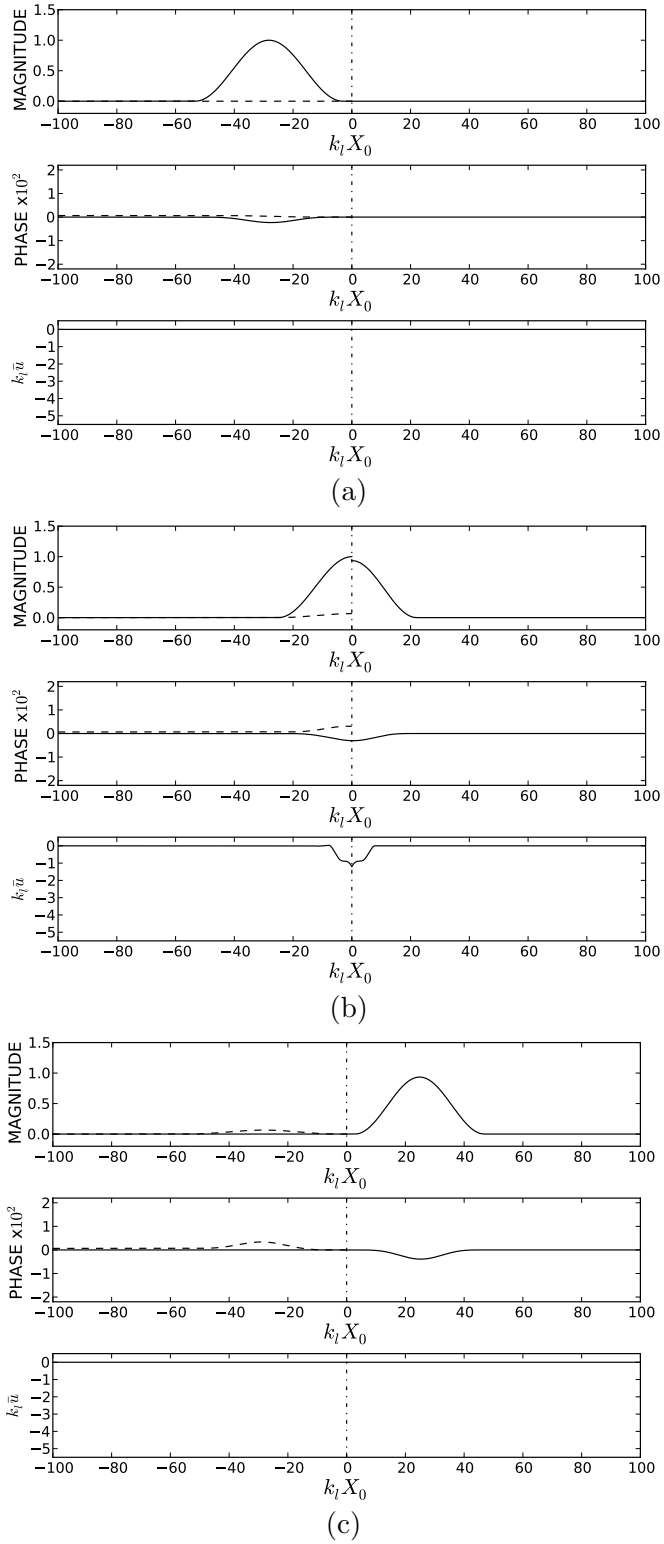

Figure 9.56: Case 6a: Results with $\rho_n = 1.3$, $(EA)_n = 1.3$, and $c_n^2 = 4.0$, at time of (a) $\hat{t} = 3.10$, (b) $\hat{t} = 3.78$, and (c) $\hat{t} = 4.54$.

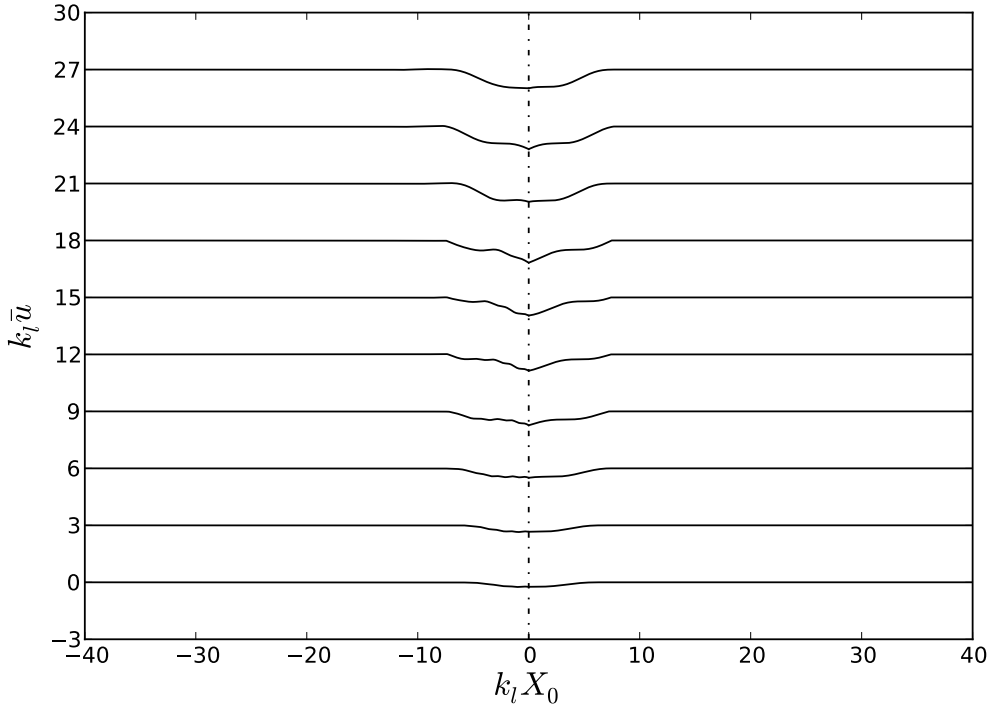

Figure 9.57: Case 6a: Mean longitudinal displacement evolution versus time from $\hat{t} = 3.10$ (bottom) through $\hat{t} = 3.90$ (top) in increments of $\Delta\hat{t} = 0.08$ each separated by 3.0 units vertically.

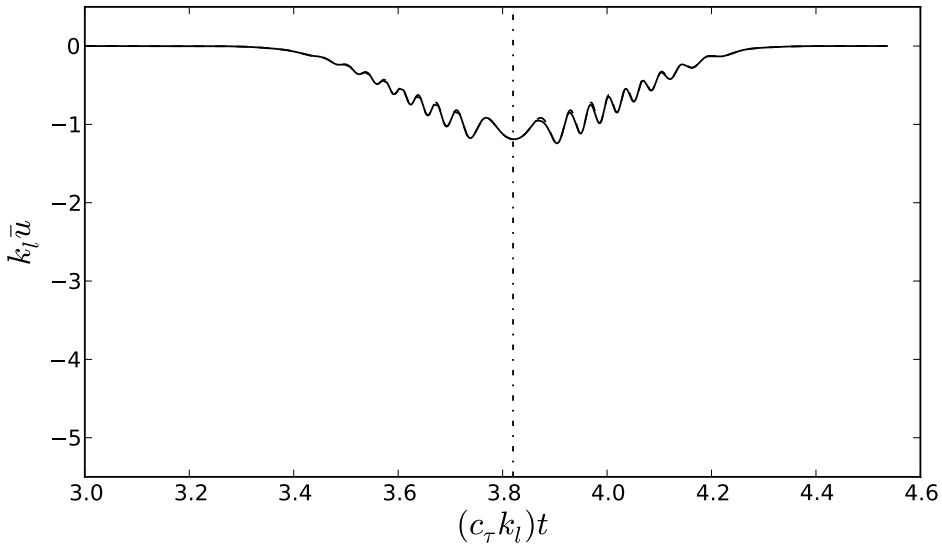

Figure 9.58: Case 6a: Mean longitudinal displacement maximum versus time plot - solid line is mean maximum and dashed line is mean at the interface.

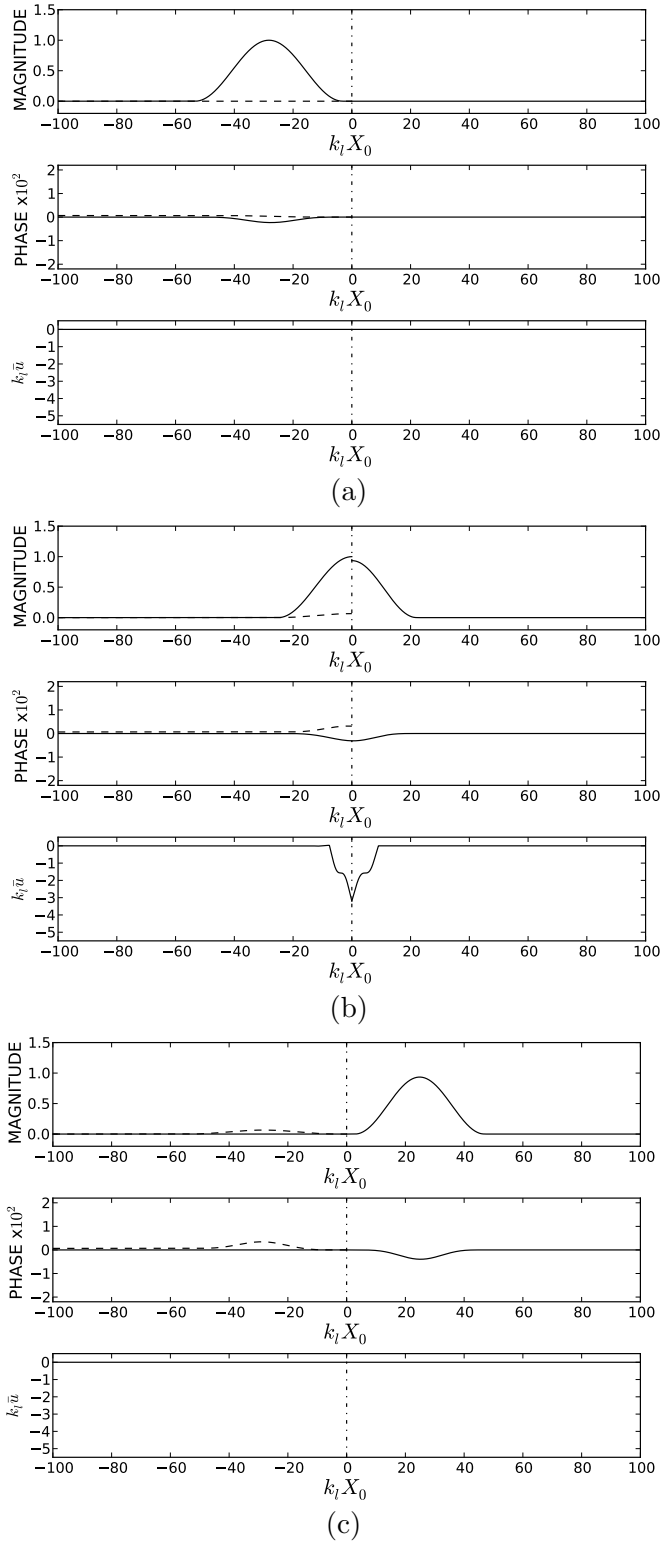

Figure 9.59: Case 6b: Results with $\rho_n = 1.3$, $(EA)_n = 1.8$, and $c_n^2 = 4.0$, at time of (a) $\hat{t} = 3.10$, (b) $\hat{t} = 3.78$, and (c) $\hat{t} = 4.54$.

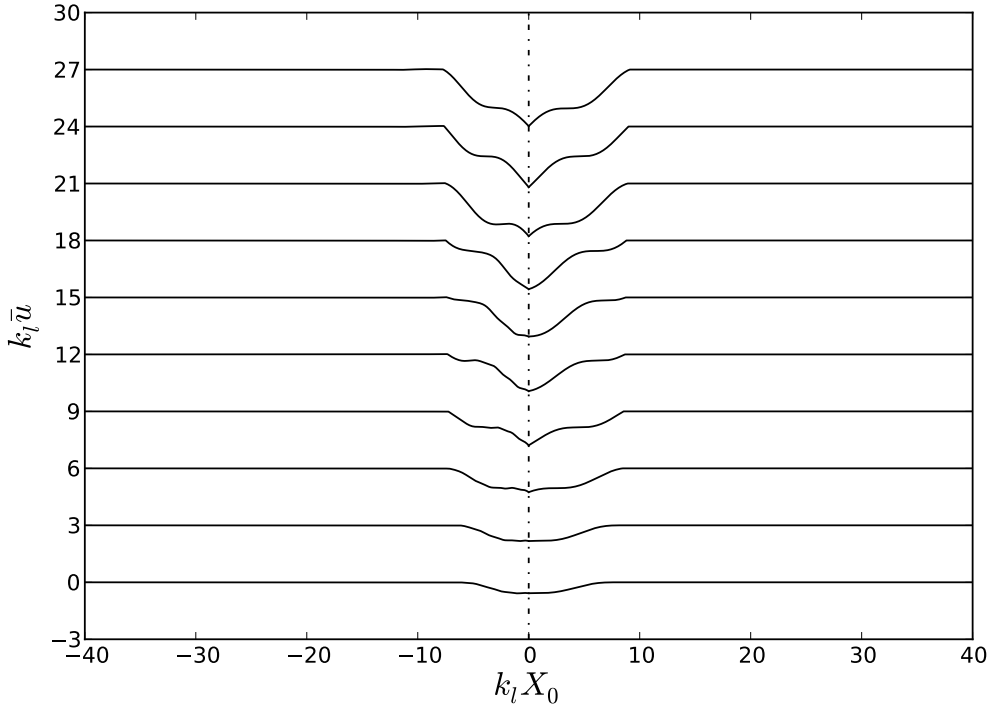

Figure 9.60: Case 6b: Mean longitudinal displacement evolution versus time from $\hat{t} = 3.10$ (bottom) through $\hat{t} = 3.90$ (top) in increments of $\Delta\hat{t} = 0.08$ each separated by 3.0 units vertically.

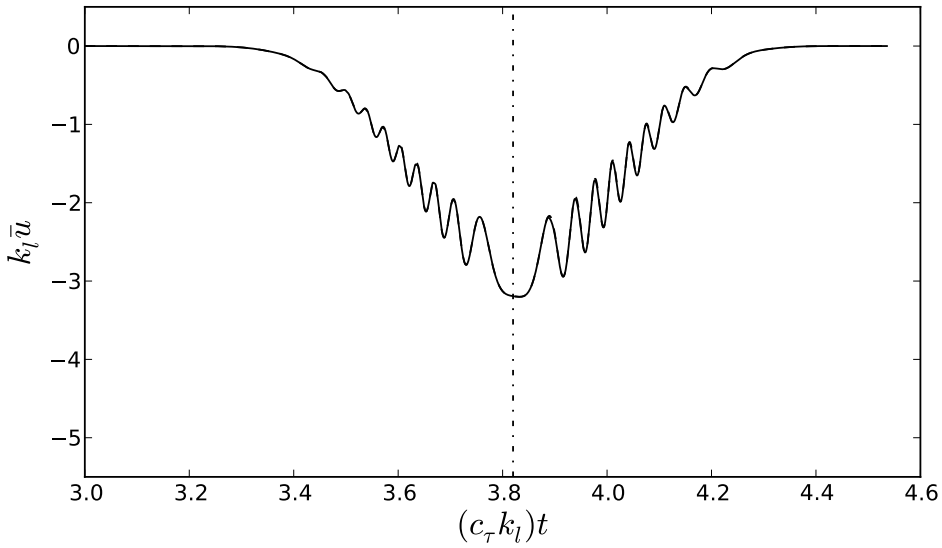

Figure 9.61: Case 6b: Mean longitudinal displacement maximum versus time plot - solid line is mean maximum and dashed line is mean at the interface.

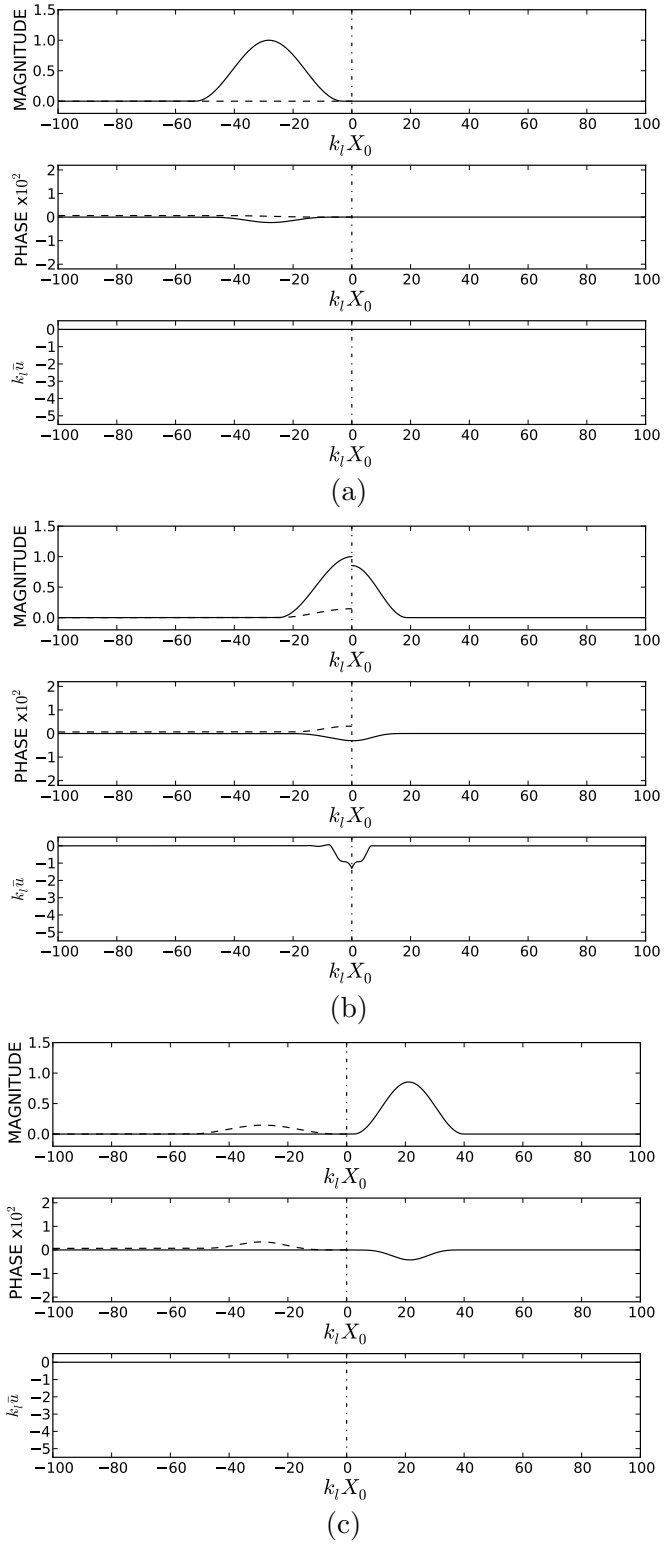

Figure 9.62: Case 6c: Results with $\rho_n = 1.8$, $(EA)_n = 1.3$, and $c_n^2 = 4.0$, at time of (a) $\hat{t} = 3.10$, (b) $\hat{t} = 3.78$, and (c) $\hat{t} = 4.54$.

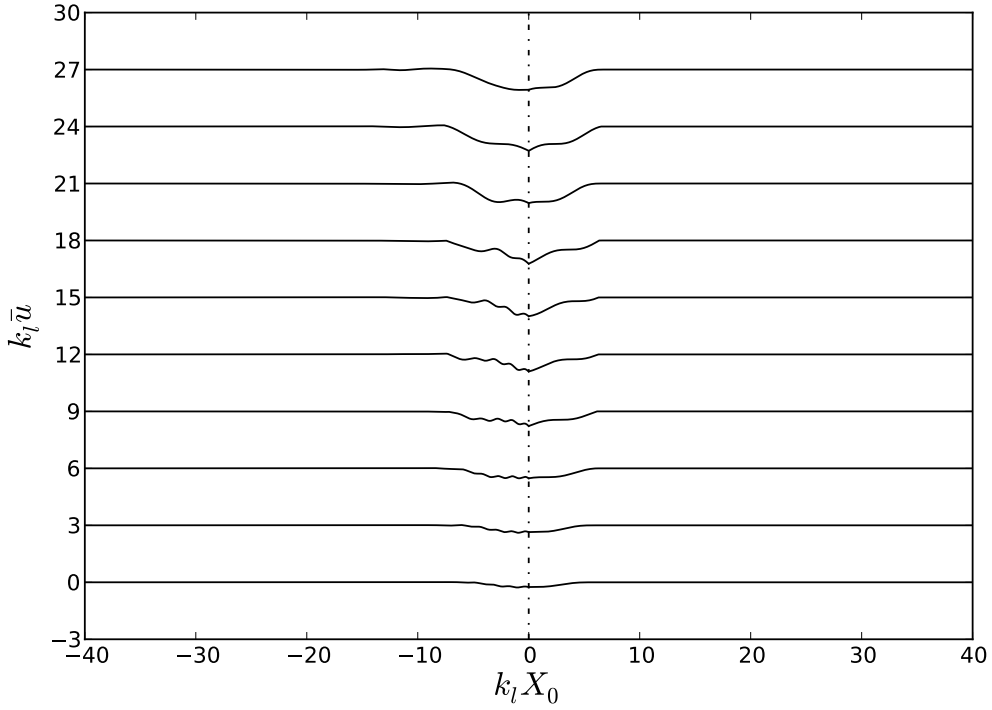

Figure 9.63: Case 6c: Mean longitudinal displacement evolution versus time from $\hat{t} = 3.10$ (bottom) through $\hat{t} = 3.90$ (top) in increments of $\Delta\hat{t} = 0.08$ each separated by 3.0 units vertically.

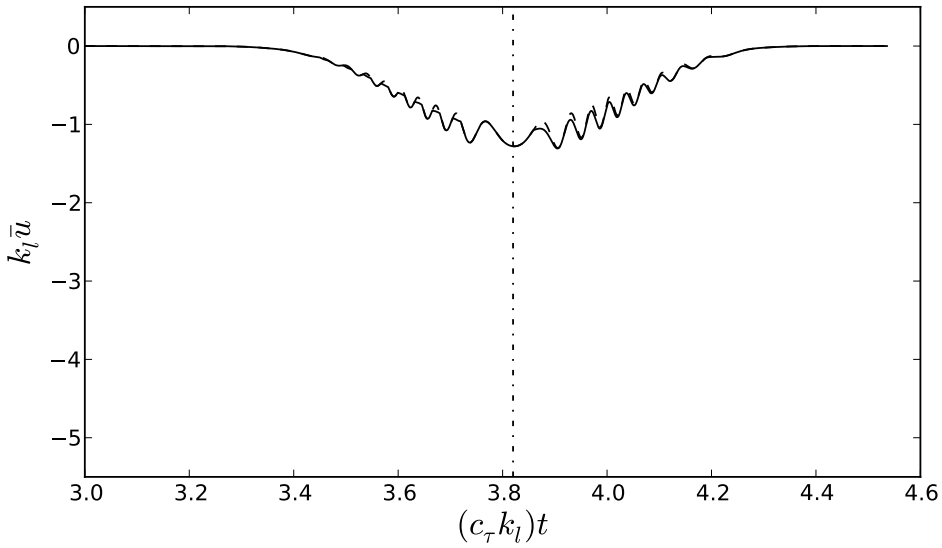

Figure 9.64: Case 6c: Mean longitudinal displacement maximum versus time plot - solid line is mean maximum and dashed line is mean at the interface.

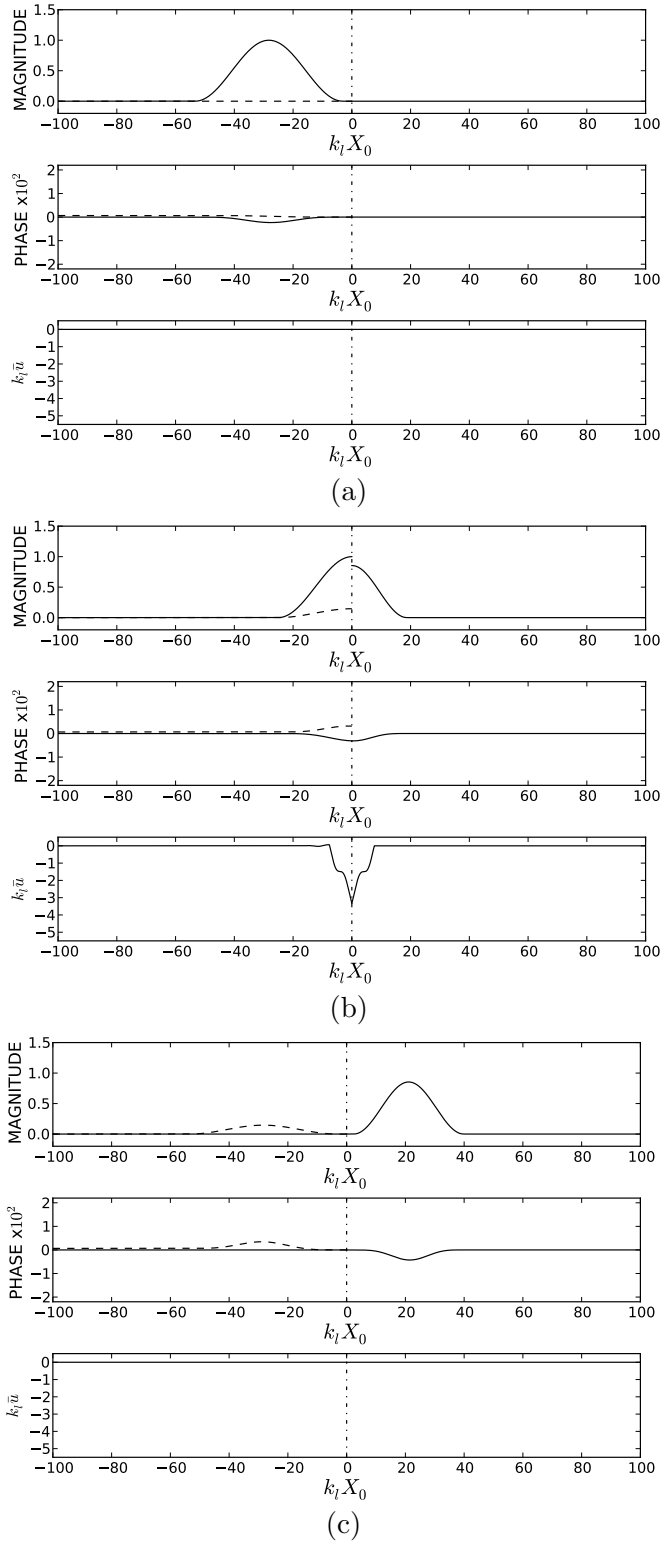

Figure 9.65: Case 6d: Results with $\rho_n = 1.8$, $(EA)_n = 1.8$, and $c_n^2 = 4.0$, at time of (a) $\hat{t} = 3.10$, (b) $\hat{t} = 3.78$, and (c) $\hat{t} = 4.54$.

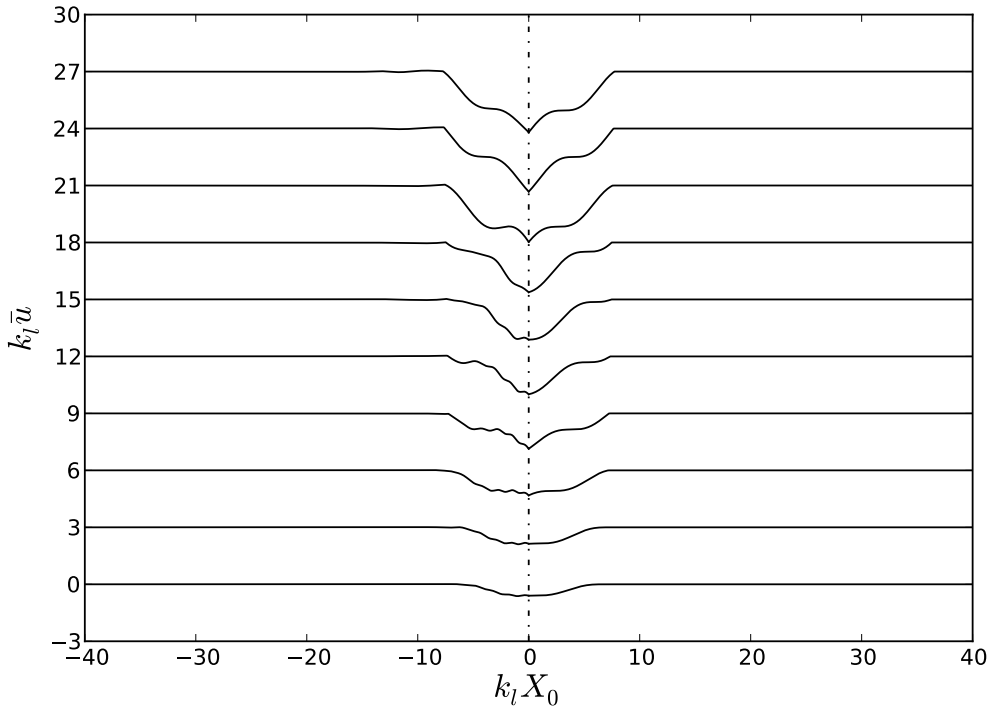

Figure 9.66: Case 6d: Mean longitudinal displacement evolution versus time from $\hat{t} = 3.10$ (bottom) through $\hat{t} = 3.90$ (top) in increments of $\Delta\hat{t} = 0.08$ each separated by 3.0 units vertically.

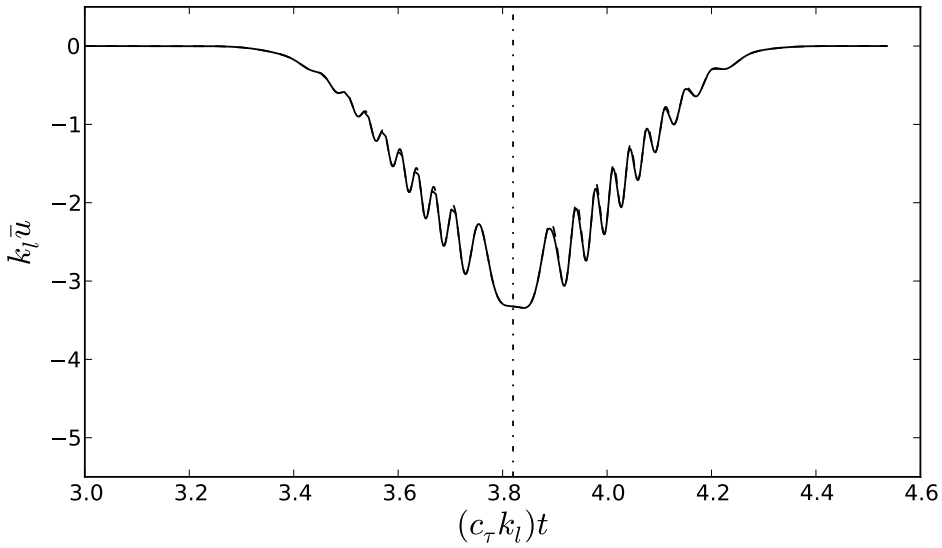

Figure 9.67: Case 6d: Mean longitudinal displacement maximum versus time plot - solid line is mean maximum and dashed line is mean at the interface.

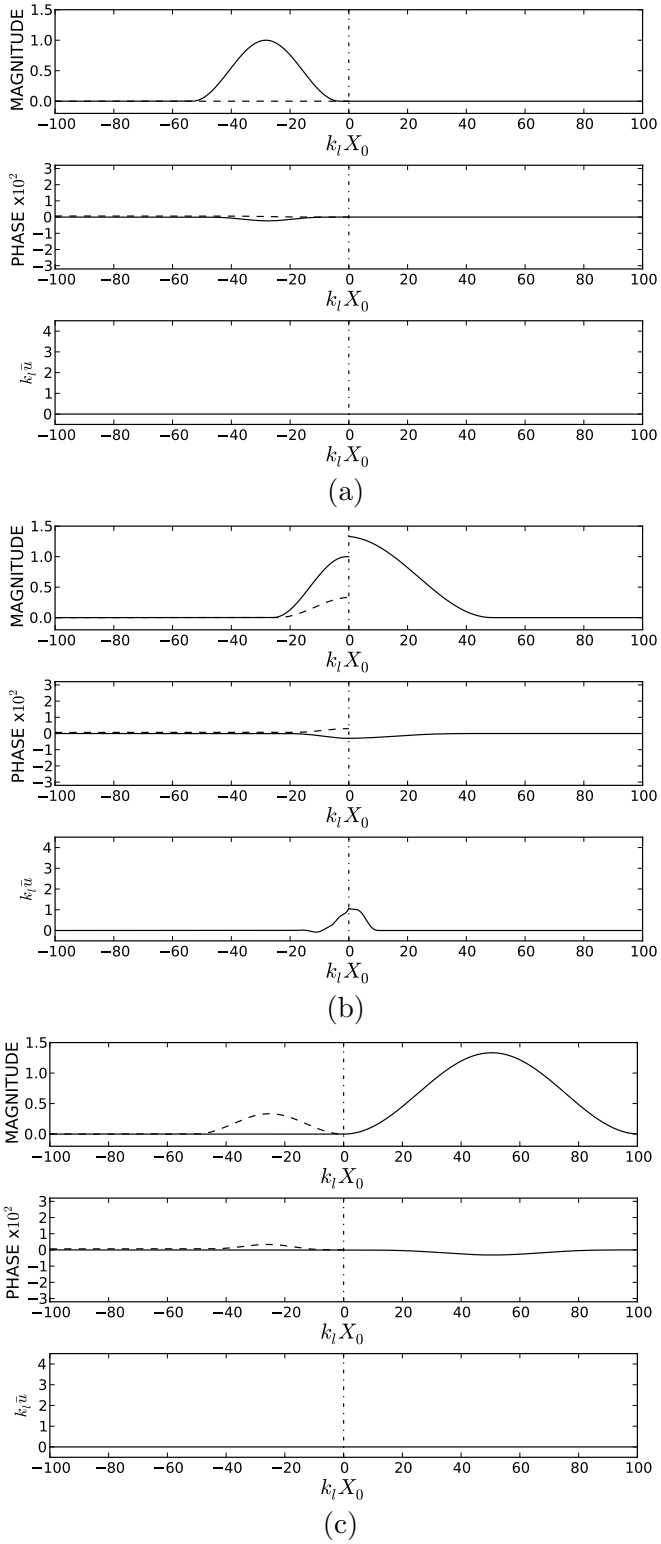

Figure 9.68: Case 7a: Results with $\rho_n = 0.25$, $(EA)_n = 0.5$, and $c_n^2 = 4.0$, at time of (a) $\hat{t} = 3.10$, (b) $\hat{t} = 3.78$, and (c) $\hat{t} = 4.54$.

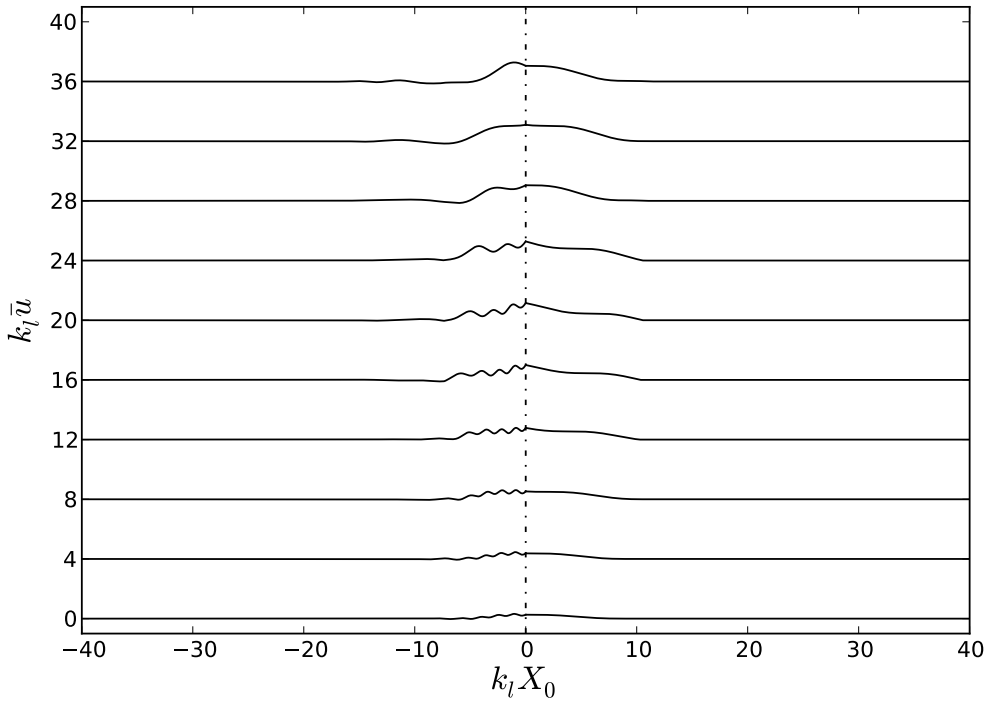

Figure 9.69: Case 7a: Mean longitudinal displacement evolution versus time from $\hat{t} = 3.10$ (bottom) through $\hat{t} = 3.90$ (top) in increments of $\Delta\hat{t} = 0.08$ each separated by 4.0 units vertically.

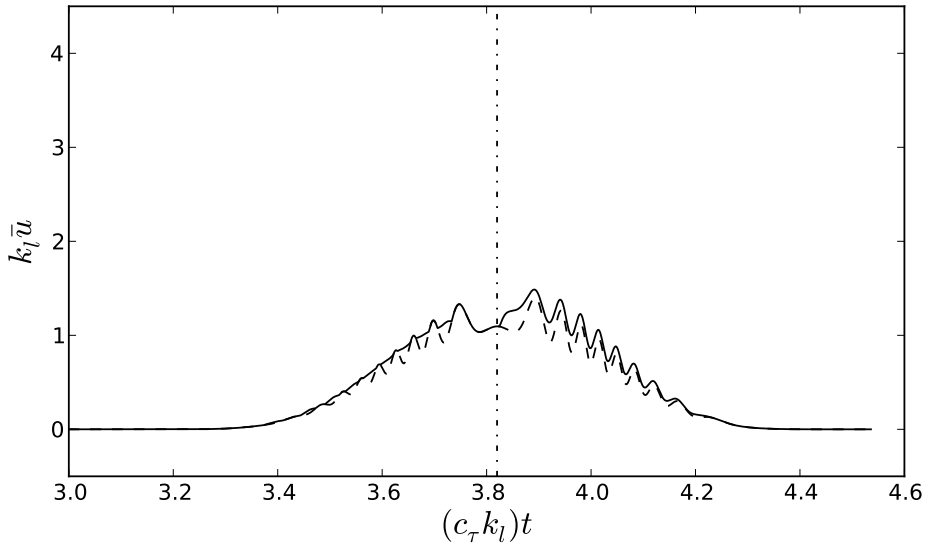

Figure 9.70: Case 7a: Mean longitudinal displacement maximum versus time plot - solid line is mean maximum and dashed line is mean at the interface.

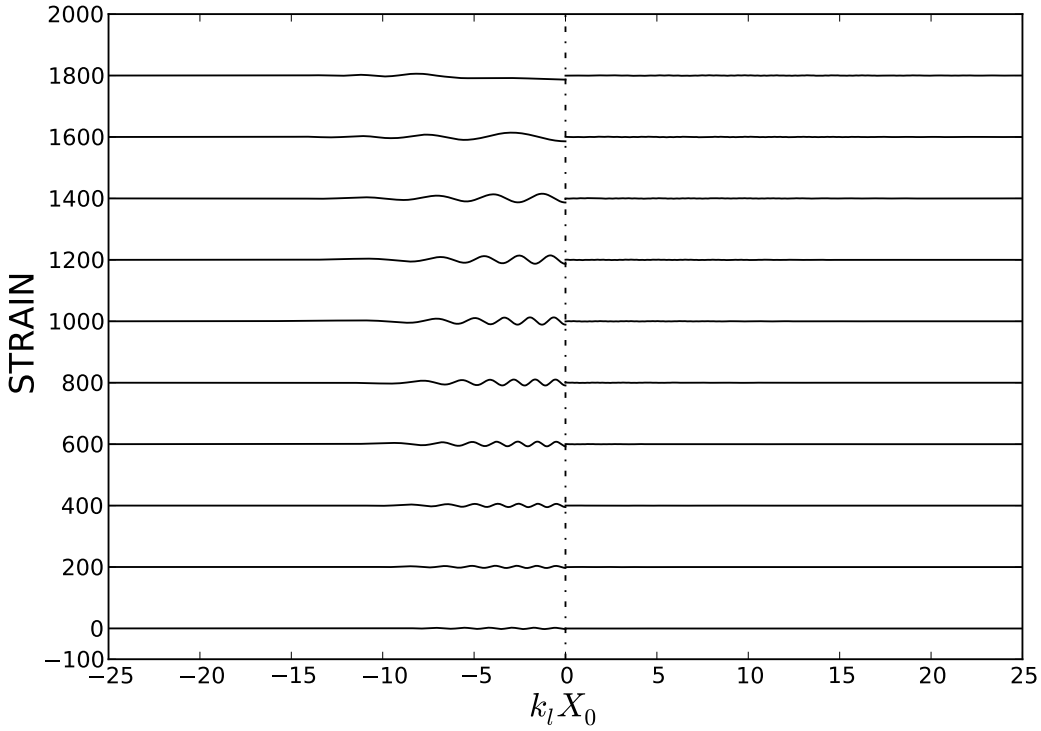

Figure 9.71: Case 7a: Strain evolution versus time from $\hat{t} = 3.10$ (bottom) through $\hat{t} = 3.90$ (top) in increments of $\Delta\hat{t} = 0.08$ each separated by 200 units vertically.

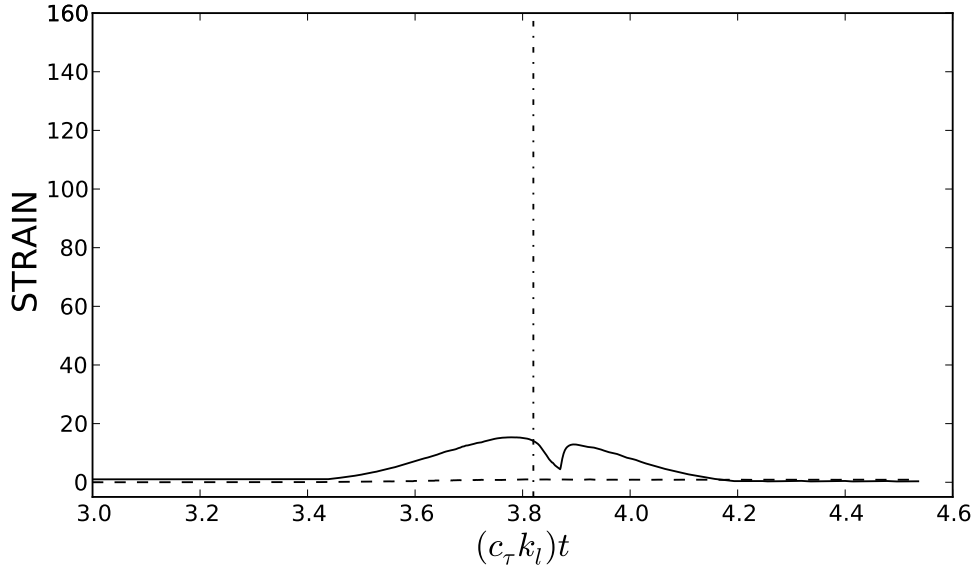

Figure 9.72: Case 7a: Strain maximum versus time plot.

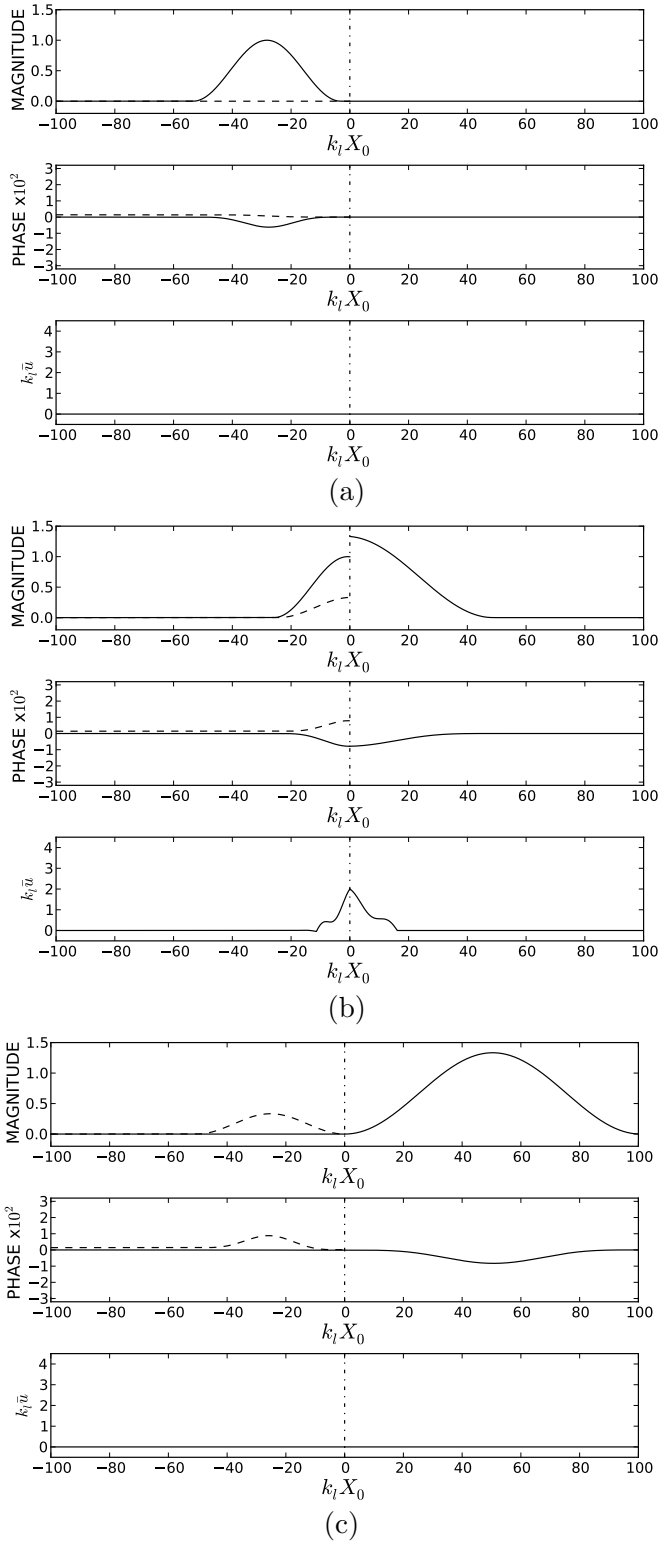

Figure 9.73: Case 7b: Results with $\rho_n = 0.25$, $(EA)_n = 0.5$, and $c_n^2 = 9.0$, at time of (a) $\hat{t} = 3.10$, (b) $\hat{t} = 3.78$, and (c) $\hat{t} = 4.54$.

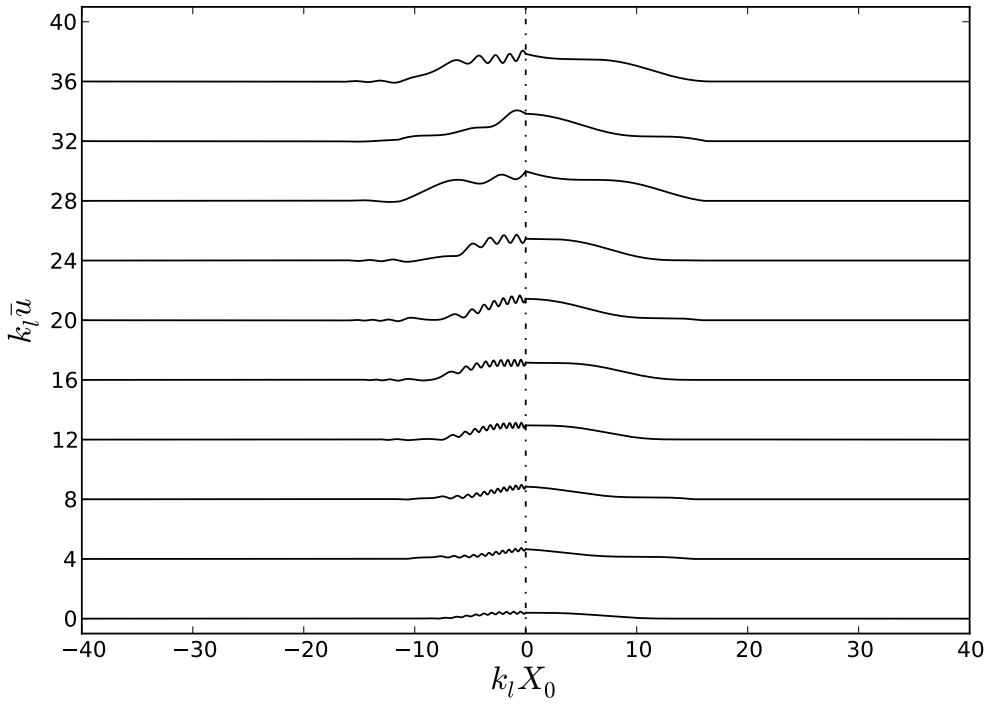

Figure 9.74: Case 7b: Mean longitudinal displacement evolution versus time from $\hat{t} = 3.10$ (bottom) through $\hat{t} = 3.90$ (top) in increments of $\Delta\hat{t} = 0.08$ each separated by 4.0 units vertically.

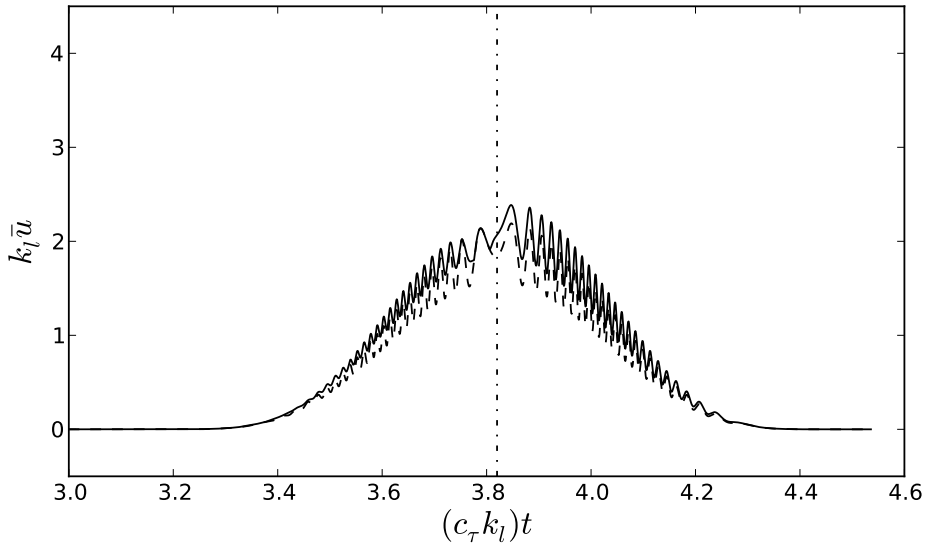

Figure 9.75: Case 7b: Mean longitudinal displacement maximum versus time plot - solid line is mean maximum and dashed line is mean at the interface.

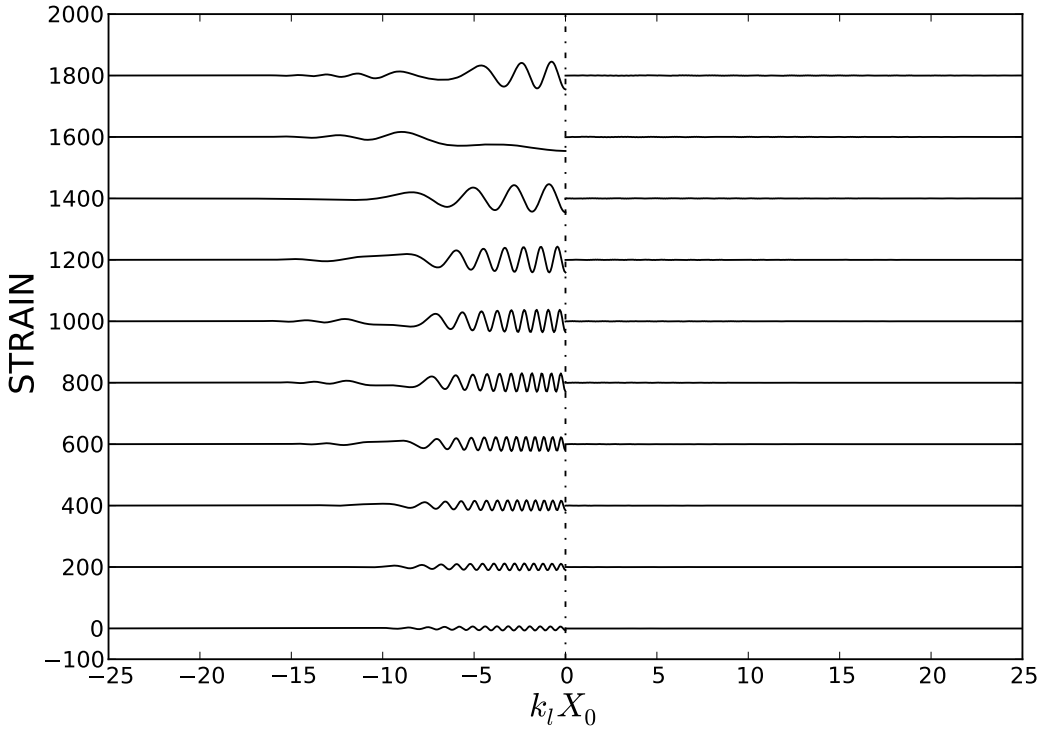

Figure 9.76: Case 7b: Strain evolution versus time from $\hat{t} = 3.10$ (bottom) through $\hat{t} = 3.90$ (top) in increments of $\Delta\hat{t} = 0.08$ each separated by 200 units vertically.

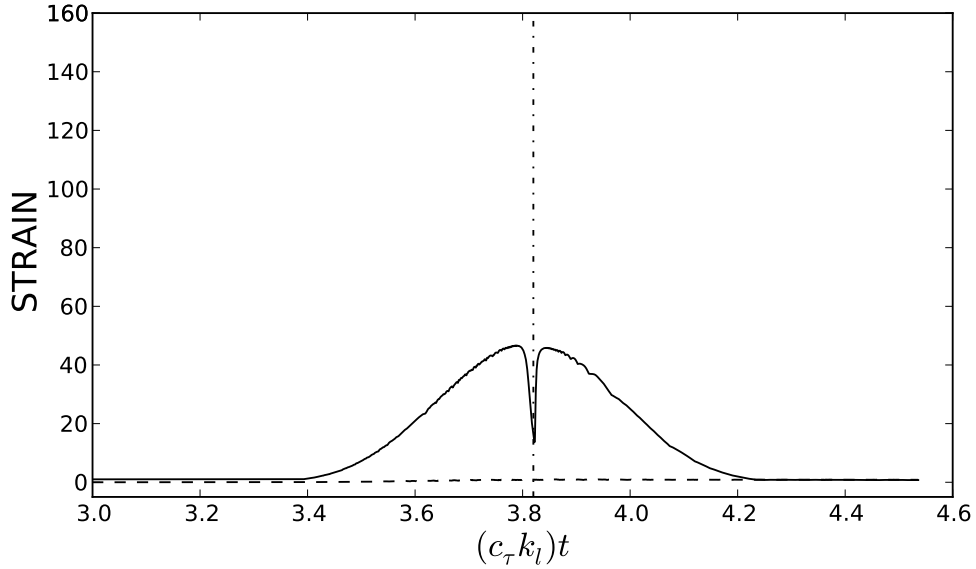

Figure 9.77: Case 7b: Strain maximum versus time plot.

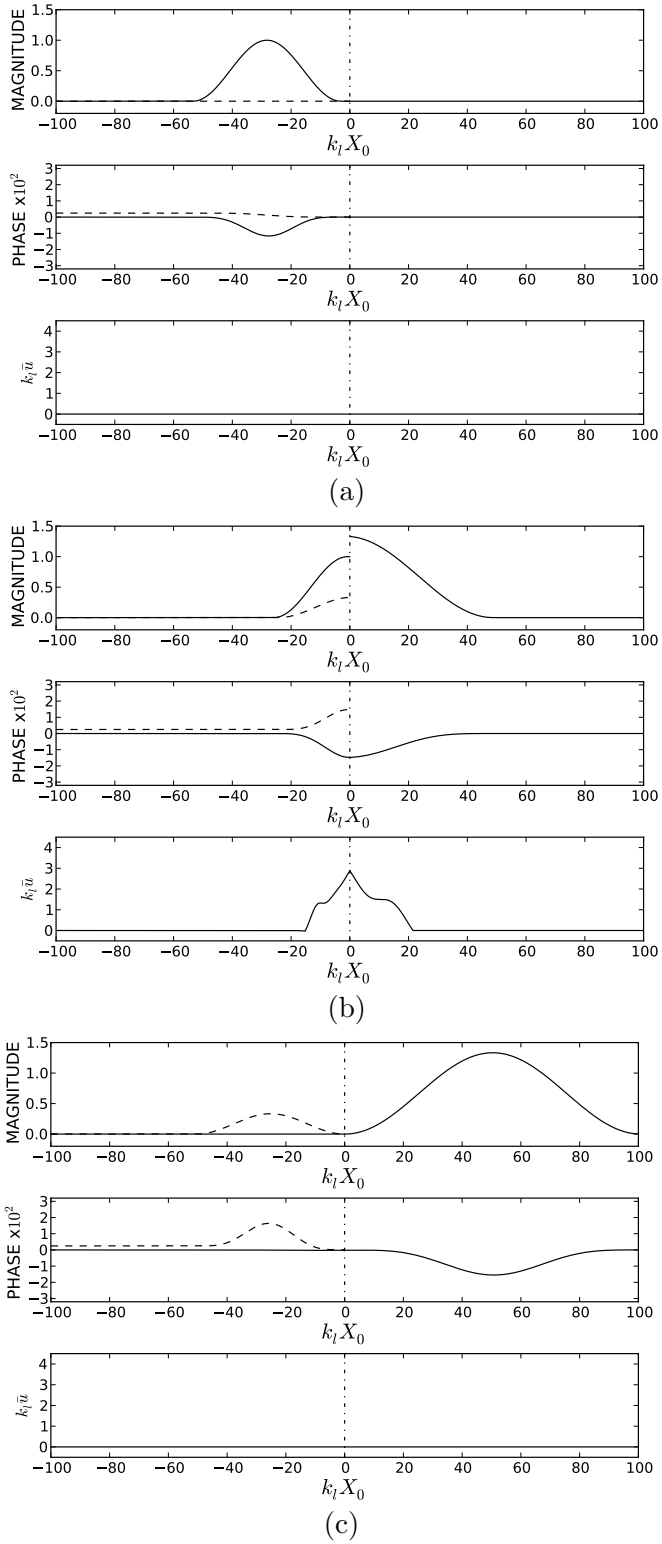

Figure 9.78: Case 7c: Results with $\rho_n = 0.25$, $(EA)_n = 0.5$, and $c_n^2 = 16.0$, at time of (a) $\hat{t} = 3.10$, (b) $\hat{t} = 3.78$, and (c) $\hat{t} = 4.54$.

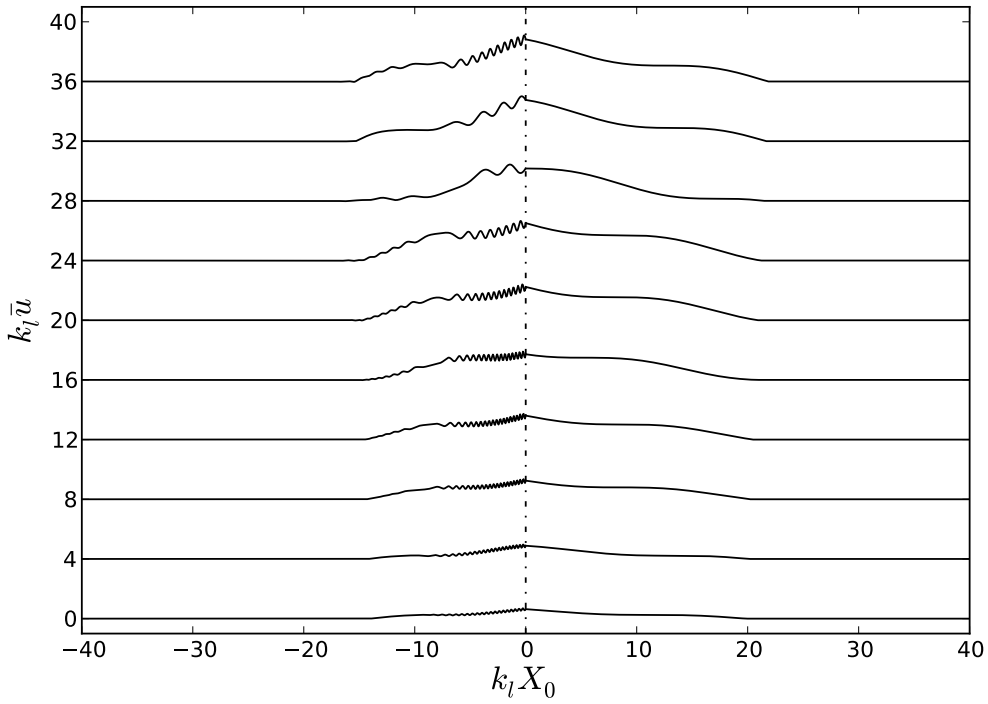

Figure 9.79: Case 7c: Mean longitudinal displacement evolution versus time from $\hat{t} = 3.10$ (bottom) through $\hat{t} = 3.90$ (top) in increments of $\Delta\hat{t} = 0.08$ each separated by 4.0 units vertically.

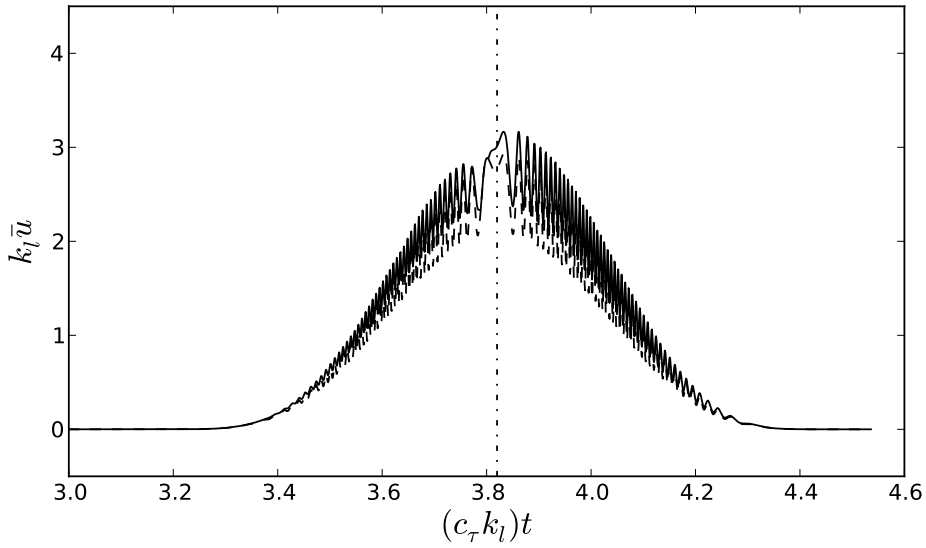

Figure 9.80: Case 7c: Mean longitudinal displacement maximum versus time plot - solid line is mean maximum and dashed line is mean at the interface.

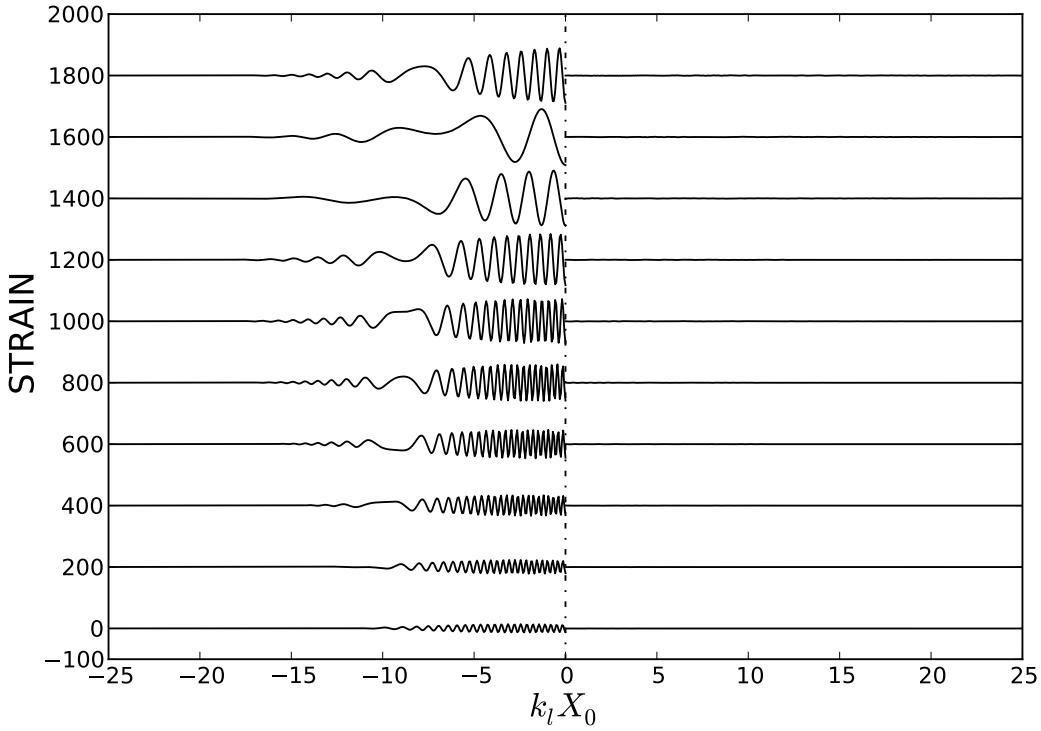

Figure 9.81: Case 7c: Strain evolution versus time from $\hat{t} = 3.10$ (bottom) through $\hat{t} = 3.90$ (top) in increments of $\Delta\hat{t} = 0.08$ each separated by 200 units vertically.

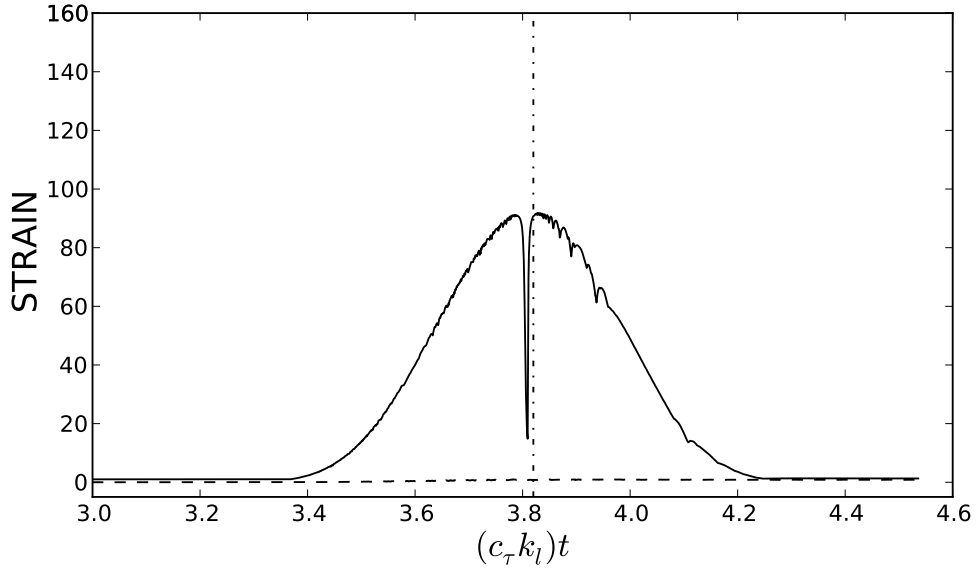

Figure 9.82: Case 7c: Strain maximum versus time plot.

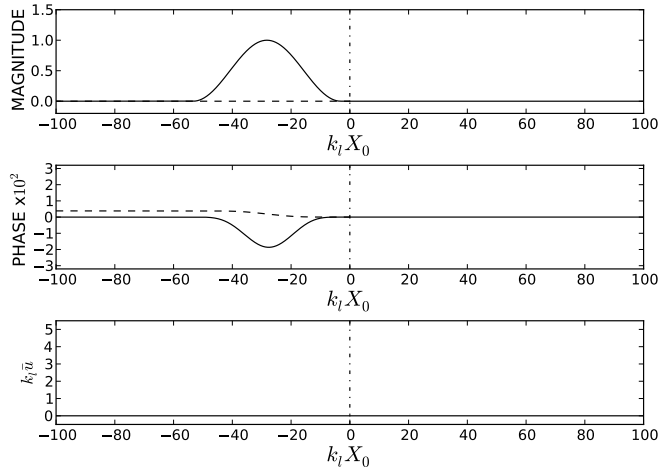

(a)

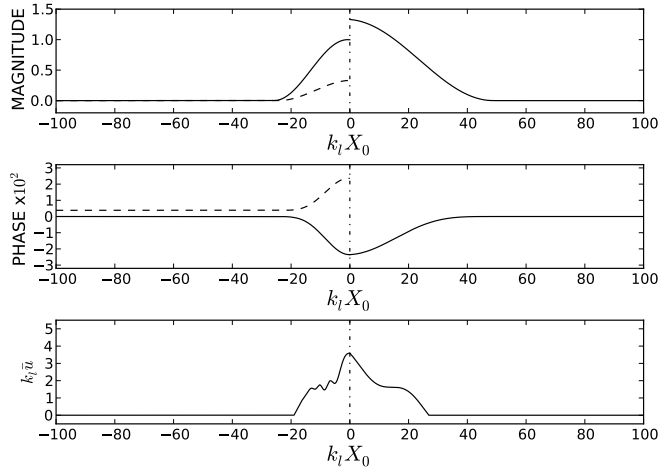

(b)

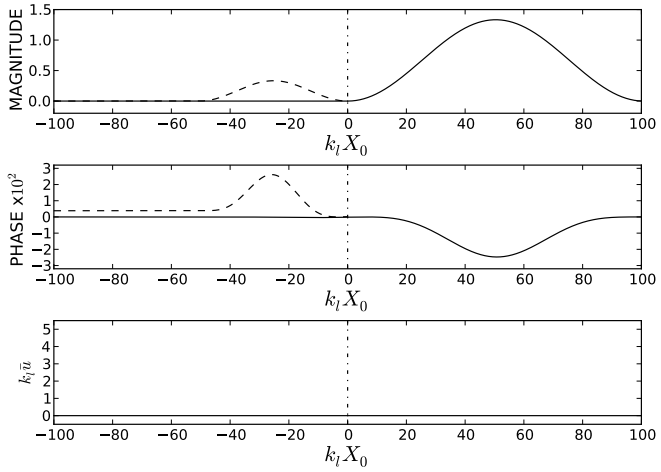

(c)

Figure 9.83: Case 7d: Results with $\rho_n = 0.25$, $(EA)_n = 0.5$, and $c_n^2 = 25.0$, at times of (a) $\hat{t} = 3.10$, (b) $\hat{t} = 3.78$, and (c) $\hat{t} = 4.54$.

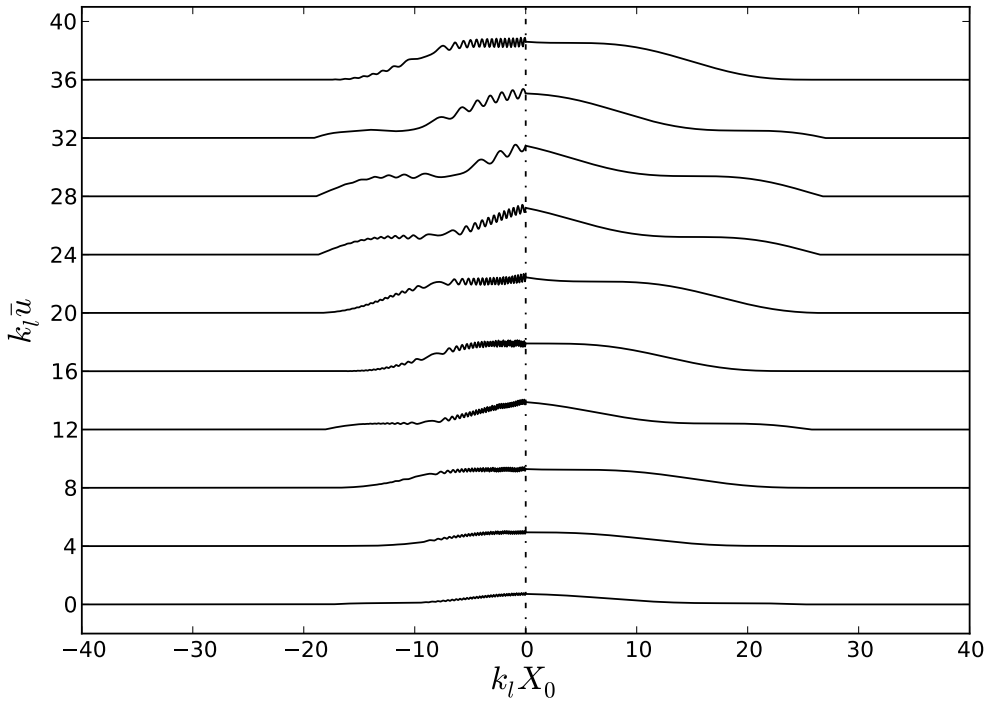

Figure 9.84: Case 7d: Mean longitudinal displacement evolution versus time from $\hat{t} = 3.10$ (bottom) through $\hat{t} = 3.90$ (top) in increments of $\Delta\hat{t} = 0.08$ each separated by 4.0 units vertically.

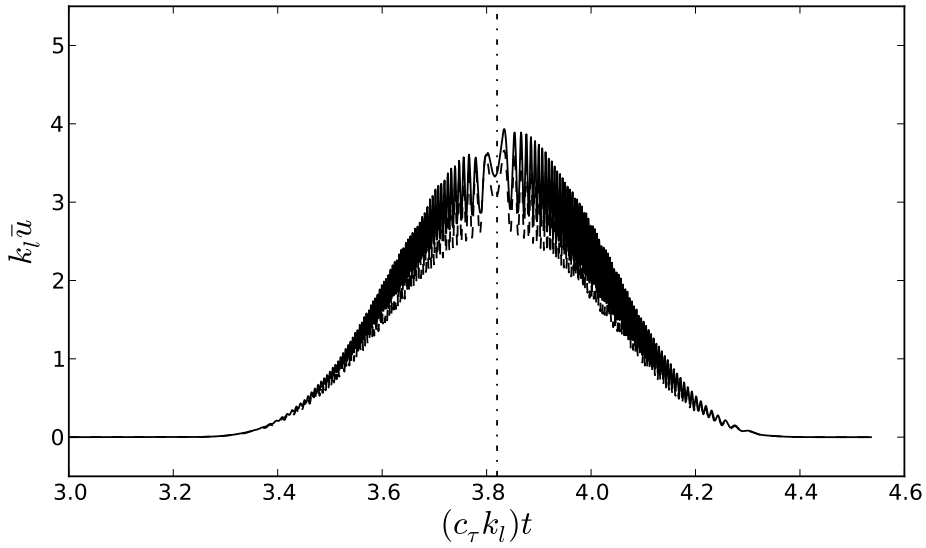

Figure 9.85: Case 7d: Mean longitudinal displacement maximum versus time plot - solid line is mean maximum and dashed line is mean at the interface.

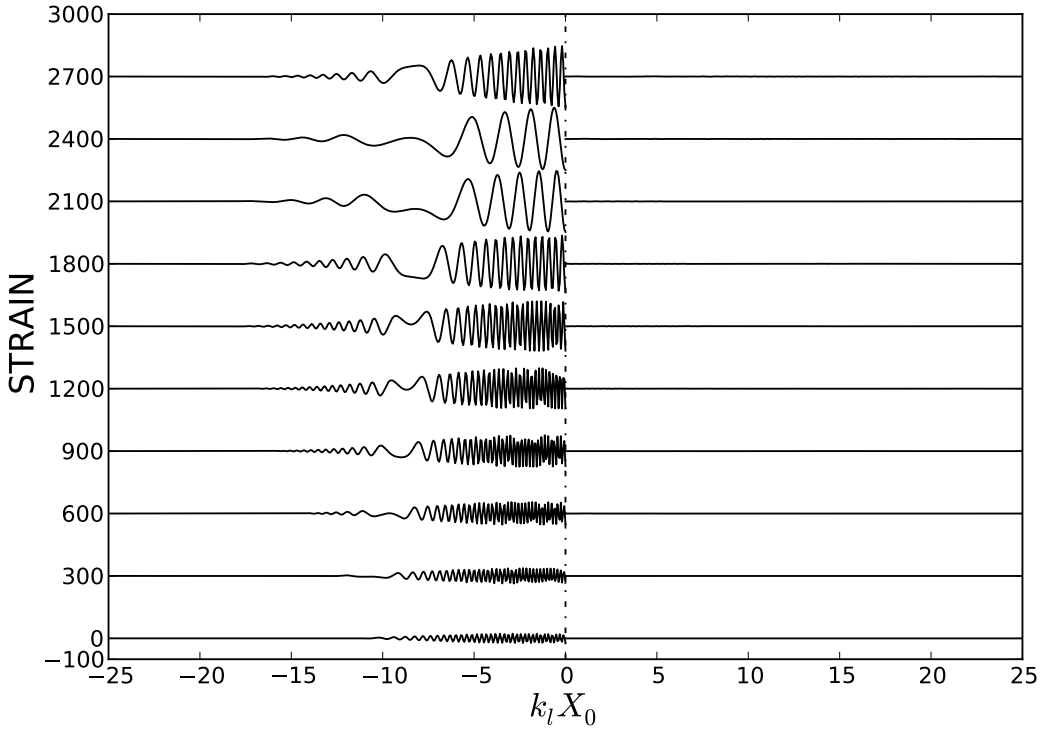

Figure 9.86: Case 7d: Strain evolution versus time from $\hat{t} = 3.10$ (bottom) through $\hat{t} = 3.90$ (top) in increments of $\Delta\hat{t} = 0.08$ each separated by 300 units vertically.

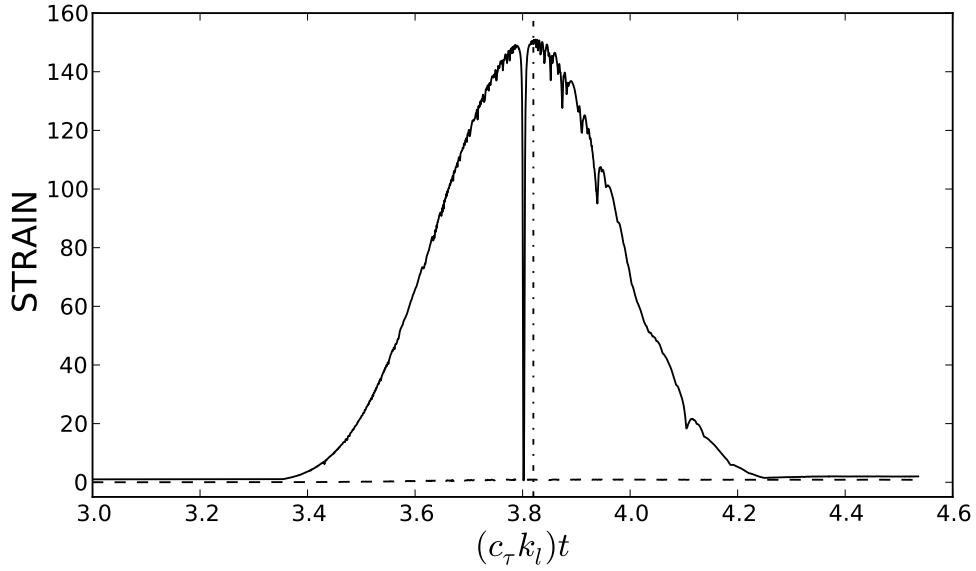

Figure 9.87: Case 7d: Strain maximum versus time plot.

Chapter 10

CONCLUSION

Waves on an infinite string have been treated here. The string has two regions, each region having constant properties. The interface between the two regions has a very sudden change in properties. A packet of waves are allowed to approach this interface from one side. The results are related to a variety of applications, in particular, the dynamics of ocean waves propagating through an ice sheet of non-uniform thickness. Such ocean waves are believed to contribute to the disintegration of polar ice.

The waves in the string are assumed to be modeled by continuum elastic effects. Geometric nonlinearities are included using a weakly nonlinear approach, but material nonlinearities are neglected. The present results focus on purely transverse waves. Linear theory shows that the incident waves will create reflected and transmitted waves, depending on the material properties. The weakly nonlinear theory considered here produces three nonlinear Schrödinger equations, one for the incident, reflected, and transmitted wave packets. The amplitude of the waves is measured by α and the length of the wave packet is measured by $1/\epsilon$. Both parameters are assumed small, and the further assumption that $\alpha = \epsilon$ is made for simplification.

The results show that these transverse waves generate a longitudinal mean displacement in the string in the vicinity of the interface. The mean longitudinal displacement is determined with a Laplace transform technique. This mean longitudinal displacement is composed of three parts. One part is due to the direct interaction of the incident and reflected waves, and has a spatial oscillation with twice the wavenumber of the incident waves. The other two parts are driven by the motion of the interface itself, with one part having a temporal oscillation at twice the frequency

of the incident waves.

The results depend on three parameters, ρ_n, $(EA)_n$, and c_n^2. The value of ρ_n directly affects the amplitude and shape of the reflected and transmitted waves through the reflection and transmission coefficients. The value of $(EA)_n$ plays a dominate role in the magnitude of interfacial mean longitudinal displacement terms. However, ρ_n and c_n^2 also contribute in a smaller way to the interfacial mean longitudinal displacement terms.

The value of c_n^2 contributes to the phase angle of the three waves and is present in the coefficient of the interfacial mean longitudinal displacement terms and contributes to the span of influence of the mean displacement. In general, an increase in c_n^2 results in an increase in the length of the span of influence. The span of influence is also not always equal on each side of the interface.

When the left side of the string has greater material properties than the right, the mean longitudinal displacement is positive. When the right side of the string has material properties greater than the left, the mean longitudinal displacement is negative. A positive mean longitudinal displacement indicates that the string is shifting toward the right, while a negative mean longitudinal displacement causes the string to shift to the left.

The maximum strain is on the left side of the string near the interface, and occurs when the incident wave is past the halfway point through the interface.

Bibliography

[1] Campbell, A.J. & Bechle, A.J. & Wu, C.H. 2014 Observations of surface waves interacting with ice using stereo imaging. *J. Geophysical Research:Oceans* 10.1002/2014JC009894.

[2] Wang, Z. & Parau, E.I. & Milewski, P.A. & Vanden-Broeck, J-M. 2014 Numerical study of interfacial solitary waves propagating under an elastic sheet. *Proc. R. Soc. A* **470**:20140111.

[3] Korobkin, A.A. & Khabakhpasheve, T.I.& Papin, A.A. 2014 Waves propagating along a channel with ice cover. *European J. of Mech. B/Fluids* **47**,166-175.

[4] Whitham, G.B. 1999 *Linear and Nonlinear Waves.* Wiley Interscience.

[5] Bland, D.R. 1965 *Vibrating Strings.* Dover.

[6] Antman, S.S. 2005 *Nonlinear Problems of Elasticity.* Springer.

[7] Fetter, A.L. & Walecka, J.D. 2003 *Theoretical Mechanics for Particles and Continua.* Dover.

[8] Morse, P.M. & Ingard, K.U. 1968 *Theoretical Acoustics.* McGraw Hill.

[9] Beyer, R.T. 1997 *Nonlinear Acoustics.* Acoust. Soc. of Am.

[10] Ellermeier, W. 1993 Nonlinear acoustics in non-uniform infinite and finite layers. *J. Fluid Mech.* **257**, 183-200.

[11] Chakraborty, A. & Gopalakrishnan, S. 2004 Wave propagation in inhomogeneous layered media: solution of forward and inverse problems. *Acta Mechanica* **169**, 153-184.

[12] Chakraborty, A. & Gopalakrishnan, S. 2003 Various numerical techniques for analysis of longitudinal wave propagation in inhomogeneous one-dimensional waveguides. *Acta Mechanica* **162**, 1-27.

[13] Mortell, M.P. & Seymour, B.R. 2011 The propagation of small amplitude nonlinear waves in a strongly inhomogeneous medium. *Math. Mech. Solids* **16(6)**, 637-651.

[14] Iizuka T. & Wadati, M. 1992 Nonlinear waves in inhomogeneous lattices. *J. Phys. Soc. Jpn.* **61**, No.7, 2235-2240.

[15] Yajima, N. 1977 Reflection and transmission of lattice solitons. *Prog. Theor. Phys.* **58**, No.4, 1114-1126.

[16] Iizuka, T. & Wadati, M. 1992 Soliton transmission and reflection in discontinuous media. *J. Phys. Soc. Jpn.* **61**, No.9, 3077-3085.

[17] Bland, D.R. 1988 *Wave Theory and Applications.* Oxford.

[18] Ames, W.F. 1992 *Numerical Methods for Partial Differential Equations.* Academic Press.

[19] Gear, C.W. 1971 *Numerical Initial Value Problems in Ordinary Differential Equations.* Prentice-Hall.